The morphology of solid-liquid contacting efficiency in trickle-flow

Arjan van Houwelingen

The morphology of solid-liquid contacting efficiency in trickle-flow

by

Arjan van Houwelingen

A dissertation submitted in partial fulfillment
of the requirements for the degree

Masters of Chemical Engineering

in the

Department of Chemical Engineering
Faculty of Engineering, the Built Environment and Information Technology

University of Pretoria
Pretoria

17th March 2006

The morphology of solid-liquid contacting efficiency in trickle-bed reactors

Author:	Arjan van Houwelingen
Supervisor:	W. Nicol
Department:	Department of Chemical Engineering University of Pretoria
Degree:	Master of Engineering (Chemical Engineering)

Synopsis

Trickle-flow is traditionally modeled by means of hydrodynamic parameters such as liquid holdup, two-phase pressure drop and wetting efficiency. Several studies showed that these parameters are not only a function of flow conditions and bed properties, but also of the flow history and morphology of flow. These can have a major influence on the distribution in the bed. The effect of flow morphology on liquid holdup and pressure drop is widely discussed in literature, but little attention is paid to its effect on wetting efficiency.

Trickle-bed reactor models suggest that not a only bed-averaged but also the distribution of wetting efficiency may be of importance for reactor performance. Both the average wetting efficiency and the distribution of wetting are probably a function flow history and morphology.

The distribution of wetting efficiency for different flow morphologies were investigated by means of a colorometric method that was developed for this purpose. Representative wetting distributions could be obtained. Flow morphologies and liquid distributions were manipulated by means of the pre-wetting procedure that was performed prior to flow. Pulse and Levec pre-wetted beds were investigated.

These distributions were explained in detail in terms of flow morphology. It was found that the average wetting efficiency in pulse pre-wetted beds are much higher than in Levec pre-wetted beds. All particles in the pulse pre-wetted beds at all investigated flow conditions were contacted by the flowing liquid. This was not the case for the Levec pre-wetted beds. It was found that the flow in Levec pre-wetted beds become similar to that in pulse pre-wetted beds at high liquid flow rates.

It was investigated how these distributions can affect reactor modeling, based on popular particle-scale models that relate reactor efficiency to wetting efficiency. According to these models, the wetting efficiency distribution in pulse pre-wetted beds can be characterised by means of only its average value. This is not the case for Levec pre-wetted beds. These results are however a strong function of the models that were employed.

Finally, some recommendations are made in terms of the preferred pre-wetting method or flow morphology for different types of reactions. These recommendations are also based

on models and have not been verified with experiments.

KEYWORDS: Trickle-bed reactors, trickle flow, wetting efficiency, solid-liquid contacting efficiency, particle wetting distributions, colorimetrics

CONTENTS

LIST OF FIGURES

LIST OF TABLES

NOMENCLATURE

δ	Film thickness, m
ϵ	Bed porosity
ϵ_L	External liquid holdup
ϵ_p	Catalyst particle porosity
ϵ_p	Particle porosity
η	Particle efficiency
$\eta_{1/2}$	Catalyst effectivity of half-wetted pellet ($\eta_{CE,pellet} = 0.5$)
$\eta_{CE,st}$	External area fraction contacted by stagnant liquid
η_{CE}	External contacting efficiency
η_d	Catalyst efficiency for completely dry pellet
η_d	Particle efficiency in terms of dry external surface area concentration
η_i	Internal wetting efficiency
$\eta_{TB,w}$	Trickle bed efficiency for externally wetted fraction of catalyst surface
η_{TB}	Effectivity of trickle-bed reactor as compared to a perfect plug-flow reactor
η_w	Particle efficiency in terms of wetted external surface area concentration
μ	Viscosity, Pa.s
ω	Fraction internal area of catalyst where no reaction takes place for a gas-limited reaction

ϕ	Particle Thiele modulus
ϕ_k	Spherical coordinate of pixel on 2-dimensional image projected in the 3-dimensional plane, radians
ρ_b	Bulk density of bed, kg/m^3
ρ_G	Gas density, kg/m^3
ρ_L	Liquid density, kg/m^3
σ	Standard deviation of a wetting distribution sample
σ_L	Liquid surface tension, Pa.m
τ	Average liquid residence time in TBR, s
τ_{lg}	Shear stress at gas-liquid interface, Pa
τ_{lw}	Shear stress between liquid and wall in the model of Holub et al. (1992), Pa
θ	Dimensionless time, $\frac{tu}{l}$
θ_p	Spherical coordinate of pixel on 2-dimensional image projected in the 3-dimensional plane, radians
ξ	Dimensionless radial position in pellet, $\xi = \frac{r}{r_p}$
$_{cw}$	Refers to completely wetted pellet
$_{lf}$	Refers to liquid-filled bed
$_{pw}$	Refers to partially wetted pellet
A	Gas-side reagent
A	Reagent species supplied in gas phase
a	External catalyst surface area per volume of reactor, m^{-1}
a_{ab}	Fractional area available for physical absorption
A_c	Cross-sectional area of bed, m^2
a_c	Fractional area available for physical absorption accompanied by chemical reaction in an absorption column
a_d	Fractional solid area contacted by dynamic liquid in an absorption column

a_{kp} Area represented by one pixel in the ϕ-θ plane, m^2

a_{st} Fractional solid area contacted by stagnant liquid in an absorption column

a_v Fractional area available for vapourisation in an absorption column

A_w Total active catalyst surface area contacted by liquid, m^2

a_w Fractional wetted solid area in an absorption column

B Reagent species supplied in liquid phase

b Stoichiometric coefficient for the reaction $A + bB \rightarrow$ products

C_i^* Concentration of i that would be in the liquid phase, if it were in equilibrium with its gas phase concentration

C_{ad} Surface concentration of adsorbed tracer species, $^{kmol}/_{m^2}$

$C_{i,s,d}$ Concentration of reagent i at dry external catalyst surface, $kmol/m^3$

$C_{i,s,w}$ Concentration of reagent i at wetted external catalyst surface, $kmol/m^3$

$C_{i,s}$ Concentration of reagent i at external catalyst surface, $kmol/m^3$

C_i Tracer concentration in catalyst pores, $^{kmol}/_{m^3}$

D_A Dispersion coefficient, $^{m^2}/_s$

D_{eff} Effective diffusivity, $^{m^2}/_s$

D_i Diffusion coefficient for component i, $^{m^2}/_s$

E_1 First Ergun constant for prediction of single phase pressure drop over bed

E_2 Second Ergun constant for prediction of single phase pressure drop over bed

f Fractional wetting as determined by a physical method

f_{ij} Pixel wetting in 2-D Cartesian coordinates, 0 or 1

f_{kp} Pixel wetting (0 or 1) in the ϕ-θ plane, dimensionless

f_n Range of fractional wetting values as used in histogram plots

f_p Particle wetting, dimensionless

Fr_L Liquid Fraude number, $Fr = \frac{L^2(1-\epsilon)}{d_p \rho_L^2 g}$

G Gas superficial mass flux, $^{kg}/_{m^2 s}$

g Gravitational acceleration, $g = 9.81$ $^{m^2}/_{s}$

Ga_L Liquid Galileo number, $Ga_L = \frac{d_p^3 \rho_L^2 g \epsilon^3}{\mu_L^2 (1-\epsilon)}$

H_i Henry's constant for reagent i

k First order reaction rate constant, $^{m^3}/_{\text{kg catalyst.s}}$

k_{ad} Equilibrium constant for adsorption of tracer species, m

K_a Constant describing time tracer spend adsorbed on catalyst surface

K_{gLs} Overall mass transfer coefficient from gas phase to particle surface, through the liquid phase, based on liquid-solid area, m/s

K_{gL} Mass transfer coefficient from gas phase to liquid phase, based on liquid-solid area, m/s

k_{gs} Gas-solid mass transfer coefficient in terms of dry external particle surface

k_{ls} Liquid-solid mass transfer coefficient, $^{m}/_{s}$

L Liquid superficial mass flux, $^{kg}/_{m^2 s}$

P Pressure, Pa

$P(f)$ Fraction of particles in the bed for which the fractional wetting lies within f_n

p_i Partial pressure of reagent i in the gas phase, kPa

P_w Probability of a completely wetted pellet in reactor

Pe Peclet number, $Pe = \frac{h v_{SL}}{D_A}$

Q_L Liquid volumetric flow-rate, m^3/s

r Radial position in spherical pellet, m

R' Reaction rate, $^{kmol}/_{m^3 s}$

$R'_{i,G}$ Rate of production of reagent i present in gas phase, kmol/s

$R'_{i,L}$ Rate of production of reagent i present in the liquid phase, kmol/s

r/R Fraction of image radius that can be taken into account before the boundary effect is encountered

R_p Particle radius, pixels

r_p Radius of catalyst particle, m

Re_L Liquid Reynolds number, $Re_L = \frac{v_{SL}\rho_L d_p}{\mu_L(1-\epsilon)}$

S_{ext} Effective external area of catalyst particle, m^2

Sh_{LS} Liquid-solid sherwood number, $\frac{k_{LS}d_p}{6D_{eff}}$

T Bed tortuosity

u_l Intrinsic liquid velocity, $u_l = \frac{v_{SL}}{\epsilon_L}$, m/s

V_b Bed volume, m^3

v_{SG} Gas superficial velocity, m/s

v_{SL} Liquid superficial velocity, m/s

We_L Liquid Weber number, $We = \frac{L^2 d_p}{(1-\epsilon)\rho_L \sigma_L}$

$WHSV$ Weight hourly space velocity, $^{m^3}/_{\text{kg catalyst.s}}$

X Reactor conversion, dimensionless

x Dimensionless position in reactor, $\frac{z}{h}$

Z Total bed length, m

z Axial position in reactor, m

z Reactor position, m

W Width of catalyst slab for the geometry illustrated in figure 2.3, m

CHAPTER 1

Introduction

Trickle-bed reactors are catalytic three-phase reactors where the gas and the liquid phase reagent flow concurrently down a packed catalyst bed, and find their main applications in oil refining, petrochemical, chemical and biochemical processes. Examples of these are hydrotreating and desulferisation of oil refining and petrochemical process streams, catalytic hydrogenation of chemical compounds and oxidation of harmful biochemical compounds in wastewater streams (Gianetto & Specchia, 1992). As catalyst research progresses, it is likely that new applications will be found (Dudukovic et al., 1999).

For modeling of these reactors, the flow over the catalyst bed is traditionally described in terms of bed average hydrodynamic parameters, such as two-phase pressure drop, liquid holdup, and solid-liquid contacting efficiency (also called wetting efficiency). These parameters are then predicted from the liquid and gas flow rates and properties, and the properties of the bed packing. Considerable scatter in data regarding this parameters, suggest that trickle-flow is too complex for such an approach (Dudukovic et al., 1999). It was for example found that the nature of trickle-flow is a strong function of flow history (Kan & Greenfield, 1978; Christensen et al., 1986; Lazzaroni et al., 1989; Ravindra et al., 1997; Moller et al., 1996). Many of these authors explain this hysteresis behaviour in trickle-flow by means of the nature of trickle-flow *morphology* (i.e. the manner in which the liquid flows down the packing).

A large amount of literature focuses on the description of trickle-flow morphology, and various possible forms of liquid flow have been suggested (Zimmerman & Ng, 1986; Lutran et al., 1991; Christensen et al., 1986; Ravindra et al., 1997), of which the most important are film flow and filament flow. The natures of these two types of flow differ considerably, and the effect of these has been described in terms of liquid holdup and pressure drop (Melli & Scriven, 1991; Ravindra et al., 1997; Christensen et al., 1986). Reactor models that take into account flow morphology, are also based on these two

parameters (Melli & Scriven, 1991). It was found that trickle-flow morphology can be manipulated by the manner in which a bed is pre-wetted prior to flow (van der Merwe & Nicol, 2005).

Some description of wetting efficiency in terms of flow morphology was given by Sederman & Gladden (2001), but was discussed only very briefly. No definite attention had been paid to the nature of wetting efficiency for different flow patterns in a trickle-bed reactor, and current reactor models still make use of an overall (bed-averaged) wetting efficiency, that is estimated by correlations that do not account for flow history or morphology.

Wetting efficiency can however play an important role in trickle-bed reactor performance, influencing external and internal mass transfer rates from the gas and liquid reagent onto catalyst sites. Available models suggest that this effect should be viewed on particle scale (Dudukovic, 1977; Ramachandran & Smith, 1979; Tan & Smith, 1980; Herskowitz et al., 1979). Most of these models are non-linear so that the *distribution of particle-scale wetting* (i.e. how many particles are wetted to what extend?) and not only the average wetting may be of importance. In almost all available data, wetting efficiency is however presented as an overall bed-averaged parameter.

The aim of this study is to give a more detailed description of wetting efficiency in trickle-bed reactors, by measuring the particle wetting distribution under trickle-flow conditions. It is investigated how the pre-wetting procedure can affect particle wetting distributions and how these distributions of can affect reactor modeling and performance. To achieve this aim a new experimental technique had to be developed in order to determine the distribution of wetting in trickle-bed reactors for different flow conditions.

The nature of wetting efficiency was studied by means of a colorometric experiments that were performed for atmospheric N_2-water flow over a porous γ-alumina packing.

CHAPTER 2

Literature Study

2.1 Background

2.1.1 Flow regime

Due to the two flowing phases present in a trickle-bed reactor, many different flow regimes can be encountered, depending on the liquid and gas flow rates and properties. These regimes can be categorized into the high interaction flow regime (HIR) and the low interaction flow regime (LIR).

The LIR is characterised by weak gas-liquid interaction, low gas-liquid mass transfer coefficients and shear stresses, and gravity driven liquid flow. Liquid trickles down the packing, whereas the gas phase process stream fill up the remaining available space in the reactor. In trickle-bed reactors, only the trickle-flow regime can be classified as a low interaction flow regime (Gianetto & Specchia, 1992).

The HIR consists of the following flow regimes:

- *Pulsing flow.* Liquid-rich and gas-rich slugs flow alternately through the bed. High catalyst wetting efficiency and mass transfer coefficients are encountered. Pulse flow also induces pseudo-unsteady state, which can be beneficial for reaction rates. As a result, a vast amount of literature is available on inducing pulsating flow at acceptable liquid hourly space velocities.

- At low gas flow rates, *bubble flow* will be encountered on increasing the liquid flow rate. The liquid phase is continuous and the gas is trapped in the liquid as small bubbles. On increasing the gas flow rate, the bubbles will coalesce to form larger, elongated gas bubbles. This flow regime is often referred to as the *dispersed bubble flow* regime.

- *Spray flow* is encountered at high gas flow rates where the liquid is entrained in a continuous gas phase as small droplets.

The HIR is characterised by a high level of interaction between the liquid and gas phase.

2.1.2 Liquid holdup

External liquid holdup, ϵ_L is defined as the volume fraction of external[1] liquid in the bed, and plays a role in trickle-bed reactor performance in the following fashion :

- For a certain volumetric liquid flow rate, liquid holdup determines the intrinsic velocity of the liquid and hence the external gas-liquid and liquid-solid mass transfer coefficients.
- The more external liquid present in the bed, the more solid-liquid contacting area will be present, influencing external liquid-solid and internal gas-solid and liquid-solid mass transfer coefficients.
- Higher liquid holdup results in less area for flow for the gas, and therefore increased pressure drop.
- Liquid is far more efficient in heat removal from catalyst particles than gas. To prevent hot spots in exothermic reactors, a good liquid distribution is needed.

In the modeling of trickle-bed reactors, liquid holdup is often divided into a stagnant ($\epsilon_{L,st}$) and dynamic liquid holdup ($\epsilon_{L,d}$) (Villermaux & vanSwaaij, 1969). This is done since it is believed that at the contact points of the catalyst particles, liquid is trapped as stagnant globules. Static liquid holdup was defined to describe deviations from ideal plug flow in a trickle-bed reactor (Villermaux & vanSwaaij, 1969; Nigam et al., 2001), but it is also believed that these areas are highly ineffective for mass transfer (Sicardi et al., 1980, 1981; Nigam et al., 2001; Iliuta et al., 1999). In the past, stagnant liquid holdup was determined by weighing the bed after draining it. The dynamic liquid holdup was then defined as the amount of liquid that remain in the bed when it is drained. Nowadays, with improved computing power, dynamic and static liquid holdup is determined from tracer experiments together with the other flow parameters in R.T.D.-models. The static and dynamic liquid holdup determined from tracer experiments differs from that determined by draining the bed, and the holdups determined by bed draining is referred to as residual and free-draining liquid holdup ($\epsilon_{L,r}$ and $\epsilon_{L,d}$). The tracer determined holdups are believed to be more representative, since it is determined *during* trickle flow.

[1]Liquid in the bed can divided into two groups: Internal and external liquid. Internal liquid volume refers to the volume of liquid inside catalyst pores, and is often assumed to be equal to the total catalyst pore volume, except when the liquid phase process stream is volatile.

Due to its importance as a hydrodynamic parameter, liquid holdup has been subject of a vast amount of literature, and several correlations has been developed to predict its value. An overview of these is given in Dudukovic et al. (2002). Data from these studies is subject to significant scatter, which is an indication that trickle-flow is still not fully understood (Dudukovic et al., 1999).

2.1.3 Pressure drop

The pressure drop over a trickle-bed reactor is of importance due to the pumping costs involved when a large gas recycle stream is needed. It can also influence reactor performance due to its influence on radial distribution, wetting efficiency, gas-liquid mass transfer and liquid holdup.

Liquid holdup and pressure drop are closely coupled parameters in a trickle-bed reactor, and several recent pressure drop correlations are coupled with that of liquid holdup (Holub et al., 1992; Iliuta & Larachi, 2000). The relationship between holdup and pressure drop can be presented as follows (Hutton & Leung, 1974):

$$\epsilon_L = \epsilon_L \left(\frac{\Delta P}{Z}, L, \text{ bed properties} \right) \tag{2.1}$$

$$\frac{\Delta P}{Z} = \frac{\Delta P}{Z} \left(\epsilon_L, G, \text{ bed properties} \right) \tag{2.2}$$

Or, in words: The holdup in the bed is increased by liquid flow and decreased by the pressure drop, where as the pressure drop over the bed is increased by increased holdup (less cross-sectional area for gas flow and increased gas-liquid shear) and by increased gas flow rates.

2.2 Trickle-flow morphology

2.2.1 Flow Types

In the trickle-flow regime the liquid is suggested to be present in the following forms (Zimmerman & Ng, 1986; Lutran et al., 1991; Ravindra et al., 1997; Sederman & Gladden, 2001):

- *Film flow* occurs when the flowing liquid covers the particles in the bed with a thin film. These films can provide either complete surface coverage or partial surface coverage, depending on liquid and gas flow rates and packing properties. This type of flow is highly effective for liquid-limited reactors, since it provides high external wetting and a high gas-liquid interfacial areas.

- It is believed that some of the liquid flows in the form of a stream down the bed, completely filling large areas in the packing. This is often referred to as *channel flow*. Although most of the particles that are subject to channel flow are completely wetted, this type of flow can be extremely detrimental for reactor performance, since very low gas-liquid interfacial area to liquid volume ratio's are experienced (Ravindra et al., 1997).

- *Filament flow.* Liquid streams over the packing without following the shape of the packing as is the case for film. Filament flow is sometimes referred to as rivulet flow (e.g. Christensen et al. (1986)).

The flow types discussed are illustrated in figure 2.1. Flow type appear to be a strong

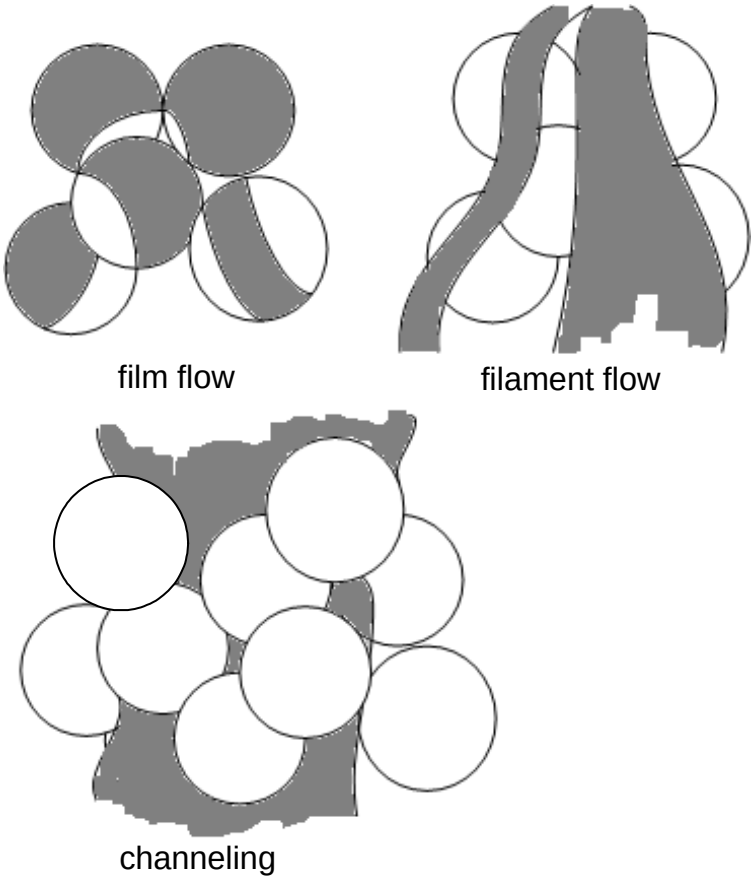

Figure 2.1: Flow types in the trickle-flow regime.

function of bed pre-wetting. The pre-wetting procedures that are reported in literature are:

- *Initially dry.* The bed is not pre-wetted prior to irrigation. Initially dry beds are often used as a limiting case to stress the importance of pre-wetting (Sedriks & Kenney, 1972; Lazzaroni et al., 1988; Ravindra et al., 1997; Sederman & Gladden, 2001; Lutran et al., 1991).

- *Levec pre-wetting.* This type of pre-wetting refers to the case where the bed is flooded and then drained before irrigation of the liquid starts (Sederman & Gladden, 2001). Bed draining can take place under gas flow or no gas flow conditions.

- *Pulse pre-wetting.* A popular method of pre-wetting is to increase the liquid flow until the pulsing regime is encountered. The liquid flow is then gradually set back to the required rate. It is also possible to achieve the pulsing flow regime by increasing the gas flow rate. The term "pulse pre-wetting" refers to pre-wetting by pulsing with the liquid in this report, except when it is clearly stated that the gas was used to achieve pulsing flow.

- *Super pre-wetting.* The packing is flooded with the liquid and then drained gradually after the liquid flow rate is set to the desired rate.

In a initially dry bed, Lutran et al. (1991) found primarily filament flow. The position and the number of filaments appeared to be determined by the top few layers of packing material. On increasing liquid flow rate, few new rivulets were formed and as a result, existing filaments were expanded. In order to identify the flow types, axial sections throughout a bed were visualised by means of X-ray tomography. Liquid that followed the geometry of the packing closely (even on a particle scale level) was classified as film flow, whereas large localised continuous streams were classified as filaments. Another tomographic method, magnetic resonance imaging (MRI), was employed by Sederman & Gladden (2001) who found severe wall flow in an initially dry bed. This did not change much on increasing the liquid flow rate. These observations suggest that for an initially dry bed, liquid flow and distribution is primarily a function of the packing configuration, until the liquid flow is high enough to force new flow paths. Making use of a colorometric method, Ravindra et al. (1997) observed severe channel flow in initially dry beds. The channels appeared to be completely liquid-filled, resulting in a very low gas-liquid interfacial area in the bed.

For a Levec pre-wetted bed, Sederman & Gladden (2001) found the following trend: At low liquid flow rates, liquid flow, in the form of filaments, flows primarily over the parts of the bed that exhibit a high particle surface to void volume ratio. Few filaments are present. On increasing the liquid flow rate the number of filaments are increased. At a certain liquid flow rate, no new rivulet filaments are formed and the existing ones are only thickened. Christensen et al. (1986) found that at low to moderate liquid flow rates filament flow prevails, with the flow morphology rapidly changing to predominantly film flow at a certain critical liquid flow rate. The magnitude of this critical flow rate was a function of the gas flow rate. The findings of Christensen et al. (1986) were not based on visual observations as was the case for the other authors stated in this section but were inferred from liquid holdup and pressure drop measurements: It was assumed that,

as a limiting case, pulse pre-wetted beds exhibit exclusively film flow, and that this type of flow will have the maximum pressure drop and liquid holdup that is possible in the trickling flow regime for the given liquid and gas flow rate and flow system. Any pressure drop and liquid holdup values that are lower than for this limiting case would then be a result of filament flow.

In pulse- and super-wetted beds, it appears as though film flow prevails. For a pulse pre-wetted bed, Lutran et al. (1991) found that the liquid flow is present where the solid surface to void space ratio is high (low porosity). Liquid flow rate did not affect the flow pattern. Ravindra et al. (1997) found a very good liquid distribution throughout the bed and overall complete wetting suggested film flow.

Although the different studies on trickle-flow morphology does support one another, some important limitations may have influenced the current "visualisation" of trickle-flow morphology:

- All above trickle-flow morphology studies were performed on *atmospheric air-water systems*. The high surface tension of water as compared to petrochemical process streams may accentuate maldistribution. Although Al-Dahhan et al. (1997) showed that wetting efficiency and pressure drop is dependent on gas density rather than absolute pressure, there is no evidence that trickle-flow morphology at atmospheric pressure is representative of flow morphology at high pressures.

- All observations were made over a *limited time span*. It is possible that in industrial trickle-bed reactors, the effect of pre-wetting diminishes over a long time, due to small flow fluctuations and change of liquid paths. The observation of Sederman & Gladden (2001) that the liquid flow path is relatively insensitive to liquid flow rate but rather a function of packing properties and pre-wetting procedure does however give some confidence that pre-wetting may influence flow in a trickle-bed reactor permanently.

2.2.2 Hysteresis

Since the liquid flow appears to be dependent on where the liquid has been in the packing, and new liquid flow "paths" do not form over time but can only be formed on increasing the liquid flow rate, it is not surprising that trickle flow exhibits hysteresis.

Hysteresis in trickle flow was first reported by Kan & Greenfield (1978), who studied liquid holdup and pressure drop as a function of flow history. They observed the following trend for a pulse pre-wetted bed: When the gas flow is increased, pressure drop over the bed will increase accordingly with a certain trend, say "path 1". Then, when the gas flow is decreased again, the pressure drop does not follow "path 1" back to the original gas flow and pressure drop, but follows another path where the pressure drops for all

gas flow rates are *lower* than the corresponding pressure drops of "path 1". In the same experiment, *higher* liquid holdups were observed for a certain gas flow when the gas flow rate was decreased from a certain maximum flow rate than when it was increased from the minimum flow rate. Trickle flow for all the reported data points was stable, suggesting multiple hydrodynamic states. The observations were explained as follows. Increased gas flow rate tend to "align" the liquid in the bed in the preferred direction of gas flow (which is vertically down the bed), thus reducing the effective tortuosity of the bed. This result in lower pressure drop over the bed, which in turn leads to a higher holdup. In these authors' opinion, this effect will only be significant for beds of small packings. A model for these observations that deals with the effect of gas flow rate history on effective bed tortuosity, was presented by Kan & Greenfield (1979).

Christensen et al. (1986) investigated liquid holdup and pressure drop hysteresis loops on a Levec pre-wetted bed containing glass beads for constant gas flow and constant liquid flow conditions. With constant gas flow conditions, pressure drop was higher when the liquid operating flow rate was set by decreasing it from a maximum flow rate, than when it was set by increasing it from the minimum flow rate. Liquid holdup did not show any hysteresis. For constant liquid flow conditions, the pressure gradient over the bed was *larger* when decreasing from the maximum gas flow rate than when the gas flow was increased from the minimum gas flow rate. This observation is in sharp contrast with that of Kan & Greenfield (1978), indicating that hysteresis behaviour may also be a function of bed pre-wetting. This is most likely due to the effect of pre-wetting on trickle flow type. Christensen et al. (1986) explained hysteresis in a Levec pre-wetted bed in terms of the fraction of the liquid in the bed that flows in the form of films, which is determined primarily by the maximum liquid flow rate.

Lazzaroni et al. (1989) and Ravindra et al. (1997) found that an initially dry bed also exhibits hysteresis in pressure drop and liquid holdup. Pressure drop and liquid holdup was higher when the working flow rate was approached from the maximum liquid flow rate than when it was approached from the minimum liquid flow rate. For an initially dry bed, this can easily be explained: the wettability of already wet particles is higher than that for initially dry particles, and better liquid distribution will be observed in a bed that was close to flooding due to high liquid flow rates, than for an initially dry bed where the liquid flow rate was gradually increased from a low value. The same explanation was given by Levec et al. (1988) for pressure drop and liquid holdup hysteresis in a Levec pre-wetted bed.

2.2.3 Radial and axial variations in trickle flow

The study of hysteresis behaviour in trickle-bed reactors resulted in new hydrodynamic models (Kan & Greenfield, 1979; Melli & Scriven, 1991; Jiang et al., 1999) and modifica-

tions of existing ones (van der Merwe & Nicol, 2005) in order to provide for trickle flow morphology, since traditional models can not describe flow hysteresis.

Another possible limitation of traditional trickle-bed reactor models is that they make use of bed averaged values for holdup and wetting efficiency (Christensen et al., 1986), and do not take into account liquid distribution. To simulate distribution in trickle bed reactors several flow models have been developed over the past two decades (Crine et al., 1980; Stanek et al., 1981; Zimmerman & Ng, 1986; Melli & Scriven, 1991; Souadnia & Latifi, 2001). Most of these are however based exclusively on theory and no experimental data is provided to verify the model. In fact, experimental observations seem to contradict these models. For example, the models of Crine et al. (1980) and Stanek et al. (1981) show a strong dependency on liquid inlet distribution, while several authors stated that their experimental results were insensitive to distributor design (Christensen et al., 1986; Moller et al., 1996; Wang et al., 1995).

Radial liquid distribution is usually measured by means of an annular collector installed at the outlet of the bed (Marcandelli et al., 2000; Ravindra et al., 1997; Moller et al., 1996). Moller et al. (1996) studied the hysteresis of radial liquid distribution in trickle-beds. The expected trend was followed for an initially dry bed: The distribution at a certain value of L is better when L is approached from the maximum flow than when approached from the minimum flow. This is in accordance to the discussion in the previous section. Pre-wetting enhanced liquid distribution significantly. No clear trend with gas flow rates was observed. It was also found that the distributor design did not affect liquid distribution in the bed very much, and that the top layers of packing compensates for poor distributor design. Using large particles for the top few layers of packing enhanced liquid distribution. Although Moller et al. (1996) found that distributor design does not influence radial liquid distribution, Tsochatzidis et al. (2002) found that it does have a very significant effect on the trickle- to pulsing flow boundary and on the pressure drop over the bed. They suggested that maldistribution in a trickle-bed can be correlated with the pressure drop over the bed. Radial liquid maldistribution as determined by means of a collector can be quantified with a maldistribution factor (Marcandelli et al., 2000):

$$M_f = \sqrt{\frac{1}{N(N-1)} \sum \left(\frac{Q_{Li} - Q_{mean}}{Q_{mean}} \right)^2} \tag{2.3}$$

Where N is the number of equal-area parts in which the collector is divided and Q_{Li} the liquid volumetric flow rate through part i of the bed. Q_{mean} is defined as the total liquid flow rate divided by N. An ideal distribution would result in $M_f = 0$ ($Q_{Li} = Q_{mean}$ for all i), whereas severe maldistribution would result in $M_f \to 1$ ($Q_{Li} = 0$ for $N-1$ zones and $Q_{Li} = N.Q_{mean}$ for one of the zones).The disadvantage of above defined maldistribution factor is that the value of M_f is not only a function of the liquid flow conditions, but also

of the number and position of partitions in the collector. Another drawback of radial distribution measurements by means of a collector is that the results are averaged over the bed length, and no axial liquid flow variations can be measured.

Wang et al. (1995) addressed this problem by measuring liquid maldistribution for different bed heights, by means of an annular collector. They distinguished between large scale, and small scale flow distribution fluctuations. Large scale fluctuations is an indication of wall flow versus central flow, whereas the small scale variations are characteristic to the flow morphology. It was found that wall flow intensity is independent of gas and liquid flow rates, but the small scale variations in the central flow was a strong function of bed height and flow conditions. Gas and liquid flow rates had an enhancing effect on the liquid distribution. The maldistribution in the bed asymptotically decreased along the bed length to some equilibrium distribution.

Roy et al. (2004) investigated liquid distribution as a function of bed depth making use of γ-ray tomography. To quantify liquid maldistribution, a uniformity factor was computed as follows: A cross-sectional image was divided into several sub-domains. Hypothesis testing is then used to test if the pixels in such a sub-domain is statistically the same as the total (pixel) population. The uniformity factor is given by the percentage of pixel groups that are statistically similar to the overall cross-section. Unlike collector experiments, distribution could be examined a specific cross-sections of the bed, and results are not averaged over the bed length. The uniformity factor is however still a function of grid size as was the case for collector experiments.

2.3 Wetting Efficiency

The most basic definition of wetting efficiency is the fraction of external catalyst particle area exposed to the liquid phase. It is of importance mainly because of its influence of external and internal mass transfer rates of the two flowing phases with regards to solid catalyst particles, thereby influencing *reactor conversions*. Numerous methods of its *determination* have been employed, leading to a large number of *correlations* that attempt to predict wetting efficiency for different flow conditions. In this section, these three aspects of wetting efficiency will be discussed consecutively.

2.3.1 Wetting efficiency as used in reactor models

Liquid limited reactions

The simplest way to model a trickle-bed reactor is by assuming ideal plug flow and no mass transfer effects for the limiting reagent. The design equation for a first order reaction

will then simply be the same as for a single phase ideal packed bed reactor:

$$\ln\left(\frac{1}{1-X}\right) = \frac{k}{WHSV} \tag{2.4}$$

A common design method was therefore to optimise pilot-scale trickle-bed reactors, after which it is simply scaled up to industrial size by keeping the weight hourly space velocity (WHSV) constant. Ross (1965) showed out that the ideal (plug flow) trickle-bed reactor can usually not be assumed and most authors began to make use of a more generalised approach:

$$\ln\left(\frac{1}{1-X}\right) = \frac{k}{WHSV}\eta_{TB} \tag{2.5}$$

with the trickle-bed efficiency, η_{TB}, is then a function of internal or external mass transfer rates of the limiting reagent and deviations from ideal plug flow.

For liquid-limited reactions, Henry & Gilbert (1973) proposed that η_{TB} is directly proportional the liquid holdup in a trickle-bed reactor. They studied trickle-bed reactor efficiencies in pilot- and industrial scale reactors and found the following relationship that can be used for trickle-bed reactor scale-up:

$$\ln\left(\frac{1}{1-X}\right) \propto WHSV^{-2/3} \tag{2.6}$$

Equation 2.6 indicates that η_{TB} is proportional to WHSV$^{1/3}$. Since most available holdup correlations then contained a term $v_{SL}^{1/3}$ and the weight hourly space velocity is proportional to v_{SL}, Henry & Gilbert (1973) suggested that external holdup in a trickle-bed reactor determines its efficiency.

Satterfield (1975) stated that the direct relationship between liquid holdup and η_{TB} has no theoretical justification, and pointed out that the observed proportionality could be due to other mechanisms:

- Holdup is proportional to $d_p^{-2/3}$. The fact that the reactor efficiency is proportional to holdup implies that the efficiency increases with decreased catalyst size, which is generally true for a reactor where internal diffusion limitations play a role.

- If $\eta_{TB} \propto \epsilon_L$, equation 2.6 can be written as:

$$\ln\left(\frac{1}{1-X}\right) \propto \frac{k\epsilon_L}{WHSV} \tag{2.7}$$

  With $\epsilon_L \propto v_{SL}^{1/3}$ and $v_{SL} = WHSV.\rho_b.Z$ one obtains:

$$\ln\left(\frac{1}{1-X}\right) \propto \frac{kZ_b^{1/3}}{WHSV} \tag{2.8}$$

which implies an increase in reactor performance with increased bed length for a constant weight hourly space velocity (i.e. increased Z_b, decreased A_c). Even if holdup does not determine trickle-bed efficiency, this could still be true, due to higher linear liquid velocities and less dispersion.

Furthermore, Bondi (1971) found an increase in reactor performance with increased gas flow rate, even although the reaction was liquid limited, and the holdup decreased with increased gas flow rate.

Mears (1974) reasoned that it is not the liquid holdup, but the external contacting efficiency (i.e. the fraction of external particle area in contact with the flowing fluid) that determines the efficiency of a trickle-bed reactor, if dispersion effects can be ignored. The trickle-bed reactor design equation for a first order reaction is then:

$$\ln\left(\frac{1}{1-X}\right) = \frac{k.\eta.\eta_{CE}}{WHSV} \tag{2.9}$$

Whereas Mears (1974) viewed η_{CE} as a reactor-scale parameter, Dudukovic (1977) suggested to view partial wetting on a particle scale to derive its influence on trickle-bed reactor efficiency. Two types of incomplete wetting can be present: Partial external wetting (η_{CE}) and partial pore filling (η_i). The effectiveness factor for such a partially wetted particle was estimated with an expression that Aris (1957) developed for particles of irregular shape (it was argued that partially wetted particles are similar to particles of irregular shape, due to asymmetrical boundary conditions), where particle efficiency is related to its Thiele modulus by means of the following expression:

$$\eta = \frac{\tanh\phi}{\phi} \tag{2.10}$$

where:

$$\phi = \frac{V_p}{S_{ext}}\sqrt{\frac{k}{D_eff}}, \text{ for a first order reaction} \tag{2.11}$$

The Thiele modulus for a partially wetted particle is then:

$$\phi_{TB} = \frac{(V_p\eta_i)}{(S_p\eta_{CE})}\sqrt{\frac{k}{D_{eff}}} \tag{2.12}$$

Rearranging equations 2.10 and 2.12 gives:

$$\eta_{TB} = \eta_{CE}\frac{\tanh\left(\frac{\eta_i}{\eta_{CE}}\phi\right)}{\phi} \tag{2.13}$$

For high Thiele moduli, this expression reduces to:

$$\eta_{TB} \approx \frac{\eta_{CE}}{\phi} = \eta_{CE}.\eta \tag{2.14}$$

which is the same as Mears' expression. This result for a severely internal diffusion limited system do make sense because for such systems reaction occurs only at the outer surface of the particles, and utilization of the catalyst is proportional to the fraction of external area wetted. For small Thiele moduli:

$$\eta_{TB} \approx \eta_i \left[1 - \frac{1}{3}\left(\frac{\eta_i}{\eta_{CE}}\phi\right)^2\right] \tag{2.15}$$

Complete internal wetting is usually assumed due to capillary forces and equation 2.15 reduces to $\eta_{TB} \approx 1$ except at very low values of η_{CE} (which is usually not encountered in trickle-bed reactors, if the average wetting efficiency can be assumed for all particles).

Wu et al. (1996) have shown that equation 2.13 does give good results for a trickle-bed reactor where ϕ is equal to the intermediate value of 3.59. More extensive derivations of the relationship between η_{TB} and η_{CE} have been performed by Mills & Dudukovic (1979) for particles of different shapes and for different limiting reagents.

For an external mass transfer limited system, it is frequently assumed that the external mass transfer rate decreases linearly with decreasing contacting efficiency, due to the fact that the mass transfer area is linearly dependent on the fractional wetting (Lakota & Levec, 1990; Nigam et al., 2001; Mills & Dudukovic, 1981; Wu et al., 1996):

$$k_{ls}a_{TB} = k_{ls}a\eta_{CE}, \text{ at same } u_l \tag{2.16}$$

or, in terms of the overall trickle-bed effectiveness:

$$\frac{1}{\eta_{TB}} = \frac{1}{\eta_{TB}^{\infty}} + \frac{1}{k.k_{ls}a\eta_{CE}} \tag{2.17}$$

Where η_{TB}^{∞} is the trickle bed efficiency when no external mass transfer limitations are present.

Static wetting efficiency

It is believed that some of the liquid in a trickle-bed reactor is trapped between the contact points of the catalyst particles and is virtually stagnant. The theory of stagnant liquid holdup in a trickle-bed reactor was introduced to allow more and other forms of deviation from ideal plug flow as what can be modeled by the normal axial dispersion model (Villermaux & vanSwaaij, 1969; Iliuta et al., 1999). The external solid area fraction that is wetted by these stagnant liquid zones, is called the static wetting efficiency, or

$\eta_{CE,st}$. Sicardi et al. (1980) introduced the concept of static wetting efficiency to explain the difference between wetting efficiency as obtained from R.T.D-experiments and as obtained from reaction experiments (see section 2.3.2). Areas wetted by stagnant zones are highly ineffective in terms of mass transfer as compared areas wetted with the flowing liquid: Nigam et al. (2001) found stagnant liquid-solid mass transfer coefficients of about 20 times smaller than dynamic liquid-solid mass transfer coefficients, and Sicardi et al. (1980) even found that this ratio is about 1:100. Sicardi et al. (1980, 1981) suggested that although $\epsilon_{l,st}$ is usually very low, η_{CE} can be much higher and severely decreases trickle-bed performance, since the stagnant liquid is trapped between the contact points of the particles in the bed, where the solid-liquid area to liquid volume ratio is very high. The relationship between static liquid holdup and static wetting efficiency can be approximated by the following geometrical relationship (Sicardi et al., 1980):

$$\epsilon_{l,st} \approx \frac{\left[2\left(1-2\frac{\eta_{CE,st}}{n}\right)^3 - 3\left(1-2\frac{\eta_{CE,st}}{n}\right)^2 + 1\right](1-\epsilon)\,n}{4} \tag{2.18}$$

Where n is the number of contact points of each particle in the bed, which is 6 for a regular cubic array of spheres. This relationship gives very high values of $\eta_{CE,st}$ for realistic $\epsilon_{l,st}$, and has been readjusted by Llano et al. (1997).

Gas limited reactions

Gas-limited reactions in trickle-bed reactors can occur when the gas reagent is only slightly soluble in the liquid process stream, and the liquid is non-volatile, so that reaction can only take place in the wetted interior of the catalyst particles. For complete pore filling, a reaction is said to be gas-limited if (Khadilkar et al., 1999):

$$D_{eff,B}.C_B(\ell) \gg D_{eff,A}.C_A(\ell) \tag{2.19}$$

It is then said that the gas-side reagent concentration (C_A) at the internal catalyst surface is always much lower than that of the liquid phase reagent (C_B), so that the reaction is zeroth order with respect to B. The effect of partial wetting on gas-limited reaction rates is best observed when external liquid-solid mass transfer is very slow (Beaudry et al., 1987). Mata & Smith (1981) found that, for a gas-limited reaction, the reaction rate exhibits a minimum when plotted vs. liquid flow rate (see figure 2.2). This can be explained as follows. At low liquid flow-rates, liquid-solid mass transfer of the gas-phase reagent is extremely slow as compared to gas-solid mass transfer. Although the liquid-solid mass transfer coefficient increases with liquid flow-rate, a decrease in reaction rate with liquid flow rate is observed since the wetting efficiency increases and the area for gas-solid mass transfer (which is much faster than liquid-solid mass transfer) decreases.

At high liquid flow rates, η_{CE} becomes unity, and reaction rate increases according to the increase of the external liquid-solid mass transfer coefficient with liquid flow rate.

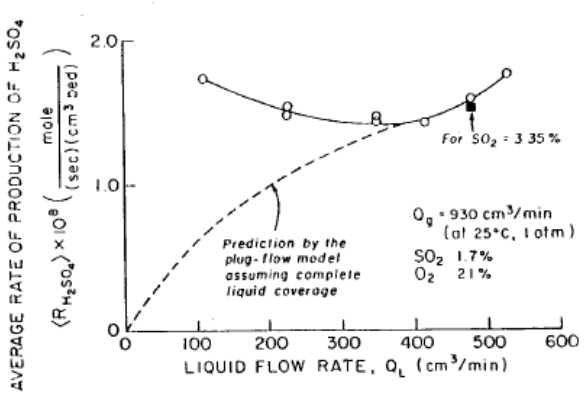

Figure 2.2: Gas-limited reaction rate vs. liquid flow rate in a trickle-bed reactor as determined by Mata & Smith (1981)

To account for this phenomenon the expression of Ramachandran & Smith (1979) for gas-limited reactions in a trickle-bed reactor can be used. These authors derived an expression for the overall trickle-bed effectiveness factor in terms of the gas phase reagent, taking into account internal and external mass transfer limitations, based on the geometry shown in figure 2.3. Reaction rates for consumption of the gas phase reagent can then be described by the following equations:

$$-r_{A,L} = K_{gLs}\,(C_A^* - C_{A,s,w})\,W\eta_{CE} = k\eta_L C_{A,s} W \eta_{CE} L \tag{2.20}$$

$$-r_{A,G} = k_{gs}\,(C_A^* - C_{A,s,d})\,W(1-\eta_{CE}) = k\eta_G C_{A,s,d} W (1-\eta_{CE}) L \tag{2.21}$$

where

$$\frac{1}{K_{gLs}} = \frac{1}{K_{gL}} + \frac{1}{k_{Ls}} \tag{2.22}$$

and

$$C_A^* = p_A/H_A \tag{2.23}$$

If the efficiency is defined as the actual rate of consumption of A divided by the maximum rate ($kC_A^* WL$) then one can derive the following TBR-efficiencies for both the wetted and

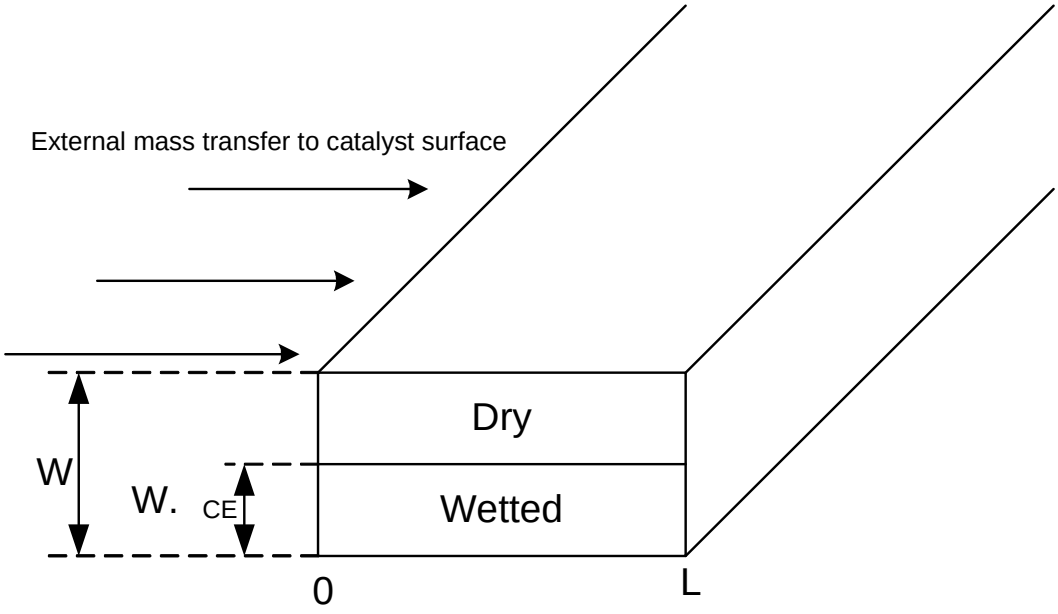

Figure 2.3: Geometry used by Ramachandran & Smith (1979) to derive an expression for η_{TB} as a function of η_{CE} for a gas-limited reaction

dry surface fractions with above equations:

$$\eta_{TB,w} = \frac{1}{\phi}.\frac{\tanh\phi}{1+\frac{\phi}{Sh_{gLS,A}}\tanh\phi} \tag{2.24}$$

$$\eta_{TB,d} = \frac{1}{\phi}.\frac{\tanh\phi}{1+\frac{\phi}{Sh_{gS,A}}\tanh\phi} \tag{2.25}$$

$$\tag{2.26}$$

These two efficiencies are weighted according to the external wetting efficiency, to get a total TBR-efficiency of:

$$\eta_{TB} = \eta_{CE}\eta_{TB,w} + (1-\eta_{CE})\eta_{TB,d} = \frac{\eta_{CE}}{\phi}.\frac{\tanh\phi}{1+\frac{\phi}{Sh_{gLS,A}}\tanh\phi} + \frac{1-\eta_{CE}}{\phi}.\frac{\tanh\phi}{1+\frac{\phi}{Sh_{gS,A}}\tanh\phi} \tag{2.27}$$

Similar models were developed by Herskowitz et al. (1979) and Tan & Smith (1980).

The main shortcoming of this model is that it cannot account for the fact that at a contacting efficiency of $\eta_{CE} = 0$, the overall reaction rate in a TBR should be equal to zero if the liquid-side reagent is non-volatile, even although the reaction is gas-limited. This is simply because the gas-side *and* the liquid-side reagent should be present on the catalyst surface for reaction to take place, and a non-volatile reagent cannot be supplied to a completely dry particle. Therefore, although a reaction may be gas-limited according to equation 2.19, the liquid side reagent should begin to play a role in the reaction rate at some low value of η_{CE}. This was observed by Ruiz et al. (1984) who found reaction rates in a trickle-bed reactor that were order 0.3 with respect to the liquid-phase reagent,

whereas for the same reaction, catalyst and feed concentrations, the reaction was zeroth order with respect to the liquid-side reagent in a slurry reactor (where all particles are completely wetted). Moreover, it was found that in order to fit gas-limited trickle-bed reaction data with a model similar to equation 2.27, unrealistic low gas-solid mass transfer coefficients had to be used(Mills & Dudukovic, 1984).

Beaudry et al. (1987) developed a model to explain these observations as follows: Liquid can only be supplied from the wetted fraction of the catalyst. Therefore the diffusional pathlength of the liquid-phase reagent is much higher than that for the gas (which can be supplied from the gas and the liquid phase) and liquid can become depleted in the pores at positions close to the dry external surface. This can lead to observed non-zero reaction orders with respect to the liquid phase. Also, if liquid is depleted in the pores closer to the dry surface, the gas-side reagent has to diffuse deeper into the pores before encountering liquid with which it can react, so that the apparent external gas-solid mass transfer coefficient is higher than the actual one. This phenomenon is only observed for gas-limited reactions: It is highly unlikely that gas-depletion in the pores can be encountered in liquid-limited reactions, since the gas-phase reagent can enter the catalyst particles from both wetted and non-wetted surfaces.

From above considerations, an expression to predict the fraction of internal area on which no reaction will take place due to depletion of liquid reagent pores was developed, using slab geometry for the reaction $A + bB \rightarrow$ products. The slab was viewed to be wetted only on one side and its pores to be filled completely with liquid (note that this corresponds *only* to $\eta_{CE} = 0.5$ and $\eta_i = 1$, see partially wetted slabs in figure 2.4):

$$\omega = \frac{2 + \frac{1}{Bi_{LS,B}} + \frac{1}{Bi_{gs,A}}}{\frac{D_{eff,B}C_{B,b}}{D_{eff,A}bC_A^*} + 1 - \frac{1/\phi_A + 1/Bi_{LS,B}}{1/\phi_A + 1/Bi_{LS,A}}} - \frac{1}{\phi_A} - \frac{1}{Bi_{gS}} \tag{2.28}$$

According to these authors this will lead to a partially wetted catalyst efficiency of:

$$\eta_{1/2} = \frac{1}{2\phi_A^2}\left(\frac{1}{\frac{1}{\phi_A} + \frac{1}{Bi_{Ls,A}}} + \frac{1}{\omega + \frac{1}{\phi_A} + \frac{1}{Bi_{gs,A}}}\right) \tag{2.29}$$

Where the Thiele modulus, ϕ_A is the Thiele modulus for a completely (internally) wetted pellet. By postulating that the bed consists of a fraction completely wetted pellets (or slabs, in their model), a fraction completely dry pellets and a fraction half-wetted pellets, they arrived at an overall bed effectiveness factor of:

$$\eta_{TB} = (1 - \eta_{CE})^2\eta_d + 2\eta_{CE}(1 - \eta_{CE})\eta_{1/2} + \eta_{CE}^2\eta \tag{2.30}$$

which is the sum of the different fractions times their effectiveness. Dry, half-wetted and completely wet fractions were calculated as follows:

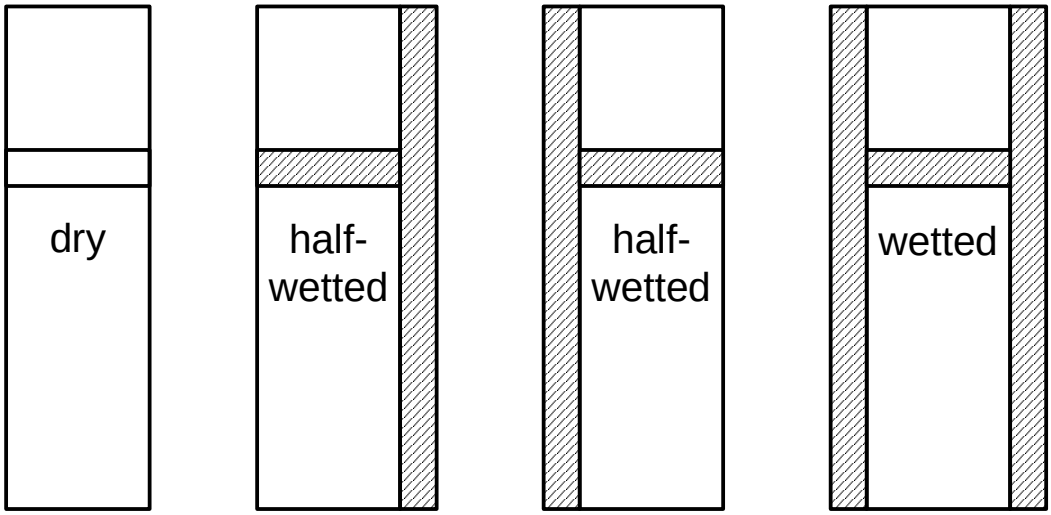

Figure 2.4: Geometry used by Beaudry et al. (1987) and proposed wetting distribution for $\eta_{CE} = 0.5$

- Take the probability that one side of the slab is wetted equal to $P = \eta_{CE}$.
- For a completely wetted pellet, both sides of the "slab" should be wetted, so that the fraction (probability) of a completely wetted pellet is: $P_w = \eta_{CE}^2$.
- A half wetted pellet, is defined to have one side of the "slab" wetted and one side dry. Both can be on either side of the slab, so that the probability for a half-wetted pellet is: $P_{1/2} = 2\eta_{CE}(1 - \eta_{CE})$.
- Likewise, the probability for a completely dry pellet is $P_d = (1 - \eta_{CE})^2$.

An illustration of the weighting by Beaudry et al. (1987) is shown in figure 2.4.

For a non-volatile liquid reagent, the dry particle effectiveness factor can be taken as zero since no liquid reagent can be supplied to a completely dry catalyst. The completely wetted particle efficiency η_w can be calculated with the Thiele modulus for a completely wetted pellet in which reagent A diffuses:

$$\eta_w = \frac{\tanh \phi_A}{\phi_A} \tag{2.31}$$

In this model, equation 2.30 accommodates for the fact that the reaction rate in a completely dry particle is zero for non-volatile liquid reagents, and equation 2.29 explains the observed high gas-solid mass transfer coefficients discussed previously. Wu et al. (1996) tested equation 2.30 for liquid-limited reactions and found good results. The effectiveness factor of a half-wetted particle was calculated with equation 2.13.

The effect of stagnant liquid zones in a gas-limited system is similar to that in a liquid-limited system. The areas covered by stagnant liquid is highly ineffective as compared to

dry areas and can practically be viewed as unavailable for external mass transfer (Llano et al., 1997).

Volatile reagents

In some trickle-bed operations volatile reagents are used, that is, both reagents are present in both phases, so that reaction can take place on dry and wetted catalyst sites. The most important differences between trickle-bed operations where volatile reagents are used and where the liquid is non-volatile are (Khadilkar et al., 1999).

- Vapour-liquid equilibrium needs to be taken into account for both reagents.
- Complete internal wetting can not be assumed.
- Holdup variations can be present due to evaporation of the liquid.
- Reaction can occur on completely dry catalyst particles. This can lead to hot spots, since reaction heat can not be removed effectively (Sedriks & Kenney, 1972).
- Not only reaction heat, but also latent heat of evaporation needs to be taken into account.

Sedriks & Kenney (1972) used partial internal wetting to model a volatile reaction in a trickle-bed reactor.

$$R'_{TB} = \eta_i R'_L + (1 - \eta_i) R'_G \tag{2.32}$$

Where R'_L and R'_G are reaction rates determined for the liquid phase and gas phase in completely wetted and completely dry catalyst particles, respectively. External mass transfer limitations were insignificant and internal mass transfer are included in R'_L and R'_G as determined for completely dry and completely wetted pellets. Llano et al. (1997); Kheshgi et al. (1992) used the same model, but with the external wetting efficiency η_{CE} replacing η_i. Khadilkar et al. (1999) modeled the effect of fractional internal wetting on reaction rate for half-wetted slabs. Since for a half-wetted slab η_{CE} can only be equal to 0.5, the external wetting efficiency does not feature in the model.

Mills & Dudukovic (1980) developed a trickle-bed efficiency model for volatile reagents, taking into account external mass transfer. If the gas and liquid phases are in equilibrium liquid-solid and gas-solid mass transfer for both components is described similar to what is discussed earlier on in the report, but if it is not, two extra possible mass transfer routes should be taken into account: If the concentration of B in the vapour phase is higher than its equilibrium concentration in the liquid, $B(g)$ will be transferred from vapour phase through the liquid phase to the wetted catalyst surface, and directly from the vapour phase to the dry catalyst surface. Likewise, if the concentration of B in the liquid phase is higher than the equilibrium concentration of $B(g)$ in the liquid

phase, $B(\ell)$ will be transferred from liquid phase through the vapour phase to the dry catalyst surface, and directly from the liquid phase to the wetted catalyst surface. This also applies for volatile reagent A. The trickle-bed efficiency can therefore be a strong function of the feed conditions when the reagents are both volatile.

2.3.2 Measurement Methods

When Mears (1974) linked reactor performance to wetting efficiency, he made use of the correlation of Puranik & Vogelpohl (1974) to predict the wetting efficiency in trickle-beds. This correlation has been developed from packed absorption column experiments. Flow in packed absorption columns was believed to be very similar to that in TBR's, since they are also packed with solid particles, which is used to provide good gas-liquid contacting.

Puranik & Vogelpohl (1974) showed the considerable scatter in literature concerning contacting efficiency in packed columns. This would be because of the different systems that were studied. Four groups of operations in packed column were identified:

- Only physical absorption of a gaseous species into a liquid solvent. In such operations, stagnant liquid pockets will become saturated in a very short time and hence ineffective for mass transfer. Therefore

$$a_{ab} = a_d \tag{2.33}$$

- Absorption accompanied by chemical reaction of the absorbed gas with a non-volatile species. If such a reaction is fast, there will be a constant driving force for mass transfer between the stagnant liquid and the gas and the active area becomes

$$a_c = a_d + a_{st} \tag{2.34}$$

  If chemical reaction is slow, the effective area would become equal to a_d.

- Liquid interfacial area as measured with colorometrics (Krauze & Scrwinski, 1971; Onda et al., 1967), will most likely include the static wetted area if the packing is exposed to the dye for long enough.

$$a_w = a_d + a_{st} \tag{2.35}$$

- Vapourisation of a liquid component into the gas. Since the gas is constantly flowing, this will also be the total gas-liquid (or liquid-solid) area:

$$a_v = a_d + a_{st} \tag{2.36}$$

Note that most of the processes described above involve gas-liquid interfacial area, and not liquid-solid interfacial area. It seems to be common practice to assume that these two are more or less the same (Pathwardan, 1978; Morita & Smith, 1978), which is definitely not true for all the different flow types (see section 2.2.1).

More than 60 sets of data from different authors were categorized into these groups, and correlations in terms of dimensionless groups were developed in order to predict a_w, a_{st} and a_d. The scatter in literature data was reduced considerably.

Soon after Mears (1974) used the correlations of Puranik & Vogelpohl (1974), the applicability of these correlations on trickle-bed reactors was questioned, mainly because absorption columns make use of solid packing materials whereas porous catalyst is used in TBR's, and various other methods to determine solid-liquid contacting in TBR's were explored.

R.T.D. Tracer Methods

One of the most powerful tools in the study of liquid flow in reactors, is the R.T.D.-tracer method, where the outlet time distribution of a tracer concentration is used to infer properties of a flow system if the inlet time distribution of the tracer concentration is known. Ever since Danckwerts (1953) started with tracer technology, it led to an explosion of research and modeling in this field (Levenspiel, 2002), and it was not long before it made its entry in the study of liquid flow in trickle-bed reactors. Lapidus (1957) was the first to use tracer technology in trickle-bed reactor research, in order to measure liquid holdup, using the following model:

$$\bar{\tau} = \frac{\epsilon_L V_b}{Q_L} \tag{2.37}$$

Schwartz et al. (1976) developed a tracer model method to measure *total* solid-liquid contacting, by means of an adsorbing and a non-adsorbing tracer whos residence time distributions were measured on the same flow system. An adsorbing tracer that adsorbs reversibly onto the solid area was selected, so that it will desorb again after some time, and the average residence time is higher than that for the non-adsorbing tracer. The difference in average residence times of the two tracer is then an indication of the total area on which absorption took place, which is the total effectively wetted area. For the adsorbing tracer,

$$\bar{\tau}_{ads} = \frac{\epsilon_L V_b}{Q_L} + \text{average time spent adsorbed onto solid surface} \tag{2.38}$$

For the non-adsorbing tracer,

$$\bar{\tau}_{non-ads} = \frac{\epsilon_L V_b}{Q_L} \tag{2.39}$$

It was assumed that the time spent on the solid surface is directly related to the amount of solid area in contact with the liquid, so that equation 2.38 can be written as:

$$\bar{\tau}_{ads} = \frac{\epsilon_L V_b}{Q_L} + \frac{A_w K_a}{Q_L} \tag{2.40}$$

Where A_w is the total solid area in contact with the liquid. To determine K_a, experiments on a liquid-filled bed were performed:

$$\tau_{lf,non-ads} = \frac{\epsilon V}{Q_L} \tag{2.41}$$

$$\tau_{lf,ads} = \frac{\epsilon V}{Q_L} + \frac{A_t K_a}{Q_L} \tag{2.42}$$

Where A_t is the total solid area. The fractional wetting of solid area in the trickle-bed reactor can then be calculated as:

$$\eta_c = \frac{A_w}{A_t} = \frac{\tau_{ads} - \tau_{non-ads}}{\tau_{lf,ads} - \tau_{lf,non-ads}} \tag{2.43}$$

The fraction of total catalyst area contacted by liquid, η_c, was found to be about 0.65, independent of liquid flow rate. This is not in agreement with the data of Satterfield (1975), who found trickle-bed efficiency to be a function of the liquid flowrate. This was later explained by Mills & Dudukovic (1989) who said that the pores of all catalyst particles in contact with the liquid were completely filled with liquid, so that the measured parameter is actually 1 minus the fraction of the bed that is completely dry. Although the fractional contacting on each particle, η_{CE}, might change with flow due to enlarged rivulets, the fraction of the bed that is completely dry seems to be more a function of inlet distribution than of flow. In the view of the discussion in section 2.2, it is more likely that is fraction is a function of pre-wetting rather than inlet distribution.

Colombo et al. (1976) suggested that solid-liquid contacting efficiency is a particle-scale phenomenon that consists of two types of wetting:

- Fractional pore filling, F_i. These authors were first to suggest that this is probably equal to one, due to capillarity.
- Particle-scale external effective wetting, η_{CE}. It was suggested that this type of wetting is the major parameter influencing trickle-bed reactor performance.

These authors suggested that dry parts on a particle will result in an increased effective pore depth, and therefore in a decreased effective diffusivity of molecules in the pores. This is illustrated in figure 2.5. The apparent effective diffusivity of a reagent in partially wetted particles versus that in completely wetted particles would then be somehow related

to the fraction external wetting of the partially wetted particle. These authors suggested:

$$\eta_{CE,n} = \frac{D_{eff,pw}}{D_{eff,cw}} \tag{2.44}$$

for a partially wetted particle, and for the whole bed:

$$\eta_{CE} = \frac{D_{eff,TB}}{D_{eff,lf}} \quad \text{at the same } u_l \tag{2.45}$$

so that the only challenge left is to determine effective diffusivities for trickle- and liquid filled beds. It was reasoned that if a system has internal mass transfer limitations, the diffusion of molecules into and out of catalyst pores will take a significant time, so that diffusivity can be determined from R.T.D. curves. The following R.T.D. model has been proposed:

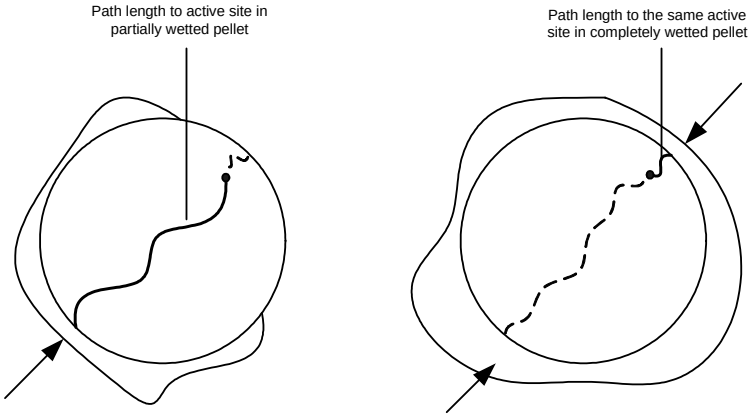

Figure 2.5: Effect of partial external wetting on apparent effective diffusivity, as proposed by Colombo et al. (1976)

Mass balance of tracer in bulk fluid over differential reactor length Δz:

Accumulation of tracer in bulk liquid = Rate in due to dispersion + rate in due to flow
− (Rate out due to dispersion + rate out due to flow)
− Rate of diffusion into or out of catalyst pores

$$\begin{aligned} \epsilon_L A_c \frac{\mathrm{d}C}{\mathrm{d}t}.\Delta z = & - D_A A_c \frac{\mathrm{d}C}{\mathrm{d}z}\bigg|_z + A_c v_{SL} C|_z - \left(-D_A A_c \frac{\mathrm{d}C}{\mathrm{d}z}\bigg|_{z+\Delta z} + A_c v_{SL} C|_{z+\Delta z} \right) \\ & - a.\Delta z A_c D_{eff} \frac{\mathrm{d}C_i}{\mathrm{d}r}\bigg|_{r=r_p} \\ \div \Delta z; \lim \Delta z \to 0: \quad \epsilon_L A_c \frac{\mathrm{d}C}{\mathrm{d}t} = & \; D_A \frac{\mathrm{d}^2 C}{\mathrm{d}z^2} - v_{SL} \frac{\mathrm{d}C}{\mathrm{d}z} - a D_{eff} \frac{\mathrm{d}C_i}{\mathrm{d}r}\bigg|_{r=r_p} \end{aligned} \tag{2.46}$$

$$\begin{aligned}
\text{Where: } a &= \frac{3(1-\epsilon)}{r_p} \\
\text{Let: } \xi &= \frac{r}{r_p} \\
\theta &= \frac{tu}{Z}; \quad u = \frac{v_{SL}}{\epsilon_L} \\
Pe &= \frac{Z v_{SL}}{D_A} \\
x &= \frac{z}{Z}
\end{aligned} \tag{2.47}$$

$$\text{then: } \frac{\mathrm{d}C}{\mathrm{d}\theta} = \frac{1}{Pe}\frac{\mathrm{d}^2C}{\mathrm{d}x^2} - \frac{\mathrm{d}C}{\mathrm{d}x} - \frac{3(1-\epsilon)D_{eff}}{u\epsilon_L r_p^2}\left.\frac{\mathrm{d}C_i}{\mathrm{d}\xi}\right|_{\xi=1} \tag{2.48}$$

If total pore filling and symmetry is assumed (view as if the particle is completely wetted), the mass balance over the particle is:

$$\begin{aligned}
\text{Rate of accumulation in particle} = &\quad \text{Rate of diffusion into or out of pores} \\
&- \text{Rate of adsorption}
\end{aligned}$$

$$\begin{aligned}
\epsilon_p.4\pi r^2\Delta r\frac{\mathrm{d}C_i}{\mathrm{d}t} &= D_{eff}4\pi\left(r^2\left.\frac{\mathrm{d}C_i}{\mathrm{d}r}\right|_r + r^2\left.\frac{\mathrm{d}C_i}{\mathrm{d}r}\right|_{r+\Delta r}\right) \\
&- 4\pi r^2\Delta r\rho_s(1-\epsilon_p)\frac{\mathrm{d}C_{ad}}{\mathrm{d}t} \\
\div\Delta r; \lim\Delta r\to 0: \quad \epsilon_p r^2\frac{\mathrm{d}C_i}{\mathrm{d}t} &= D_{eff}\frac{\mathrm{d}}{\mathrm{d}r}\left(r^2\frac{\mathrm{d}C_i}{\mathrm{d}r}\right) - r^2\rho_s(1-\epsilon_p)\frac{\mathrm{d}C_{ad}}{\mathrm{d}t} \\
\therefore D_{eff}\frac{\mathrm{d}^2C_i}{\mathrm{d}r^2} &+ \frac{2}{r}\frac{\mathrm{d}C_i}{\mathrm{d}r} - \epsilon_p\frac{\mathrm{d}C_i}{\mathrm{d}t} - \rho_s(1-\epsilon_p)\frac{\mathrm{d}C_{ad}}{\mathrm{d}t} = 0 \\
\therefore \frac{\mathrm{d}^2C_i}{\mathrm{d}\xi^2} + \frac{2}{\xi}\frac{\mathrm{d}C_i}{\mathrm{d}\xi} &- \frac{r_p^2u_l\epsilon_p}{D_{eff}Z}\left(\frac{\mathrm{d}C_i}{\mathrm{d}\theta} + \rho_s\frac{(1-\epsilon_p)}{\epsilon_p}\frac{\mathrm{d}C_{ad}}{\mathrm{d}\theta}\right) = 0
\end{aligned} \tag{2.49}$$

If adsorption goes to equilibrium fast enough for the kinetics to be neglected, C_{ad} can be written as:

$$C_{ad} = k_{ad}C_i \tag{2.50}$$

The contacting efficiency as defined in equation 2.45 agreed reasonably with the data of Satterfield (1975), who defined solid liquid contacting efficiency as the ratio of the liquid-limited reaction rate constant in a TBR to that in a liquid-filled reactor.

After Dudukovic (1977) suggested that the Thiele modulus for a partially externally wetted pellet with completely filled pores is given by:

$$\phi_{TB} = \frac{V_p}{\eta_{CE} S_{ext}} \sqrt{\frac{k}{D_{eff}}} \tag{2.51}$$

Sicardi et al. (1980) derived an expression for η_{CE} in terms of effective diffusivities:

$$\phi_{TB} = \frac{V_p}{\eta_{CE} S_{ext}} \sqrt{\frac{k}{D_{eff}}} = \frac{V_p}{S_{ext}} \sqrt{\frac{k}{D_{eff,TB}}} \tag{2.52}$$

Therefore

$$\eta_{CE} = \sqrt{\frac{D_{eff,TB}}{D_{eff,LF}}} \quad \text{at the same } u_l \tag{2.53}$$

Mills & Dudukovic (1981) repeated the work of Colombo et al. (1976) to determine η_{CE} and of Schwartz et al. (1976) to determine η_c (which is about the same as η_i). It was found that equation 2.53 brings tracer-determined wetting efficiency data closer to the data from reaction experiments than when equation 2.45 is used. Complete pore fill-up ($\eta_i = 1$) was also found independent of flow rate, so that this assumption of Colombo et al. (1976) seems to hold true. A rigorous fundamental proof of equation 2.53 however still seem to be elusive.

A more rigorous model for intraparticular diffusion was developed by Ramachandran et al. (1986). These authors took into account fractional external wetting and different boundary conditions (wetted and dry) to model intraparticular diffusion thereby disposing of the term $D_{eff,TB}$ used in the model of Colombo et al. (1976). It is assumed that the wetting on each particle is in the form of a spherical cap (see figure 2.6. The wetted fraction is defined by:

$$\begin{aligned} \text{Wetted:} \quad & 0 \leq \phi \leq \alpha \\ \text{Non-wetted:} \quad & \alpha \leq \phi \leq \pi \end{aligned} \tag{2.54}$$

Wetted cap geometry is assumed in order to dispose of one of the angular coordinates in the spherical coordinate system and the diffusion equation becomes:

$$\epsilon_p = D_{eff} \left[\frac{1}{r^2} \frac{\mathrm{d}}{\mathrm{d}r} \left(r^2 \frac{\mathrm{d}C_i}{\mathrm{d}r} \right) + \frac{1}{r^2 \sin\phi} \frac{\mathrm{d}}{\mathrm{d}\phi} \left(\sin\phi \frac{\mathrm{d}C_i}{\mathrm{d}\phi} \right) \right] \tag{2.55}$$

With boundary conditions:

$$\begin{array}{ll} \lim r \rightarrow 0 \left(r^2 \frac{\mathrm{d}C_i}{\mathrm{d}r}\right) = 0 & : \\ \phi = 0, \pi \frac{\mathrm{d}C_i}{\mathrm{d}\phi} = 0 & \text{Symmetry and geometry of sphere} \end{array} \tag{2.56}$$

$$r = R \begin{cases} -D_{eff} \frac{\mathrm{d}C_i}{\mathrm{d}r} = k_s \left(C_i - C_b\right) & , 0 < \phi \leq \alpha \quad \text{Mass transfer over boundary} \\ \frac{\mathrm{d}C_i}{\mathrm{d}r} = 0 & , \alpha < \phi \leq \pi \quad \text{No mass transfer over boundary} \end{cases} \tag{2.57}$$

The variable α is fitted on the R.T.D.-response data and the wetted fraction related to α by:

$$\eta_{CE} = \frac{1 - \cos \alpha}{2} \tag{2.58}$$

The advantage of this model is that no separate liquid-filled runs for all different liquid velocities need to be performed. Reasonable agreement with results from Colombo's model was found, but it was stated that at lower particle wetting efficiencies, the two models will differ significantly. These authors pointed out that equation 2.53 is not per definition true and that the power to which the ratio of diffusivities should be raised will vary depending on the shape and magnitude of the wetted fraction.

Equation 2.53 does however still seem to be generally accepted for calculation of wetting efficiency from tracer response data (Kundu et al., 2003; Nigam et al., 2001; Iliuta et al., 1999).

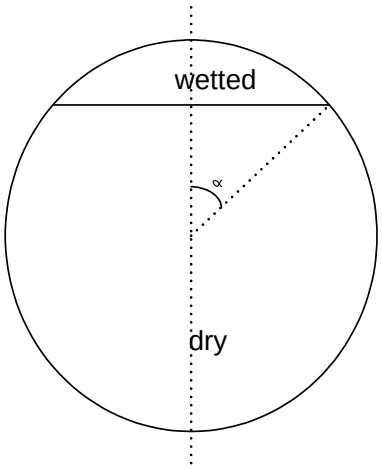

Figure 2.6: Particle-scale R.T.D.-model of Ramachandran et al. (1986)

Tsamatsoulis & Papayannakos (1996) studied the validity of equation 2.53 theoretically for different shapes of wetting on cylinders and found that this equation works well independent of shape, for external fractional wetting higher than 0.6. Since η_{CE} is usually greater than 0.6 in trickle-bed reactors, it was concluded that the effect of wetting shape on trickle-bed efficiency and tracer determined wetting efficiency is insignificant. On the other hand, all particles in a trickle-bed reactor do not have the same fractional wetting, and it is very likely that there is a certain fraction of particles that at a low

enough wetting for shape to begin to play a role (about 0.5, according to the results of these authors).

Stagnant zones

Some literature attempt to quantify the effect of static wetted areas on R.T.D response curves, since these areas would have a different effect in an unsteady state tracer system than in a steady state reaction system (see section 2.3.1): In tracer experiments, stagnant liquid zones will influence the degree of mixing of the tracer, since at unsteady state (such as a pulse), tracer exchange will take place between stagnant and moving liquid zones. In steady state reactive systems, stagnant zones become saturated and are approximately "dead" zones, having very low chemical activities (Sicardi et al., 1980). To further investigate the role of stagnant wetted areas in tracer experiments, Sicardi et al. (1980) defined three types of external contacting efficiencies: External solid-liquid contacting efficiency as obtained by tracer experiments, $\sqrt{\frac{D_{eff,TB}}{D_{eff,LF}}}$, chemically active solid-liquid contacting efficiency and stagnant contacting efficiency. These three were plotted as a function liquid flowrate on the same graph, shown in figure 2.7. Chemically active area fractions were most likely obtained from a reactive method. Static areas were estimated by means of equation 2.18.

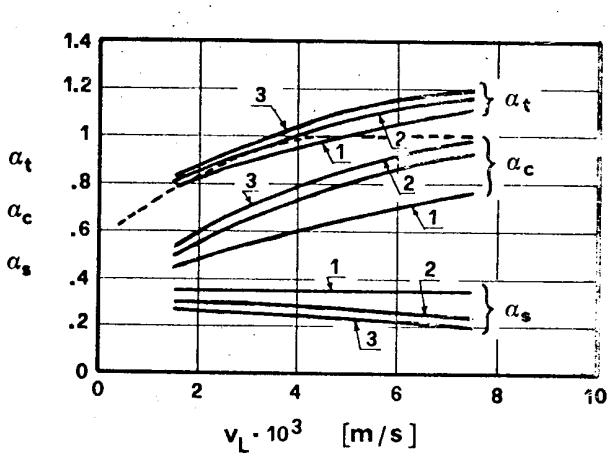

Figure 2.7: R.T.D.-evaluated, chemically active (denoted α_c), static (α_s) and total wetted area fractions ($\alpha_t = \alpha_c + \alpha_s$) as functions of liquid flowrate. 1: $v_G = 0$, 2: $v_G = 0.32$ m/s, 3: $v_G = 0.61$ m/s. The R.T.D evaluated contacting efficiency is shown by the dashed line. From Sicardi et al. (1980)

It can be seen from the figure that tracer experiments measure not only the chemically active solid-liquid interface, but also a *part* of the stagnant wetted fraction. If one wants to decouple these two parameters in tracer experiments, stagnant and dynamic liquid zones should be modeled apart. Nigam et al. (2001) fitted tracer data onto a model considering dispersion, exchange between static and dynamic liquid holdup, internal and

external mass transfer rates, and solid-liquid contacting efficiency. This model is called the piston dispersion exchange (P.D.E.) model. Since this model contains a large number of parameters, very good fits could be obtained, but the values of these parameters were extremely scattered and did not show a very clear trend with liquid and gas flow rates.

Reaction Method

Another popular method used to determine wetting efficiency in trickle-bed reactors is the reaction method, where the wetting efficiency is inferred from reactor conversion data, by means of reactor models as discussed in section 2.3.1. This method has several advantages above the tracer method (Herskowitz & Smith, 1983):

- This method is more direct. In tracer studies, wetting efficiency is determined by some model, which should then be used in a different reactor model for prediction of reactor performance. With the reactive method, the same model that is used to predict reactor performance can be used to measure wetting efficiency, which make this a more reliable method.

- Completely dry regions in the bed can more readily be detected, by means of reaction on catalyst particles with a very low Thiele modulus. All particles in such a reactor with some degree of wetting will have an efficiency of 1, whereas completely dry particles will have an efficiency of zero.

- The tracer-determined actively wetted area might be different from the chemically active wetted area, due to stagnant zones. The reactive method directly measures the chemically active area fraction.

Sedriks & Kenney (1972) made use of reaction experiments to determine bed scale wetting efficiency, by means of equation 2.32. They found incomplete *bed-scale* wetting, but this is not surprising, since the only way in which they explained the difference between the observed trickle-bed reaction rate and the intrinsic kinetics was in terms of bed-scale incomplete wetting.

Satterfield (1975) took reaction data from various authors who found an increase in reactor performance with flow. He reasoned that this increase of reactor performance with liquid flowrate is a proof of some kind of solid-liquid contacting efficiency, for example that defined by Mears (1974), since if there was no such an effect, reactor conversion would go down with liquid flowrate (see equation 2.5). He plotted $\frac{k_{TB}}{k}$ versus liquid flowrate as a preliminary estimate of external solid-liquid contacting efficiency, which is equal to η_{CE} for high Thiele moduli.

Morita & Smith (1978) studied wetting efficiency in a trickle-bed reactor with a gas-limited reaction, and a reactor model that takes into account external and internal mass

transfer limitations, and the effect wetting has on these. The following relationship between catalyst efficiency and wetting efficiency was assumed:

$$R' = \eta_{CE} k \eta C_{A,s} + (1 - \eta_{CE})\, k \eta C_A^* \tag{2.59}$$

Using two sets of data obtained from catalyst particles with different activities at the same flow conditions, η_{CE} at each condition could be determined without the need of any knowledge of the external gas-liquid and liquid-solid mass transfer coefficients. Equation 2.59 seems to be widely accepted for the calculation of wetting efficiency from reactor conversion data for a gas-limited system (Leung et al., 1987; Ramachandran & Smith, 1979; Mata & Smith, 1981).

The problem with equation 2.59 is that it does not take into account the effect asymmetrical boundaries. To evaluate this, Herskowitz et al. (1979) estimated trickle-bed efficiencies for a gas-limited reaction for particles at $f = n/6$ (where $n = 1..5$), making use of cube-shaped geometry. Tan & Smith (1980) found that an additive procedure such as equation 2.59 gives good agreement with the values obtained by Herskowitz et al. (1979) when separate effectiveness factors for an external completely dry and an external completely wetted particle are used:

$$R = \left[\eta_{CE}.\eta_w k + (1 - \eta_{CE})\,.\eta_d k\right] C_A^* \tag{2.60}$$

The effectiveness factors η_w and η_d are functions of the respective external mass transfer coefficients and the particle Thiele modulus, similar to the model derived by Ramachandran & Smith (1979), discussed in section 2.3.1. Llano et al. (1997) made use of equation 2.60. The effectiveness factor η_d was measured for a internally wetted particle in the presence of only vapour phase reagents as recommended by Tan & Smith (1980). A very similar shape of the tendency of η_{CE} with liquid flow-rate as obtained from most tracer experiments was found, but the exact values were significantly smaller. This was explained in terms of stagnant liquid, which are approximately dead zones, but does influence the residence time distribution of a tracer. They suggested that the relationship between chemically- and tracer-determined external contacting efficiency is given by:

$$\eta_{CE,tracer} = \eta_{CE,reaction}(1 - \eta_{CE,st}) + \eta_{CE,st} \tag{2.61}$$

The experimental results were accordingly compared with values of η_{CE} predicted by several correlations which were based on tracer-determined values for η_{CE}. Examples of these are the correlations of Ring & Missen (1991) and Al-Dahhan & Dudukovic (1995). Assuming that static wetted fraction does not change with liquid flow-rate, a best fit of $\eta_{CE,st} = 0.16$ was obtained.

Wu et al. (1996) evaluated reactor models for liquid-limited reactions, making use of the liquid phase decomposition of hydrogen peroxide over different types of catalyst. It was found that the model of Dudukovic (1977) (equation 2.13) is in close agreement with the obtained results. Wetting efficiency was approximated by the correlation of Al-Dahhan & Dudukovic (1995) and not determined from the experimental results. Khadilkar et al. (1996) found that the model of Beaudry et al. (1987) and El-Hisnawi et al. (1982) predict trickle-bed performance adequately for both liquid-limited and gas-limited reactions.

External mass transfer coefficients

Lakota & Levec (1990) measured external solid-liquid contacting efficiency by means of measuring external solid-liquid mass transfer coefficients. The wetting efficiency will then be ratio of external liquid-solid mass transfer coefficients of a trickle- and liquid-filled bed.

$$\eta_{CE} = \frac{(k_s a)_{TB}}{(k_s a)_{lf}} \quad \text{at the same } u_l \tag{2.62}$$

They studied a trickle-flow system where naphtalene pellets were partially dissolved in water trickling over them. Air was used as inert gas-phase fluid. This approach has as advantages that it is very simple, and that external mass transfer rates are more directly related to external mass transfer than to pellet efficiency. The only drawbacks are that (once again) trickle- and liquid-filled beds has to be compared and that dissolution of the naphtalene particles may have caused change in bed properties over time. The authors reasoned that the latter could be ignored, since the dissolution was a very slow process.

Wetting efficiency was also determined from external mass transfer measurements by Specchia et al. (1978), reported as the ratio between the measured external mass transfer area and the geometrical external area of the packing. It is not stated how the external mass transfer area was decoupled from the external mass transfer coefficient in the measured term $k_s a_s$.

Pressure drop

Pironti et al. (1999) reasoned that the tracer and chemical methods that are available for the determination of η_{CE} usually requires time-consuming experiments, and makes use of models with all kinds of assumptions. The more direct method of Lakota & Levec (1990) of taking the ratio of external mass transfer coefficients makes use of less assumptions, but the experimentation is rather time-consuming and complex (dissolution of bed packing, when is steady state reached?). They proposed a similar method but instead of external mass transfer coefficients, solid liquid shear stresses, which is also a linear function with

solid-liquid contacting area, are used to approximate wetting efficiency:

$$\eta_{CE} = \frac{(\tau_{ls}a_{ls})_{TB}}{(\tau_{ls}a_{ls})_{lf}} \quad \text{at the same } u_l \tag{2.63}$$

This can be written in terms of more measurable parameters by means of force balances over the bed:

- Force balance over liquid-filled bed:

$$(\tau_{ls}a_{ls})_{ls} = \frac{\Delta P_{lf}\epsilon}{Z} + \epsilon\rho_L g \tag{2.64}$$

- Force balance for the liquid in a two-phase bed:

$$(\tau_{ls}a_{ls})_{TB} = (\tau_{lg}a_{lg})_{TB} + \frac{\Delta P_{TB}\epsilon_L}{Z} + \epsilon_L\rho_L g \tag{2.65}$$

- Force balance for the gas in a two-phase bed:

$$(\tau_{lg}a_{lg})_{TB} + (\tau_{ls}a_{ls})_{TB} = \frac{(\epsilon - \epsilon_L)\,\Delta P_{TB}}{Z} + (\epsilon - \epsilon_L)\,\rho_G g \tag{2.66}$$

- Adding equations 2.65 and 2.66 gives:

$$2(\tau_{ls}a_{ls})_{TB} = \frac{\epsilon\Delta P_{TB}}{Z} + (\epsilon - \epsilon_L)\rho_G g + \epsilon_L\rho_L g \tag{2.67}$$

Therefore only pressure drop, liquid holdup and bed porosity have to be measured in order to "measure" η_{CE}, which are all easily measured parameters. For the liquid-filled bed, Ergun's equation can be used to predict pressure drop, so that separate liquid-filled runs at all the different liquid velocities are not needed. The model makes use of the following assumptions:

- Liquid holdup, porosity and liquid velocity do not vary along the axial coordinate.
- Liquid flow is laminar.

The major limitation of this model is that it is one-dimensional and cannot provide for flow morphology, although it is based on a flow model.

Tomography

All measurement methods described thus far, are model based, can not provide for liquid flow morphology and make use of data obtained from liquid-filled beds in which flow differ completely from flow in trickle-beds. A more direct approach is to directly observe the flow as it is and then try to capture meaningful data from it.

The taking of images through sections of a bed during liquid flow is called tomography. Several means of generating these images are proposed in literature, usually making use of some signal that is affected by the bed packing and flowing liquid when transmitted through the bed. Tomography methods were originally developed for medical research, but found their applications in various industrial research fields.

Of importance in these techniques is the resolution of images that are created, and the time required to generate such an image. Long image acquisition times can blur the obtained image, if liquid flow changes over time.

Sederman & Gladden (2001) made use of magnetic resonance imaging (MRI), to measure liquid holdup, wetting efficiency and the number of rivulets in the bed trickle-bed reactors at different gas and liquid flow rates. As additional data they measured wetting efficiency for separate particles, and reported the wetting distribution of the particles in the bed. This is shown in figure 2.8.

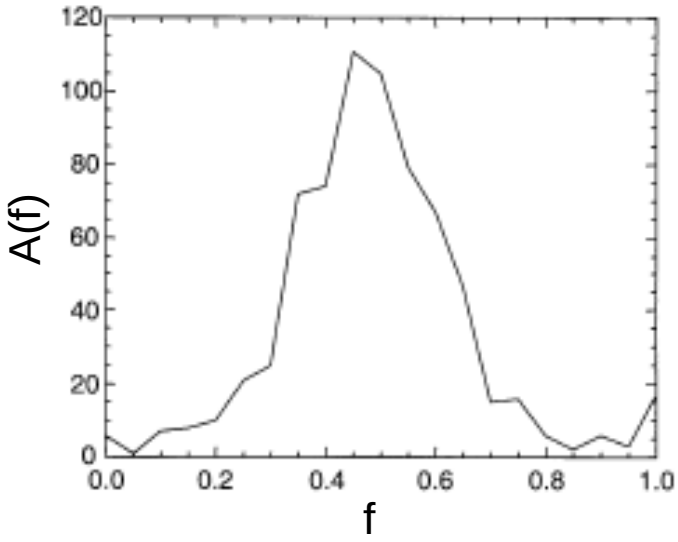

Figure 2.8: Distribution of surface wetting of particles in a trickle-bed reactor, as determined with MRI (Sederman & Gladden, 2001). $v_{SL} = 0.003m/s$ and $v_{SG} = 0.066m/s$

Even although image acquisition took as long as 3 minutes, the authors obtained sharp images, which suggests that the liquid flow was stable when at steady state.

Colorometrics

Colorometric methods for the determination of wetting efficiency makes use of doping the liquid stream with a colourant, so that particles that were contacted can be visually evaluated, and wetted fractions can be physically quantified using visual observations. This technique was first used in the study of trickle flow by Onda et al. (1967) and later by Krauze & Scrwinski (1971), who measured fractionally wetted (coloured) external areas on particle scale after injecting ink into the liquid feed. These experiments were

performed on packed absorption columns, which are similar to trickle-bed reactors, except that the particles are non-porous and usually of different shape and size.

It was only in the late 1980's when a colorometric method was again used in the study of trickling flow. Lazzaroni et al. (1988) doped the liquid feed with a component (Chrome-Azurol S) that colours red when adsorbed to the surface of porous γ-alumina particles. The time of contact (or amount adsorbed) between a certain solution of this compound and the particles was calibrated versus the intensity of the colour of contacted particles, so that they could distinct between particles constantly wetted by the steady-state liquid stream and those that were only contacted by the liquid once or twice for a short time. Before dismantling, the bed was solidified so that the degree of wetting and the position of each particle could be identified and a radial liquid distribution profile could be obtained. As a secondary indication of radial liquid distribution, the outlet liquid stream was collected in an annular collector, to measure the maldistribution of liquid flow through the bed. These two measures of radial liquid distribution did not agree at high gas flow-rates, with the distribution as measured by the particle wetting far more uniform than that obtained from the annular collector. This is an indication that solid-liquid contacting efficiency can increase with gas flow-rate even although liquid holdup is decreased: The gas tends to flow through the external parts of the bed, decreasing the liquid flow through these parts, but increasing the spreading of this liquid so that a uniform radial wetting distribution is still obtained. At low gas flow-rates, it seems as though gas flow only results in radial liquid maldistribution and a decrease in liquid holdup and wetting efficiency in the bed (Lutran et al., 1991).

Ravindra et al. (1997) stressed the importance of direct physical methods for the study of liquid flow in trickle beds, since available models fail to predict a number of experimental observations. As examples, they mentioned multiple steady states (Kan & Greenfield, 1978; Christensen et al., 1986), flickering hot spots (Germain et al., 1974) and the effect of prewetting (Kan & Greenfield, 1978). Liquid and gas distribution in various trickle-bed configurations were studied. Additionally, the liquid feed was doped with methylene blue so that solid-liquid contacting could be quantified. After beds were drained, particles were removed layer-by layer from the bed, photographing the top of the resulting bed each time when a layer was removed, so that the solid-liquid contacting could be obtained as a function of bed-height. A number of effects that are not provided for in traditional TBR models have been observed

- Solid-liquid contacting efficiency and liquid distribution is a function of bed height, and liquid tends to coagulate while going down the bed.

- If liquid channeling takes place in the bed, no gas will flow through such channels, and the gas-liquid contacting area in the bed may become very low, which can severely decrease reactor performance, even although the solid-liquid contact area

is high.

- No particle-scale partial wetting could be observed for particles smaller than $d_p \leq 6$ mm.

It was also found that liquid distribution in beds containing solid glass particles differed completely from beds containing porous alumina particles, so that wetting efficiency correlations for packed absorption columns are not applicable to trickle-bed reactors.

One of the most important drawbacks of colorometric measurements is that wetting efficiency may be greatly overestimated, if the flow in the bed changes from position during time (Schwartz et al., 1976). All the solid area that was at any time contacted by liquid will then show as wetted. There is however some evidence that the liquid flow in the trickle-flow regime is stable: Lazzaroni et al. (1988) used a colourant for which the colour intensity of the wetted solid areas are a function of time of contact. No intensity variation were reported. Also, Sederman & Gladden (2001) acquired sharp images of trickle flow with a tomographic method for which the image acquisition time was about three minutes.

Another disadvantage is that it is difficult to evaluate the wetting fraction on small particles accurately (Mills & Dudukovic, 1981).

2.3.3 Correlations

For a better understanding and to discriminate between available wetting efficiency correlations, the parameters that are believed to have the most important influence on wetting efficiency will be discussed.

Liquid flow and properties

Liquid flow-rate and properties is believed to be the main parameter influencing solid-liquid contacting efficiency because of their influence on liquid holdup: Increased liquid holdup leads to increased solid-liquid contacting.

Bondi (1971) investigated several industrial trickle-bed reactors, and compared their performance with the maximum performance (i.e. rate of reaction is equal to the intrinsic kinetics of the reaction). He suggested a trickle-bed efficiency correlation of a form for which the trickle-bed apparent reaction rate constant k_{app} would approach the intrinsic rate constant, as liquid flow-rate approaches infinity, since external mass transfer effects would then be negligible and wetting would be complete:

$$\frac{1}{k_{TB}} - \frac{1}{k} = \frac{A'}{L^{2/3}} \tag{2.68}$$

Puranik & Vogelpohl (1974) studied a wide range of data from experimental studies on packed absorption columns and found:

$$a_w = 1.05 Re_L^{0.047} We^{0.135} (\sigma/\sigma_c)^{-0.206} \tag{2.69}$$

This correlation suggests that solid-liquid contacting efficiency is proportional to $L^{0.3}$ in a packed absorption column. Mears (1974) used this correlation to "prove" that trickle-bed efficiency is proportional to η_{CE}, arguing that the flow in trickle-bed reactors is very similar to that in packed absorption columns.

There are several other correlations in literature that only take into account liquid flow and liquid and packing properties. Examples are:

Mills & Dudukovic (1980)

$$\eta_{CE} = \tanh \left[0.664 Re_L^{0.33} Fr_L^{0.195} We_L^{-0.171} \left(\frac{a d_p}{\epsilon^2} \right)^{-0.0615} \right] \tag{2.70}$$

and

$$\eta_{CE} = 1.0 - \exp \left[-2.6 Re_L^{0.40} Fr_L^{0.32} We_L^{-0.17} \left(\frac{a d_p}{\epsilon^2} \right)^{-0.043} \right] \tag{2.71}$$

Ring & Missen (1991)

$$\eta_{CE} = 1 - \exp -118 v_{SL}^{0.635} \tag{2.72}$$

El-Hisnawi et al. (1982)

$$\eta_{CE} = 1.617 Re_L^{0.1461} Ga_L^{-0.0711} \tag{2.73}$$

$$\text{where} \quad Re_L = \frac{\rho_L v_{SL} d_p}{\mu_L}, \qquad Ga_L = \frac{d_p^3 g \rho_L^2}{\mu_L^2}$$

Making use of the percolation theory [2], Crine et al. (1980) related the wetting efficiency at a certain liquid velocity to the minimum liquid velocity at which $\eta_{CE} = 1$:

$$\eta_{CE} = 1.961 \frac{u_l}{u_{l,min}} - 1.275 \left(\frac{u_l}{u_{l,min}} \right)^2 - 1.598 \left(\frac{u_l}{u_{l,min}} \right)^3 + 3.326 \left(\frac{u_l}{u_{l,min}} \right)^4 - 1.417 \left(\frac{u_l}{u_{l,min}} \right)^5 \tag{2.74}$$

The stagnant wetting efficiency, is believed to be independent of liquid flow-rate and only a function of liquid and packing properties (Puranik & Vogelpohl, 1974; Sicardi et al., 1981; Saez & Carbonell, 1975). It is believed that the major liquid properties influencing static liquid holdup (and therefore $\eta_{CE,st}$) is the surface tension of the liquid

[2] A statistical model where for each all the packing elements "activities" are ascribed in terms of the interaction with surrounding packing elements

at the gas-static liquid interface and the density of the liquid, since these two determine the capillary force to gravitational force ratio on liquid trapped between contact points of the bed particles. When the static liquid holdup is determined with a tracer, one do however find a dependency on liquid flow rate (Nigam et al., 2001).

Gas flow and pressure drop

Originally, it was thought that the effect of gas flow-rate on solid-liquid contacting efficiency is negligible. For example, Goto et al. (1975) did not find any change of solid-liquid mass transfer on increasing gas flow, and Lakota & Levec (1990) found that observed increases in solid-liquid mass transfer with increasing gas flow-rate is only due to decreased dynamic liquid holdup and therefore increased intrinsic liquid velocity, u_l. Lazzaroni et al. (1988) found that, despite a decrease in liquid holdup due to increased gas flow, the wetting efficiency in the bed did not decrease with increased gas flow. Burghardt et al. (1995) did find a *decrease* in wetting efficiency with increased gas flow rate and developed the following wetting efficiency correlation:

$$\eta_{CE} = 0.0381 L^{0.222} G^{-0.083} d_p^{-0.373} \tag{2.75}$$

All these observations were made at atmospheric pressures. At high pressures however, several authors found a significant increase in reactor performance when gas flow-rate is increased. Bondi (1971) found an increase in industrial reactor performance when increasing gas flow-rate, and suggested to multiply L in his correlation for reactor efficiency (equation 2.68) with $(\rho_G G)^{1/3}$, but Satterfield (1975) suggested that the increased performance with increased gas flow-rate is probably due to increased gaseous reagent partial pressures. Wammes et al. (1991) and Larachi et al. (1992) also found such increases and reasoned that this might be due to increased solid-liquid or gas liquid contacting. No correlation to relate gas flow to solid-liquid contacting efficiency was however developed.

To predict pressure drop and liquid holdup inside a trickle-bed reactor, Holub et al. (1992) developed a phenomenological model: The slit model. Here the bed is viewed as a slit, inclined at an angle θ, with liquid film of total thickness δ flowing over the slit walls of total thickness S_D. Gas flows through the centre of the slit. The slit is depicted in figure 2.9. Momentum balances over the slit yield:

$$-\frac{\mathrm{d}P}{\mathrm{d}z} + \rho_G g cos\theta = \frac{\tau_{lg}}{w - \delta} \tag{2.76}$$

$$-\frac{\mathrm{d}P}{\mathrm{d}z} + \rho_L g cos\theta = \frac{\tau_{wl} - \tau_{lg}}{\delta} \tag{2.77}$$

The shear stresses, τ_i can be expressed in terms of liquid and gas velocities, w and δ. The slit dimensions, w, S_D, δ and θ can be related to bed properties with the following

equations:

$$\frac{w}{S_D} = \frac{\epsilon}{(1-\epsilon)} \tag{2.78}$$

$$\frac{\delta}{S_D} = \frac{\epsilon_L}{(1-\epsilon)} \tag{2.79}$$

$$\cos\theta = \frac{1}{T}, \text{with } T \text{ the bed tortuosity} \tag{2.80}$$

From this, an overall relationship between liquid holdup and pressure drop in a TBR was derived:

$$\epsilon_L = \epsilon \left(\frac{E_1 Re_L + E_2 Re_L^2}{Ga_L \left(1 + [(\Delta P/Z)/\rho_L g]\right)} \right)^{1/3} \tag{2.81}$$

This model of Holub et al. (1992) gives good accuracy in the prediction of pressure drop and liquid holdup in the bed. It should be noted that the slit is modeled as if the walls are completely wetted, and does not take into account wetting efficiency so that the discussion of this model may seem out of place. This model has however had a significant impact in the study of solid-liquid contacting efficiency.

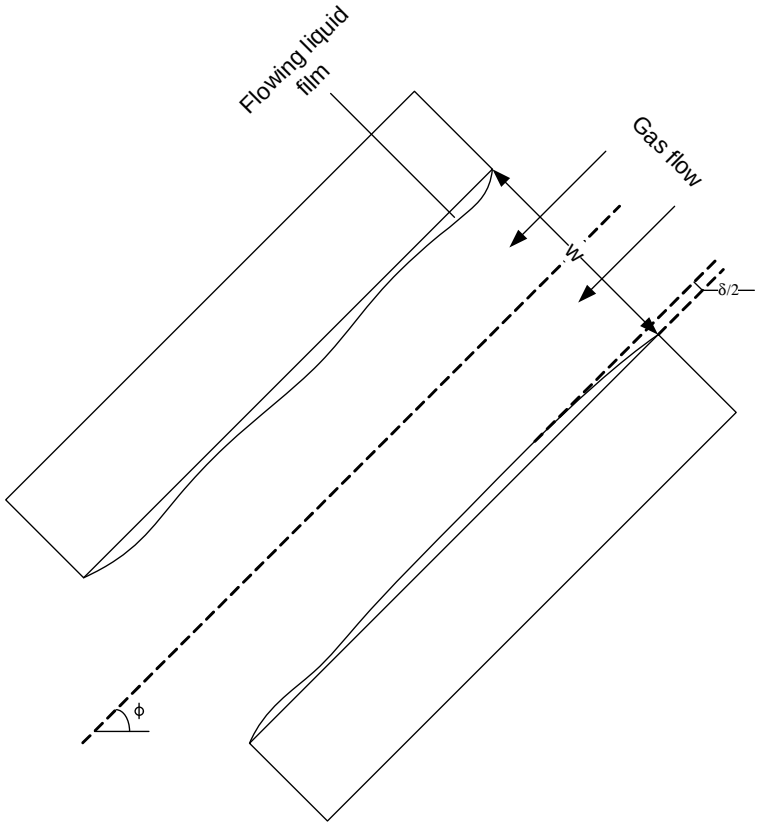

Figure 2.9: Geometry of the slit model proposed by Holub et al. (1992)

Al-Dahhan & Dudukovic (1995) noted that the slit momentum balances from which the slit-model of Holub et al. (1992) arised (equations 2.76 and 2.77), predict a decrease in film thickness, δ, with pressure drop. It was reasoned that these thinner films can

be interpreted as improved spreading of the liquid and therefore improved solid-liquid contacting, if the liquid holdup stays more or less constant. For spherical particles, the relationship between film thickness and liquid holdup is given by (assuming that all liquid completely contacts all particles in the form of films):

$$\begin{aligned} \delta &= \frac{\text{liquid volume per bed volume}}{\text{particle external area per bed volume}} \\ &= \frac{\epsilon_L}{6(1-\epsilon)/d_p} \end{aligned} \tag{2.82}$$

Substituting this in equation 2.81 yield the following relationship between liquid film thickness, flow-rate and pressure drop:

$$\delta = \left(\frac{d_p \epsilon}{6(1-\epsilon)}\right)\left(\frac{E_1 Re_L + E_2 Re_L^2}{Ga_L\left(1+[(\Delta P/Z)/\rho_L g]\right)}\right)^{1/3} \tag{2.83}$$

From this equation it can be seen that packing properties, and the ratio of pressure drop to gravitational forces exerted on the liquid directly influence the film thickness. The latter can be explained as follows:

An increase in pressure drop increases the gas-liquid shear force, which on its turn increase spreading of the liquid so that solid-liquid contacting is increased. Gravitational forces tend to decrease this effect. Therefore, it was suggested that the dependency of η_{CE} on gas flow rate will be some function of pressure drop, gravitational forces and packing properties. The authors assumed:

$$\eta_{CE} \propto \left(\frac{1+\frac{\Delta P/Z}{\rho_L g}}{Ga_L}\right)^m \tag{2.84}$$

To provide for the effect of liquid flow-rate on η_{CE}, the form of the correlation of El-Hisnawi et al. (1982) was assumed, and equation 2.84 becomes:

$$\eta_{CE} = cRe_L^n \left(\frac{1+[(\Delta P/Z)/\rho_L g]}{Ga_L}\right)^m \tag{2.85}$$

The constants c, n, and m were fitted onto a wide range of experimental data and the following correlation was obtained (Al-Dahhan & Dudukovic, 1995):

$$\eta_{CE} = 1.104 Re_L^{1/3} \left(\frac{1+[(\Delta P/Z)/\rho_L g]}{Ga_L}\right)^{1/9} \tag{2.86}$$

This correlation became very popular and is widely accepted.

The slit-model of Holub et al. (1992) also resulted in a double-slit model by Iliuta & Larachi (2000), which was suggested in order to not only model pressure drop and liquid holdup, but also solid-liquid contacting efficiency in the slit. The geometry used was

similar to that of Holub et al. (1992), but with an extra slit which is completely dry. This results in an extra force balance (gas phase over the dry slit), and alters the relationship between bed properties and geometry, for example the widths of the two slits are not only dependent on bed porosity, but also on solid-liquid contacting efficiency. The correlation was fitted on experimental results of just about all authors who worked on solid-liquid contacting efficiency.

To simulate high-pressure trickle-beds in experiments, one can make use of high molecular mass gases, since the pressure drop over the bed is mostly dependent on gas density and velocity (Al-Dahhan et al., 1997).

Packing properties

The influence of packing properties on η_{CE} is usually described in terms of the Galileo number, Ga_L, which is given by:

$$Ga_L = \frac{d_p^3 \rho_L^2 g \epsilon^3}{\mu_L^3 (1-\epsilon)^3} \tag{2.87}$$

According to most correlations, the solid-liquid contacting efficiency is proportional to some negative power of Ga_L. This can be explained as follows:

- The smaller the particles in the bed, the higher the contacting efficiency. This is due to increased capillarity of the bed.
- The gravitational force exerted on the liquid tends to decrease η_{CE}. This has already been discussed in the previous section, and results from the force balance over the bed or slit, as modeled by Holub et al. (1992).
- Bed porosity influences the pressure drop over the bed, which will directly influence η_{CE}: A higher bed porosity decreases pressure drop and therefore η_{CE}.
- Increased liquid viscosity results in increased liquid-solid shear stresses and therefore better spreading of the liquid.

Static liquid holdup is dependent on liquid surface tension, liquid density and particle diameter, since these influence the capillary force exerted on the liquid between particles. The ratio of static liquid holdup to $\eta_{CE,s}$, is dependent on bed porosity and the number of contact points between the particles in the bed, as can be seen from equation 2.18.

Puranik & Vogelpohl (1974) found that the static wetted area fraction in packed absorption columns is equal to:

$$a_{st} = 0.229 - 0.091 \ln(We/Fr) \tag{2.88}$$

where:

$$We = \frac{L^2 d_p}{(1-\epsilon)\rho_L \sigma_L},\ Fr = \frac{L^2(1-\epsilon)}{d_p \rho_L^2 g} \tag{2.89}$$

which also implies that static wetted area is not a function of liquid flow-rate and only of the bed and liquid properties mentioned earlier.

2.4 Concluding remarks

Literature on trickle-flow morphology shows out that trickle-flow can not be described with only bed-averaged parameters but one needs to take into account flow history and the types of flow that are present in the bed. Liquid holdup and pressure drop as functions of flow history and pre-wetting have therefore been subject many experimental investigations.

Wetting efficiency literature, on the other hand, pays little attention to flow history and morphology. Some comparison between dry and pre-wetted beds is available, but it is usually not stated how the beds were pre-wetted.

Reactor models and measurement methods that incorporate wetting efficiency are usually based on particle-scale phenomena, but an average wetting efficiency is used in the model. This might affect modelling and measurement of wetting efficiency. Most wetting efficiency data that are available in literature are derived from a model. To distinguish between model-based and physically determined wetting efficiency, the former will be denoted as η_{CE} and the latter as f when experimental results are discussed.

CHAPTER 3

Experimental

It was decided to investigate the effect of liquid flow morphology on wetting efficiency and reactor performance by means of a colorometric method. This method has the following advantages that are applicable to the intended investigation:

- The nature and distribution of wetting efficiency as a function of flow can be investigated, since fractional wetting of each single particle in the bed can be evaluated.
- Flow and wetting efficiency can be examined along the bed depth, and do not have to be averaged over the whole of the bed, as is the case for most wetting efficiency measurement methods.

There are a few important possible disadvantages to colorometric methods that should be kept in mind:

- If the flow in the bed changes over time during experimental operation, wetting efficiency can be severely overestimated, since all areas that were contacted by the liquid over time will register as "steady state wetting efficiency".
- It is very difficult to accurately measure area fractions on small particles (Mills & Dudukovic, 1981).

These disadvantages are addressed in sections 3.1.2 and 5.1 respectively.

3.1 Experimental setup

Figure 3.1 shows the process flow diagram for the experimental setup. This setup consists of a trickle-bed reactor with distributor, a low pressure N_2 feed system, and two separate liquid feed systems, one containing clear water whereas the other contains a colourant

which is used to colour the packing according to the flow pattern in the bed. The clear water is used to enable one to reach steady state trickle-flow before the colourant is introduced, and to wash away remaining colourant from the bed after the experimentation. The pressure drop over the bed and the liquid holdup in the bed are measured during flow.

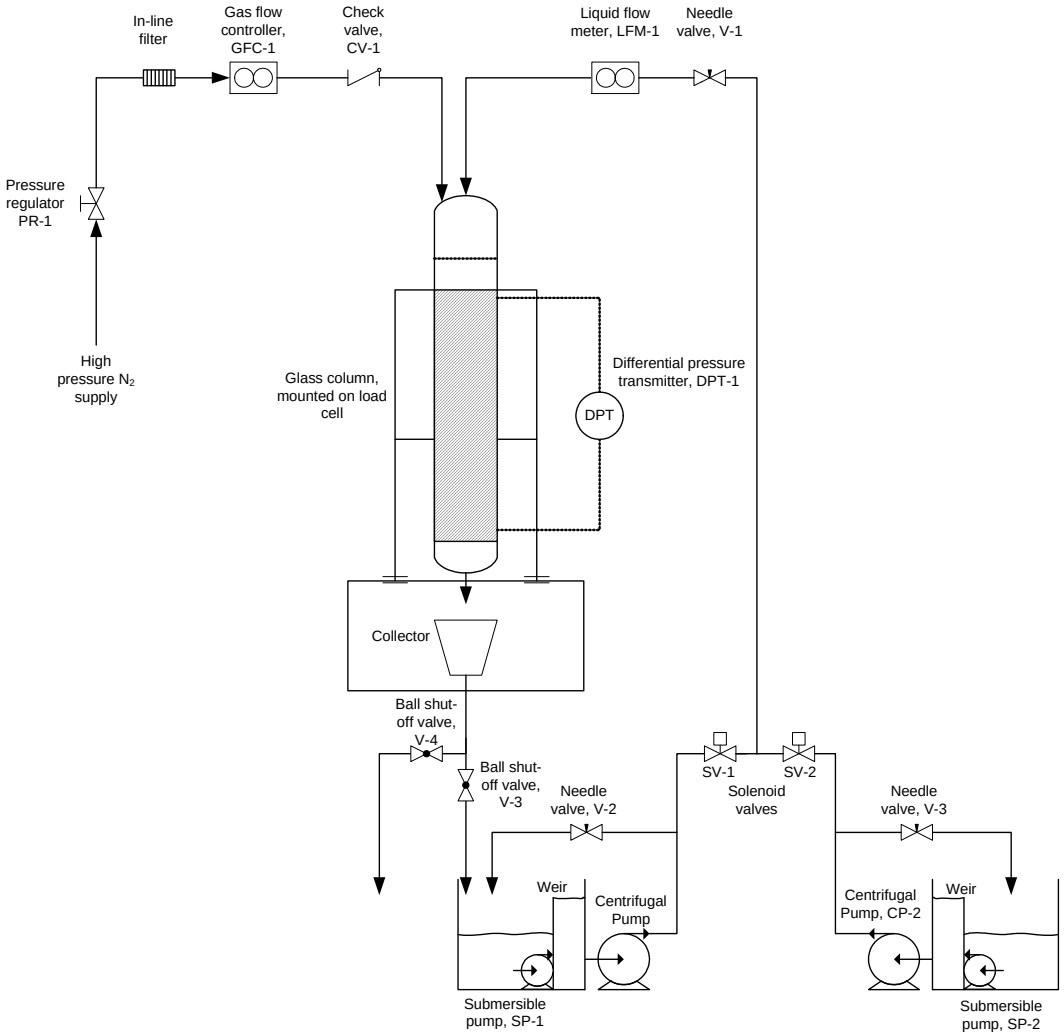

Figure 3.1: Process flow diagram (PFD) of the trickle-bed facility

3.1.1 Description of the column and packing

The reactor consists of a 63 mm I.D. column, 1.0 m long, with pressure taps spaced 800 mm from one another. A valve located at the top of the column enables one to flood the column without building up pressure. The column is made of glass to observe patterns near the wall during and after trickle flow. Since the glass column can only withstand low pressures (up to about 100 kPag), experiments are limited to atmospheric conditions but, according to Al-Dahhan et al. (1997), the *gas density* rather than pressure is a parameter influencing trickle-flow characteristics, and making use of a high molecular mass gas feed (N_2) still enables one to cover some range of trickle-flow conditions.

The packing in the column consists of 2.5 mm spherical γ-alumina supports from Sasol Germany, with internal porosity $\epsilon_{int} = 0.46$ and a particle density of 1010 $^{kg}/_{m^3}$. The resultant column to particle diameter ratio is $\frac{D_c}{d_p} \approx 25$, which meet the criterion of $\frac{D_c}{d_p} > 20$ necessary to avoid wall effects (Al-Dahhan et al., 1997).

3.1.2 Colourant characteristics

Particles are coloured by means of a 0.2 g/ℓ solution of the colourant Chromeazurol S in water to colour the packing during trickle flow. The areas on the particles in the bed that were contacted by this colourant exhibits a deep red colour. To accurately measure wetting efficiency, the colourant should comply to the following criteria:

- For the investigation of particle-scale effects, the dye should only colour parts of the particles that are in direct contact with the liquid, i.e. it may not diffuse through the particle or over the external area to colour other (non-wetted) parts of the particles. Chromeazurol-S adsorbs fast and permanently to the external γ-alumina surface, so that diffusional "errors" are minimal (Lazzaroni et al., 1988).

- When wash with water, the colourant may not desorb from the particle surfaces. Adsorption of Chromeazurol-S onto γ-alumina is permanent and irreversible.

- As previously discussed, the overall wetting efficiency can be largely overestimated, if the liquid flow pattern changes over time. To evaluate whether such changes occur, the colour intensity of wetted surfaces should be time dependent for at least a limited time period. On the other hand, if all particles are to be analysed by the same method, the colour intensity of all particles should be independent of their position in the bed. Since contacting time with a specific particle is a function of its axial position in the bed, colour intensity should become time independent after a certain period. Subsequently, a colourant should be selected for which the wetted surface colour intensity is time dependent for a reasonable time span and then becomes time independent. A 0.2 g/ℓ solution of Chromeazurol S does exhibit

these characteristics, as is shown in figure 3.2. It can be seen from the figure that all particles that were contacted for less than 10 minutes will be recognisable, so that it can be evaluated to some extend whether flow patterns has changed during the time of the experiment. Note that the time span of the experiment (±40 minutes) will still allow for changes in flow that will not be recognised, and it still has to be assumed that flow is stable and that its pattern does not change. This assumption is supported by data of van der Merwe & Nicol (2005).

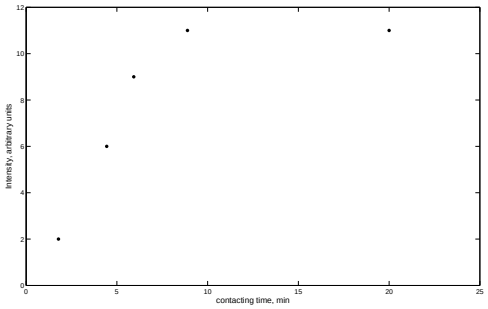

Figure 3.2: Colour intensity as a function of time of contact between particle surface and the colourant. Adapted from Lazzaroni et al. (1988).

Chromeazurol S was previously used by Lazzaroni et al. (1988) with success for colorometric studies in a trickle-bed reactors containing γ-alumina particles (see chapter 2.3).

3.1.3 Gas and liquid feed systems

The liquid feed system consists of two seperate systems, one for clear water and one for the colourant. An experiment is started with a clear water feed, so that trickle flow can be given time to reach steady state without influencing results. After steady state is reached, the colourant is introduced in the bed by switching between the two feed systems.

To achieve representative colouring of the particles during trickle flow, the liquid feed system needs to enable one to switch between two different liquid feeds without causing significant flow disturbances in the column: the flow should stabilise before the colourant enters the bed. To minimize the flow disturbance encountered when switching between the liquid in TK-1 (clear water) to TK-2 (colourant), needle valves V-2 and V-3 are installed. The switch between the two different feeds can be achieved with solenoid valves SV-1 and SV-2. These valves operate on the same signal, to switch as fast as possible. Valve SV-1 is normally open and valve SV-2 is normally closed to enable one to switch between the feed tanks with only one signal. Liquid flow rate is manipulated with needle valve V-1 and fine tuned with valve V-2 or V-3, and is measured with an Endress & Hauser model PROMAG 10H electromagnetic flow meter. The flow meter has a range of $0 - 3.8$ ℓ/min, with an accuracy of 0.5% of the measured flow at flowrates above 1 ℓ/min and

1.5% at flow-rates above 0.2 ℓ/min. A weir and submersible pump was installed in each feed tank to provide the feed pumps with a constant head. Ball shut-off valves V-3 and V-4 are installed to switch between recycling and draining of the reactor outlet flow.

The nitrogen gas is fed from a high pressure cylinder and the flow rate controlled with a Brooks Smart mass flow controller model 5853S with range $0 - 250$ standard liters per minute (slpm). Accuracy is $\pm 0.7\%$ of the flow-rate. Filter F-1 and check valve CV-1 are installed in the line to protect the controller. Data from the controller is logged on the DeltaV data-logging system to check flow stability.

Liquid and gas are distributed by means of the distributor shown in figure 3.3. The holes in the distributor plate were 0.5 mm in diameter, 8 mm spaced in a square pitch arrangement. This gives a hole density of about 16000 points/m^2. According to Burghardt et al. (1995), a uniform liquid distribution can be assumed when the distributor point density exceeds 5000 points/m^2. The gas was distributed by means of three 1/4 inch stainless steel tubes, as shown in figure 3.3. The same distributor was used for all experimental runs.

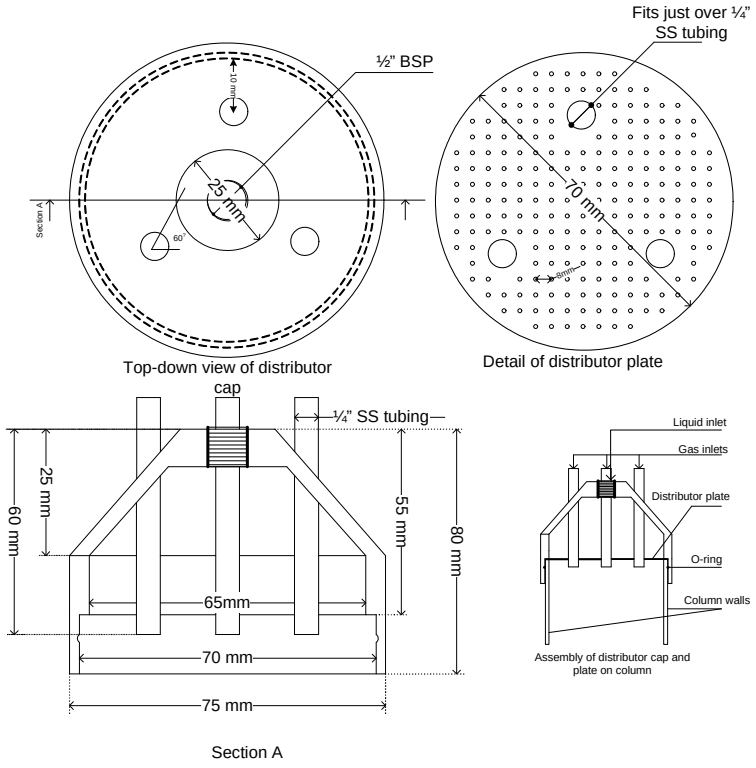

Figure 3.3: Detailed distributor design

3.1.4 Pressure drop and holdup measurements

Pressure drop over the major part of the bed was measured and recorded by means of a Rosemount model 3051CD differential pressure transmitter. The transmitter has

an accuracy of about 0.1 % of its range while it can be operated at ranges $0 - 70$ Pa, $0.07 - 6.2$ kPa and on toward 62 kPa. This translates to a ± 6 Pa accuracy under normal operating conditions. Data from the differential pressure cell was logged on a DeltaV data-logging system for access of data history, so that steady state can be easily recognised and verified during experiments.

The holdup in the bed was measured by weighing the bed during flow, by means of a model 642C3 load cell from Revere Transducers Europe, calibrated for 0-20 kg. The load cell is connected to a transmitter, and holdup data was logged on the deltaV data-logger, for access of data history and easy verification of steady state during experiments. The accuracy is about $\pm$ 4g, which is a bit inaccurate for holdup measurements and it had to be assumed that the average of 1 s interval steady state measurements over at least 5 min is a good representation of the steady state holdup.

Another problem with the holdup measurements is that the amount of liquid in the distributor cap during experiments could not be measured. In order to make corrections, separate experiments were performed where the liquid in the distributor at different flow rates was trapped by shutting of the liquid inlet above the distributor during flow, and then weighed. In these experiments the holdup in the distributor was found to be more or less constant at 133 g. The measured holdup was therefore corrected by subtracting 133 g for all liquid flow rates.

3.2 Experimental procedure

Prior to every flow experiment, the column is packed with 2.5 mm γ-alumina spheres to a height of about 800 mm. The mass of the packing is noted for bed porosity calculations.

The packing is then flooded for at least 3 h to ensure internal saturation of the particles after which it is left to drain for about half an hour. The packing is then pre-wetted with the clean water from TK-1 according to one of the pre-wetting procedures described in section 3.2.1 after which the gas and liquid flow-rates are brought to the desired magnitudes.

The experiment should be run on clear water for at least 5 min after steady state is achieved to improve accuracy of holdup measurements as discussed in section 3.1. On-line holdup and pressure drop measurements are used to verify trickle-flow steady state. After steady state is reached and the steady state liquid holdup and pressure drop measurement are obtained, the colourant is introduced by switching between the two feed systems. Before switching over to the colourant, it has to be assured that valve V-4 is opened and valve V-3 is closed, so that none of the colourant is recycled into tank TK-1.

As already discussed, the colour intensity of the contacted particle areas become contacting time independent only after 20 min of contacting. Since the colourant is initially stripped from the dye at the top of the column due to adsorption, trickle flow

with the dye should be run for about 40 min.

The dye is then washed from the column with clear water at the experimental trickle-flow conditions, to minimise "smudge" of colour on the particles. To reach all the parts where the dye has been, it is necessary that the clear water will follow the same path as where the dye has been. Since a small disturbance is induced when switching between feed systems it is likely that some of the liquid paths may have changed locally. To remove any dye that can still be present in the packing despite washing under trickle-flow conditions, the packing is washed under pulsing flow conditions. On the hand of figure 3.2, it can be assumed that the residual dye washed away under the maximum flow conditions ($\pm 4\ell$/min) will not be in contact with the particles long enough to influence results, due to the high linear liquid velocity (one residence time $\approx$ 35s).

The packing is then left to dry and the particles in the bed are ready for analysis.

3.2.1 Flow conditions

The different flow conditions that were used in experiments are shown in table 3.1. To be able to investigate different flow types, two different pre-wetting procedures were adopted: Pulse pre-wetting and Levec pre-wetting. According to literature the former will result in film flow, whereas the latter will result in both film flow and filament flow.

Table 3.1: Experimental flow conditions

$L[\frac{kg}{m^2 s}]$	$G[\frac{kg}{m^2 s}]$	Pre-wetting Procedure
1.60	0.023	Pulse
1.60	0.152	Pulse
5.35	0.023	Pulse
5.35	0.152	Pulse
1.60	0.152	Levec
5.35	0.152	Levec

3.3 Particle sampling and analysis

For fast sampling and analysis of a representative amount of particles in the bed a sampling grid was constructed, which consists of a plate in which a 17×17 grid of holes was drilled. Particles from each sample were captured in this grid, and then photographed, as shown in figure 3.4. The particles are retained by two clear PVC plates fastened on both sides of the grid.

The sample is then photographed from *both sides* in a light box to obtain consistent images. The grid is marked in each corner so that the "half particles" from the two sides

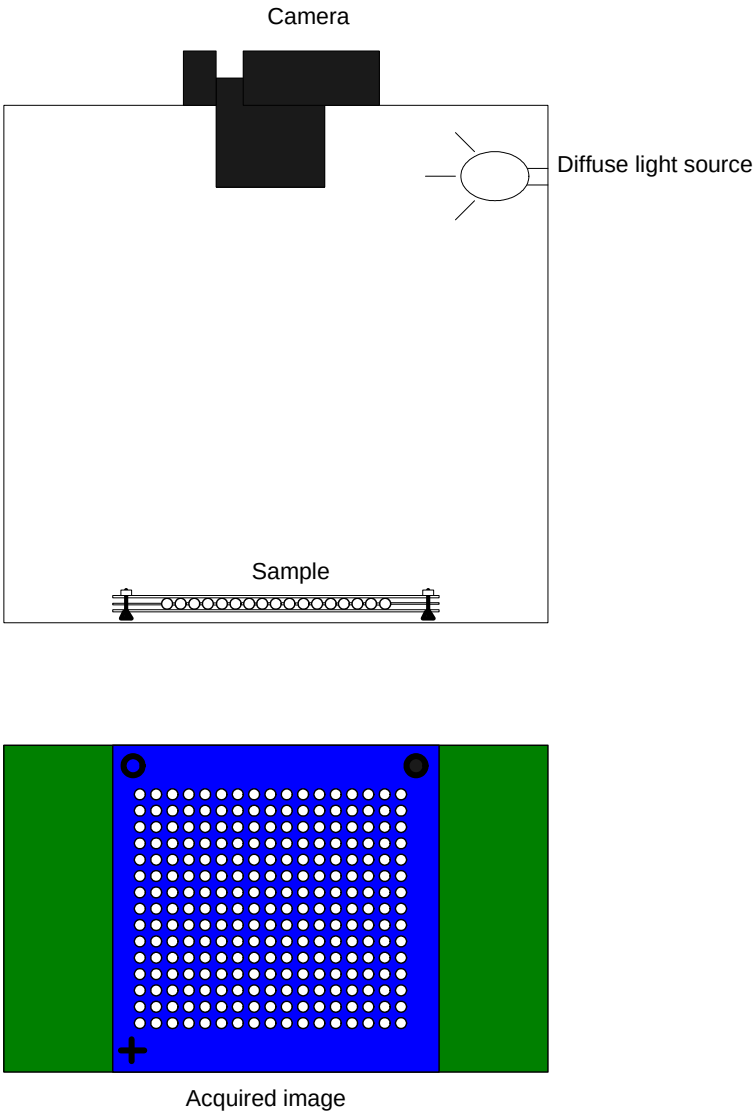

Figure 3.4: Image acquisition for the determination of particle wetting distributions

taken from each sample can be matched.

The images are processed in Matlab's Image Processing toolbox to calculate the wetting of each particle. One of the most important aspects in the image processing is to correctly recognise all the particles in the image. To simplify this process the images are taken against a green background, whereas the grid background is blue: Images are stored in Matlab as 3-dimensional matrices describing the red, blue and green intensities at each point on the image. The particles, that are either red or white or both, then has by far the highest percentage red intensities as compared to the rest of the image, so that they can easily be identified by the following image processing step:

$$\text{Filtered image} = K_1 \times \text{Blue Intensities} - K_2 \times \text{Red Intensities}$$

When the two constants are optimised the particles appear black against a light grey background and can easily be identified. Objects on the image that are incorrectly identified as particles, are filtered by using known properties of the particles, i.e area to diameter ratio, overall area etc. Care should be taken that K_1 and K_2 are chosen in such a way that white particles shows as clear as red particles, so that overall wetting measurements are not skew toward high or low wetting. The grid colour is chosen different from the background colour for easily alignment of the image if it is skew.

Each particle is extracted as a separate image and each pixel on each particle is then identified as wetted or non-wetted. This information (1 or 0 for each Cartesian coordinate on the particle) is rewritten in terms of polar coordinates, with the following transformation:

$$F_{kp} = F_{ij}$$

with

$$\begin{aligned} r_k \sin\theta_p &= x_j - x_{j,mid} \\ -r_k \cos\theta_p &= y_i - y_{i,mid} \end{aligned} \tag{3.1}$$

Where:

F_{ij} = wetting of each pixel in the x-y plane, binary 2×2 matrix

F_{kp} = wetting of each pixel in the ϕ-θ plane (spherical coordinates with R constant), binary2×2 matrix

r_k = distance of pixel from centrepoint$(x_{j,mid}, y_{i,mid})$, pixels.
This value is a function of the spherical coordinate ϕ only, since R is constant

$x_{j,mid}$ = x-coordinate of centre pixel, pixels

$y_{i,mid}$ = y-coordinate of centre pixel, pixels

For illustration, the coordinate systems and variables used for this transformation are depicted in figure 3.5.

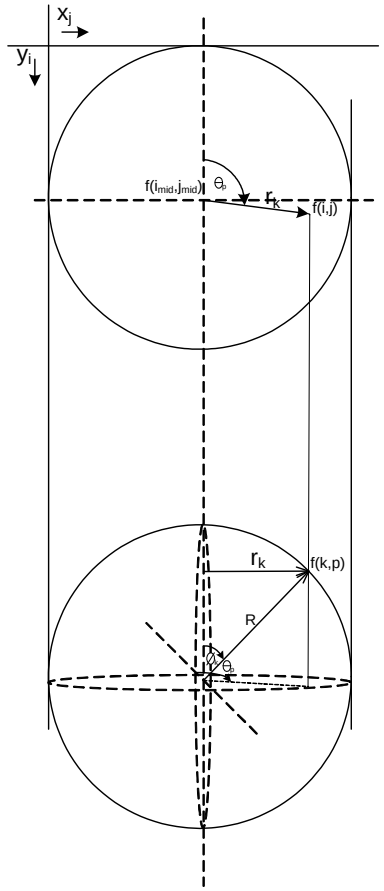

Figure 3.5: Image transformation from 2-D Cartesian coordinates to 3-D spherical coordinates

Since the image is a 2-dimensional projection of 3-dimensional spheres, each pixel has to be weighted according to the fractional area of the sphere that it represents. Weighting

is performed by the following equations:

$$a_{kp} = R^2.sin\phi_p d\phi_p d\theta_k \tag{3.2}$$

$$W_{kp} = \frac{a_{kp}}{\sum a_{kp}} \tag{3.3}$$

Where:

$$a_{kp} = \text{area represented by one pixel in the } \phi\text{-}\theta \text{ plane} \tag{3.4}$$

$$W_{kp} = \text{Weighting factor for each seperate pixel} \tag{3.5}$$

$$\phi_k = \sin^{-1}\left(\frac{r_{kp}}{R_p}\right) \tag{3.6}$$

$$\theta_p = \sin^{-1}\left(\frac{x_j - x_{j,mid}}{R_p}\right) \tag{3.7}$$

And the fractional wetting of each particle is:

$$f_p = \sum^{k}\sum^{p} W_{kp}.f_{kp} \tag{3.8}$$

Using the procedure described in this section, not only average wetting but also the distribution of particle wetting efficiency was calculated for samples taken from different bed sections of the bed as well as for several samples taken from the well-mixed bed packing.

3.4 Wetting data acquisition

One of the major advantages of colorometric experiments on trickle-bed reactors is the high amount of information that is "stored" in the reactor after a such an experiment is performed. The question is how one should extract this information when unpacking the column. Lazzaroni et al. (1988) solidified the packing before removing it from the column to retain all information "stored" in the packing and then studied the radial variation of wetting efficiency in the column. Ravindra et al. (1997) unpacked the column with adhesive tape, so that the path of liquid flow could be followed down the column.

3.4.1 Bed section data

To obtain information of the nature of trickle-flow as a function of bed depth, it was initially decided to follow the method of Ravindra et al. (1997), using adhesive tape to unpack the column. It was however found that their method is extremely cumbersome and only viable if the particles are either completely wetted or completely dry, since removing particles with the tape resulted in turning of the particles. This conceals the

path of the liquid if these particles are only partially wetted but not completely dry. This method would therefore only be able to describe particle wetting as a function of height, but not the path of the liquid flow when the particles are partially wetted.

A less cumbersome method was developed to extract the same information: A "pouring cap" was fastened on top of the column to pour out the particles in a controlled fashion. The column is then turned upside down as fast as possible to minimise relative displacement of the particles in the axial direction. The particles are then poured out up to a mass corresponding to the depth of the bed where a sample is desired, and the cap is closed. The cap is opened again, and a small sample, corresponding to one or to bed sections, is taken and the cap is closed a gain. The process is repeated until all required samples are taken.

To optimise the accuracy of this method of unpacking, an experiment was done where the column was packed with layers of coloured and white particles alternately. It was attempted to separate the layers by pouring the particles out of the column without mixing the coloured and the white particles. The pouring cap design was altered until this attempt was successful, so that it can be said with confidence that the samples taken from each section of the column are representative in terms of their axial position.

One sample of about 250 particles were examined for each bed section.

3.4.2 Overall bed data

To characterise the wetting efficiency for the complete packing, the particles were well mixed after the column was unpacked and 15 samples of about 250 particles were taken from this mixture and photographed for further analysis.

CHAPTER 4

Results

4.1 Operational measurements

The measured pressure drop and liquid holdup data are presented in table 4.1. Repeated data are present in the last two column of the table. Repeatability runs were performed on clear water, so that the repeatability of the obtained wetting efficiencies were not evaluated. The repeated values of external liquid holdup and pressure drop for the pulse pre-wetted beds are all within 6% of the experimental values. For the Levec pre-wetted beds, holdup measurements gave poor repeatability. Good repeatability on the pressure drop data (within 3%) suggests liquid holdup measurement errors. Measured

Table 4.1: Experimental external liquid holdup and pressure drop data

Pre-wetting	L (kg/m^2s)	G (kg/m^2s)	ϵ_L	$\frac{\Delta P}{Z}$(Pa/m)	ϵ_L	$\frac{\Delta P}{Z}$(Pa/m)
Pulse	1.60	0.023	0.162	139	0.153	140
Pulse	1.60	0.152	0.158	2020	0.152	1950
Levec	1.60	0.152	0.10	910	0.07	890
Pulse	5.34	0.023	0.230	540	0.240	558
Pulse	5.34	0.152	0.228	4510	0.218	4258
Levec	5.34	0.152	0.18	1879	0.14	1865

average wetting efficiencies are compared with some existing wetting efficiency data and correlations in figures 4.1 and 4.2.

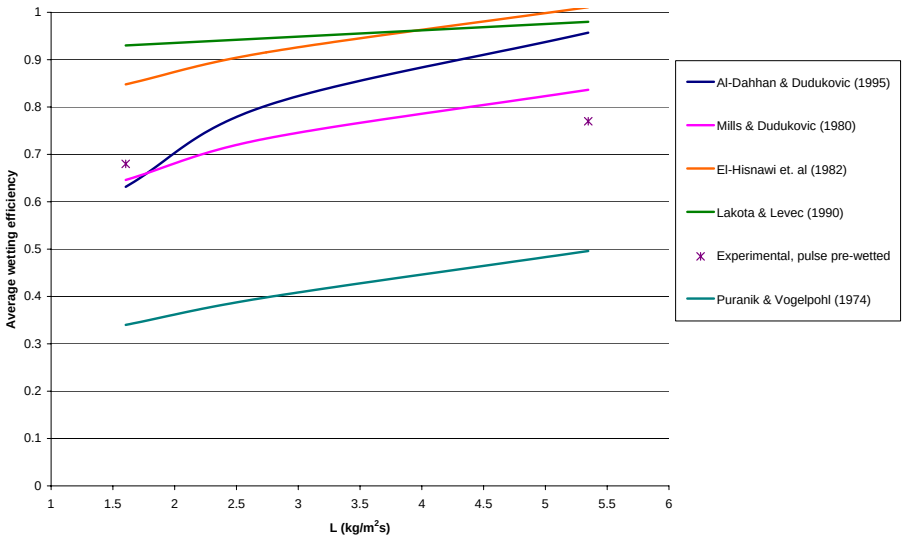

Figure 4.1: Comparison of experimental average wetting efficiencies with existing data and correlations. G = 0.023 kg/m^{2}s

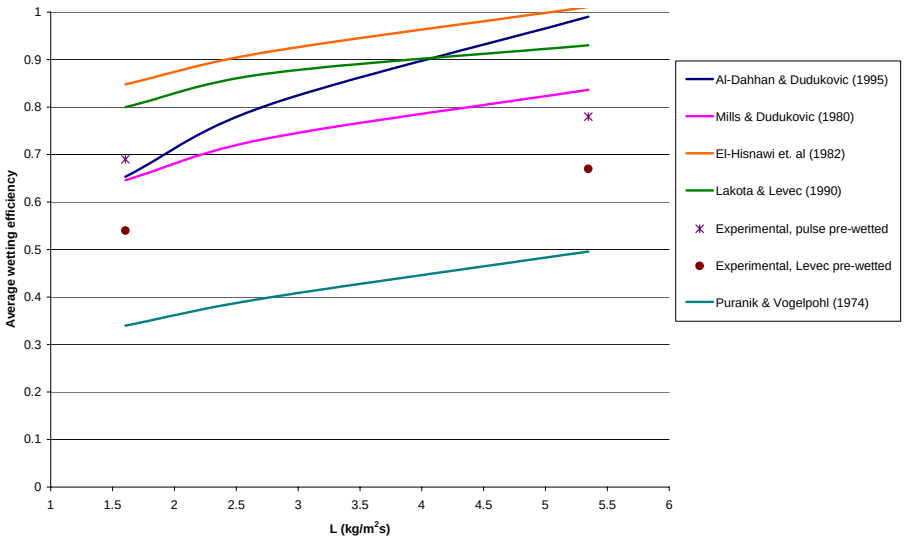

Figure 4.2: Comparison of experimental average wetting efficiencies with existing data and correlations. G = 0.152 kg/m^{2}s

4.2 Images

A typical example of the particle images that were extracted from the photos (taken as described in chapter 3) is shown in figure 4.3. Overall bed data was generated from 15 of these samples each, whereas one such a sample was prepared for each bed section reported. A resolution of 70 pixels × 70 pixels was obtained for most of the particles. For smaller or larger particles, the images were resized to contain the same amount of pixels. Weighting factors, as calculated according to equations 3.2 and 3.3, are not affected hereby, since these equations can be written as dimensionless in terms of particle radius. Each particle was photographed from both sides, to obtain information from the maximum possible particle area.

It can be seen from figure 4.3 that the light source was not perfectly diffuse and the illumination can differ from particle to particle. Therefore, the image processing method had to be optimised in such a way that the classification of the wetting of each pixel, f_{ij}, is independent of overall light intensity. Figure 4.4 shows particles and matrices that contain the corresponding wetting value of each pixel for particles that were exposed to a high and a low overall light intensity, respectively. It can be safely concluded that wetting of each particle could be estimated independent of its illumination.

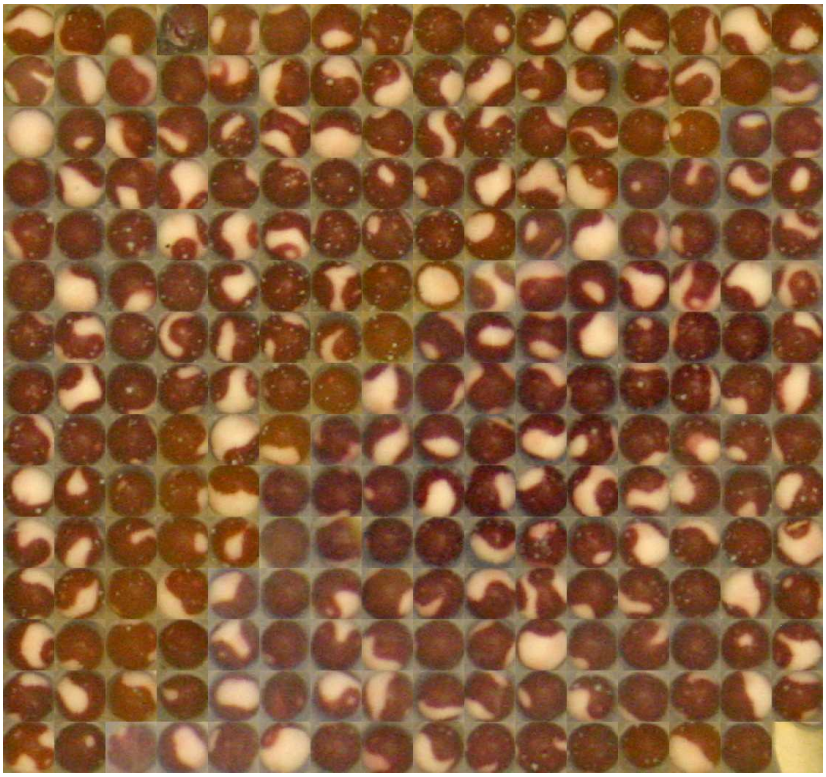

Figure 4.3: An example of the particle images extracted from a photo

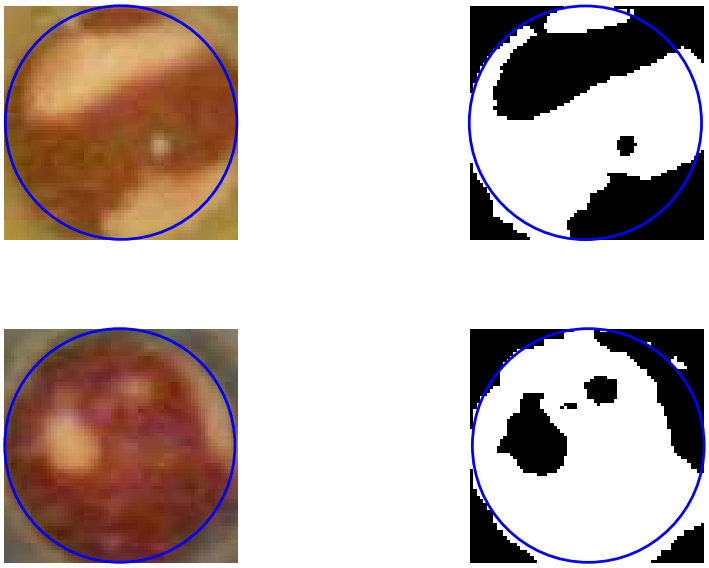

Figure 4.4: Images of particles that were exposed to different light intensities, and their corresponding pixel wetting matrices. Black pixels correspond to $f_{ij} = 0$ and white pixels to $f_{ij} = 1$. The estimated particle boundaries are indicated by means of a blue line.

As shown in figure 4.3, the colour intensities of the wetted parts of the particles from a certain experimental run were all more or less the same, indicating flow stability. A sharp boundary between non-wetted and wetted parts of the particles was obtained, showing that the flow is stable even on small scale. This clear evidence of particle-scale partial wetting even on small particles has never been reported before in literature, and is even contradicted (Ravindra et al., 1997).

4.3 Wetting distributions

After calculating the wetted area fraction on each particle, a particle wetting distribution for each bed and bed section is obtained. The obtained results are summarised in figures 4.5 to 4.7.

The overall bed wetting distributions are depicted as normalised histograms, were the height of each bar represents the fraction of the particles in the bed that have a fractional wetting between the limits of the bar. Bed section data is represented by plots of the sample averages and standard deviations as a function of the bed depth from which these samples were obtained.

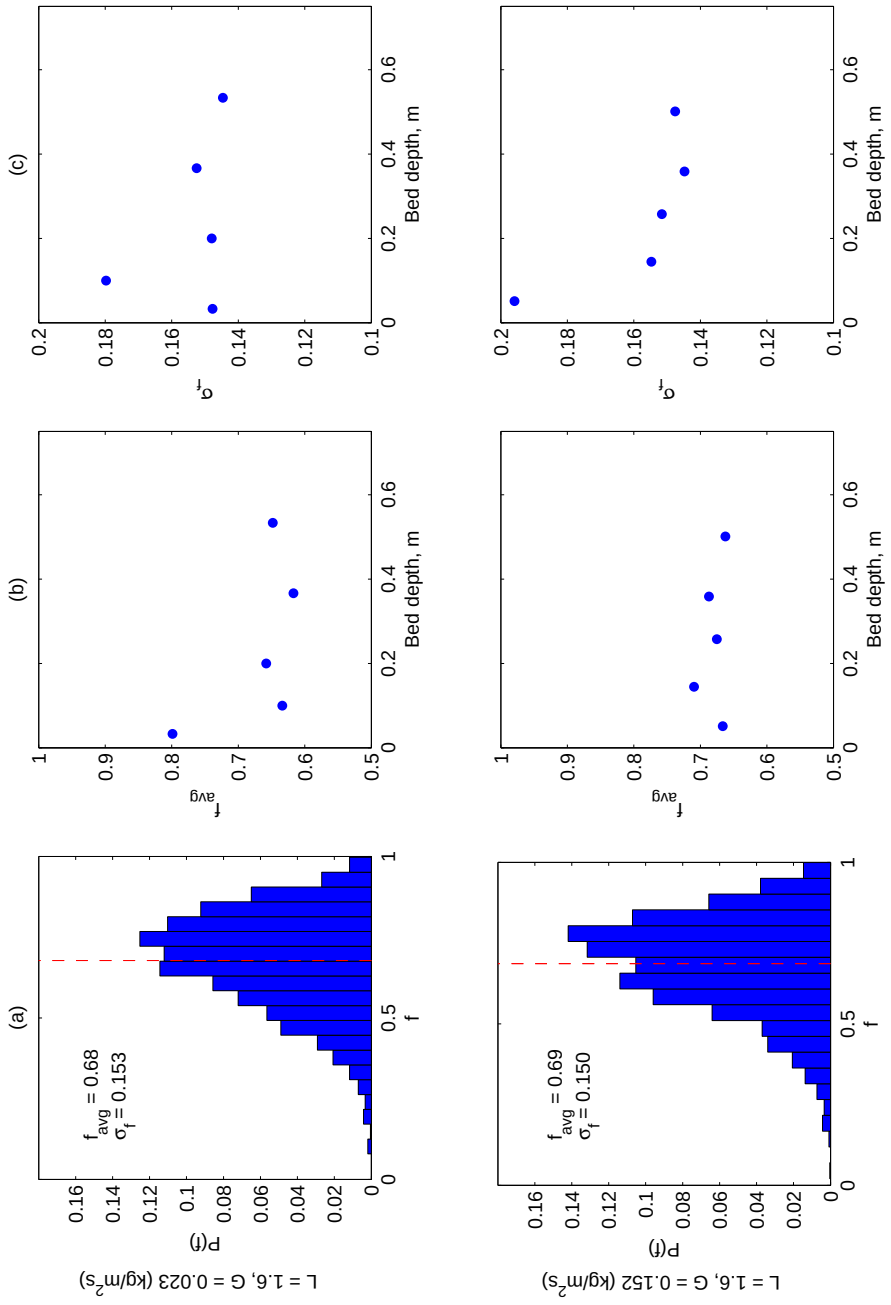

Figure 4.5: Wetting distribution data for pulse pre-wetted beds, where L = 1.60 kg/m^{2}s and varying gas flow rates. (a) Overall bed wetting distribution and (b) the average wetting efficiency and (c) standard deviation as a function of bed depth

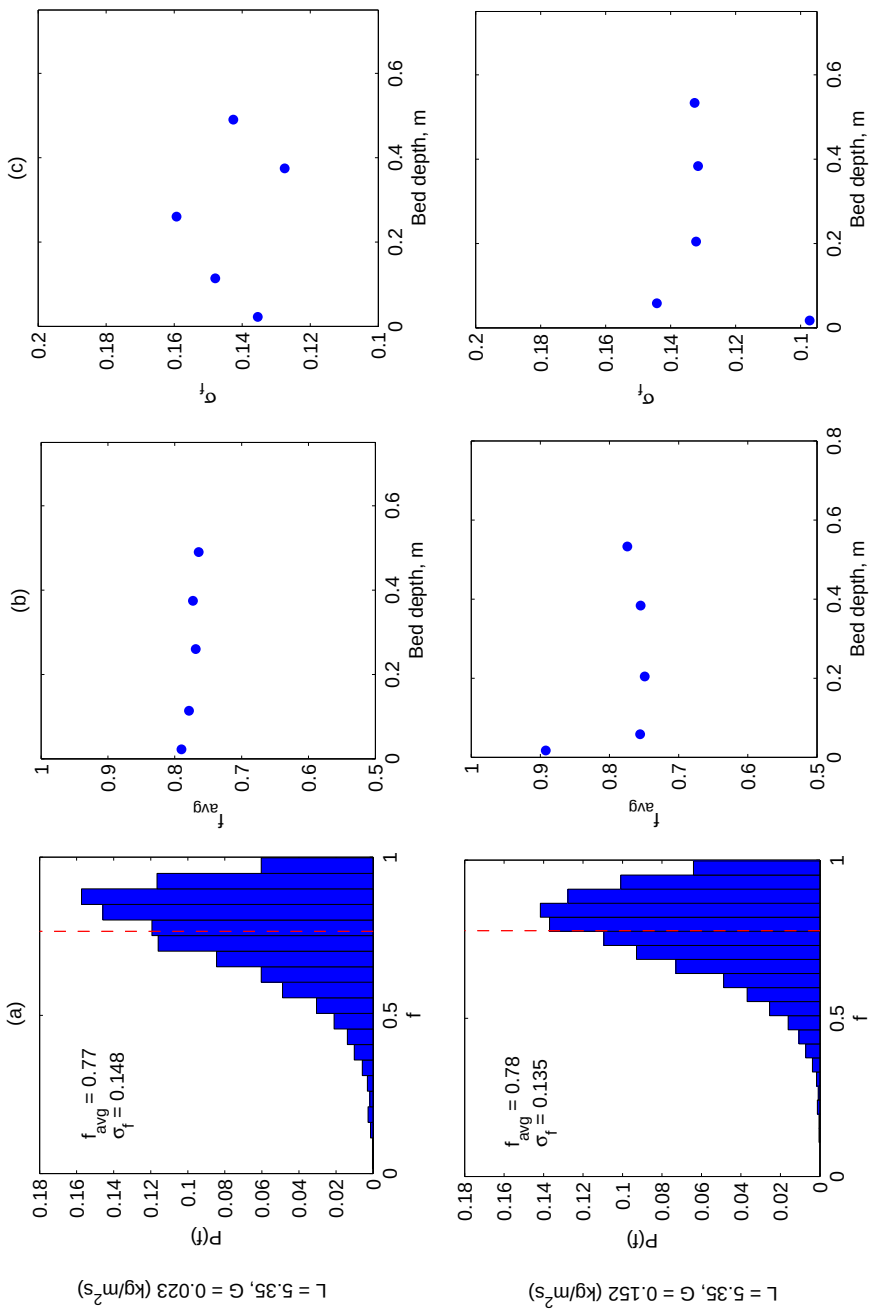

Figure 4.6: Wetting distribution data for pulse pre-wetted beds, where L = 5.35 kg/m^{2}s and varying gas flow rates. (a) Overall bed wetting distribution and (b) the average wetting efficiency and (c) standard deviation as a function of bed depth

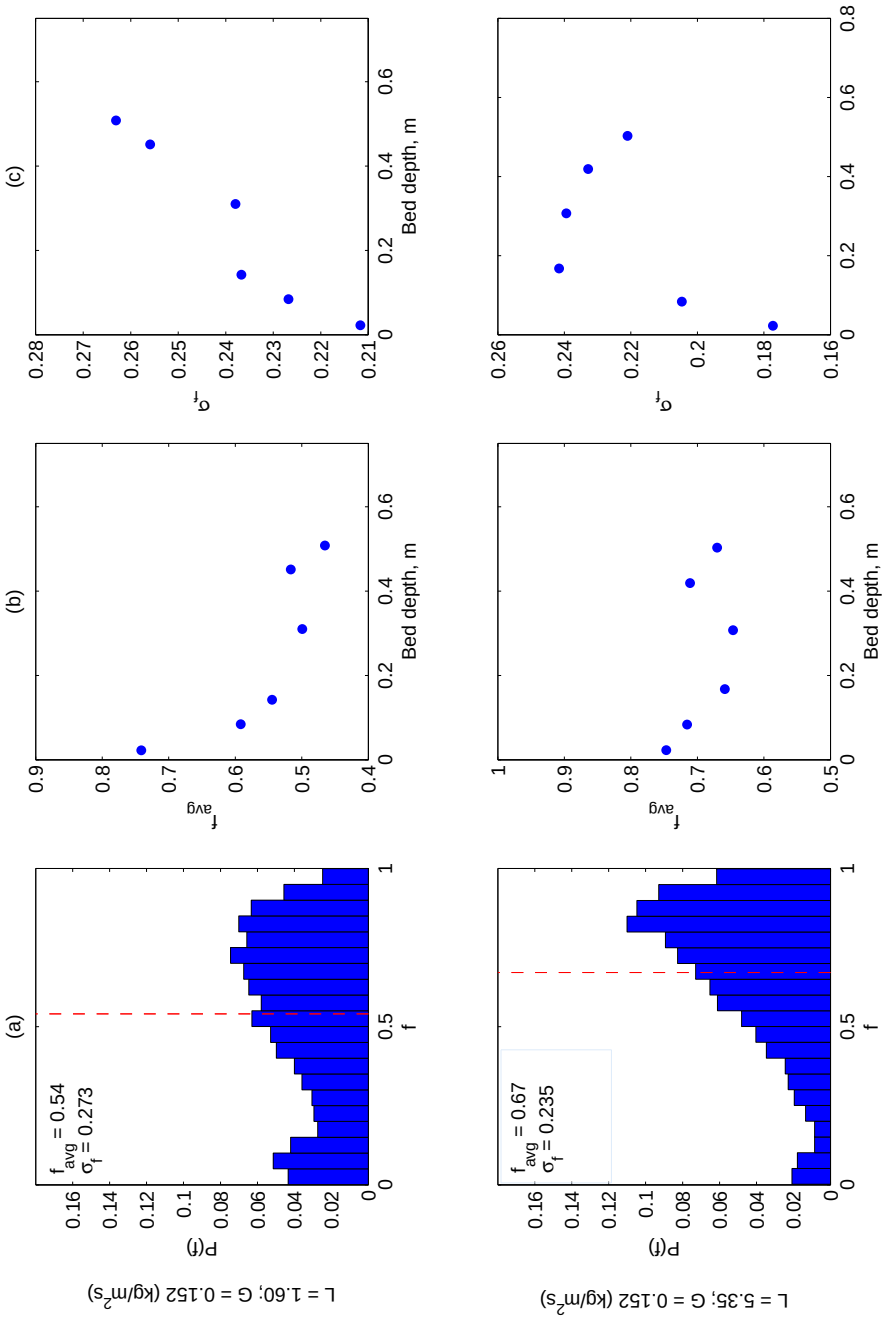

Figure 4.7: Wetting distribution data for Levec pre-wetted beds, where L = 1.60 kg/m^{2}s and 5.35 kg/m^{2}s and varying gas flow rates. (a) Overall bed wetting distribution and (b) the average wetting efficiency and (c) standard deviation as a function of bed depth

CHAPTER 5

Data evaluation

Before the data is discussed it necessary to get an idea of the level of detail that it represents. The following discussions aim to provide the reader such an idea.

5.1 Particle measurements

The pixel analysis is straightforward, except for the pixels on the boundary of the two-dimensional projection of each particle. At the particle boundaries, pixels can easily be incorrectly classified. This was primarily due to colour smudge (which is a result of the format of the digital images), loose pick-up of the particles (a small ring of pixels surrounding a particle image is classified as being part of it by the particle extraction program) and shadows on the image. Being a 2-D projection of a hemisphere, these boundary pixels represent a very large fraction of the true spherical area and incorrect classification of their wetting lead to severe errors in the estimation of the wetting of a particle. Any boundary pixel that can be incorrectly classified therefore needs to be discarded. This have as a result that only a part of the area of the particles can be evaluated, and instead of the full hemisphere each image represents, only a spherical cap with base radius $r < R$ can be evaluated for each image. This boundary effect is illustrated in figure 5.1. Note how large an area only a few boundary pixels represent.

Since the area fraction that is taken into account is such a strong function of r/R, it is important to discard as few as possible rings of boundary pixels, but enough to avoid the large errors that are caused by the boundary effect. To find this optimum "operating point", the apparent wetted fraction of a completely wetted, completely dry, and partially wetted particle was calculated as a function of r/R. Results are shown in figure 5.2. It can be seen from the figure that all pixels further away than $r/R = 0.91$ from the centre point had to be discarded due to the boundary effect (the outer three rings of pixels in

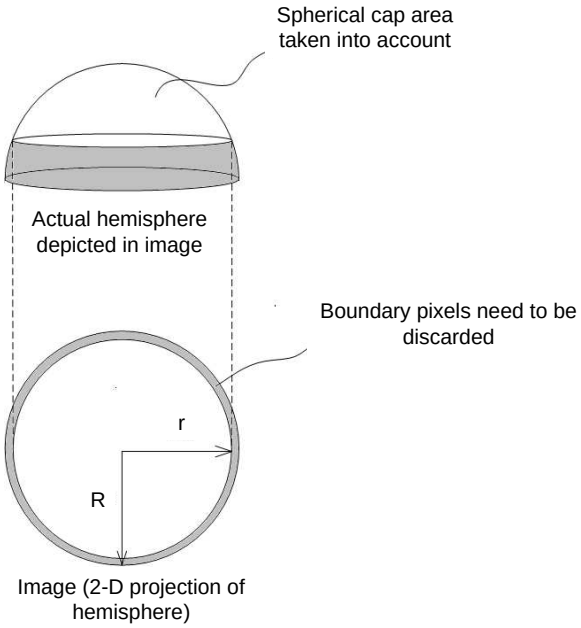

Figure 5.1: The boundary effect: Blurriness around edges of particles has as a result that some of the outer pixels of the 2-D image has to be discarded. This translates into a large spherical area that cannot be taken into account.

a 70 pixels x 70 pixels image exhibit boundary errors). This means that only 59% of the total area of a particle can be taken into account.

If only 59% of each particle's area can be evaluated, it is necessary to evaluate whether the particle wetting distributions that are obtained are representative of the true particle wetting distributions. In other words, the dependency of the particle wetting distributions on the area that is taken into account needs to be evaluated. Figure 5.3 shows the dependency of some of the particle wetting distribution histogram bins on the fractional area taken into account.

The figure is explained as follows:

- The evaluated fraction of completely wetted ($0.95 < f_n < 1$) particles has a high starting value, since dry areas on well-wetted (but partially wetted particles) are not yet encountered. As the area that is taken into account is increased dry areas are encountered on more and more particles, and the fraction of completely wetted particles decreases with increasing r/R.

- Dry areas that are encountered cause particles that were previously classified as completely wetted to shift into a "partially wetted" bin. The magnitudes of "partially wetted" bins are therefore mostly increasing with increasing r/R. The sample shown in this figure is for a well-wetted bed ($f_{avg} = 0.78$) so that the percentage of well-wetted particles ($0.75 < f_n < 0.8$) increases fast with increasing area.

- When the boundary effect is encountered, the particles that are close to completely

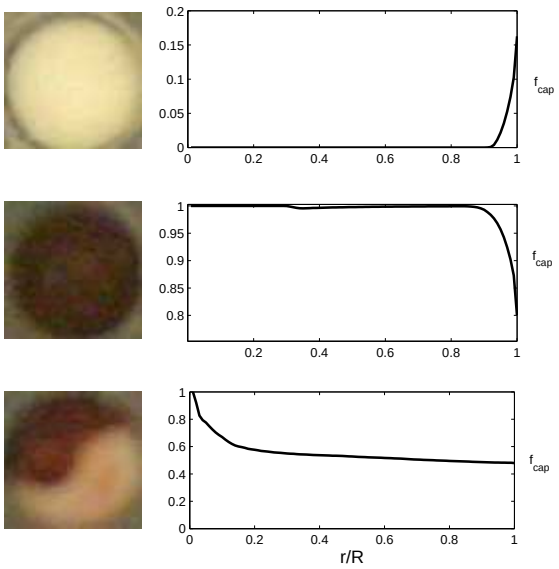

Figure 5.2: Estimation of the maximum distance, r, from the centre point for which pixels can be taken into account. Sudden errors in the evaluated fractional wetting of the completely wetted and completely dry particles indicate the boundary effect.

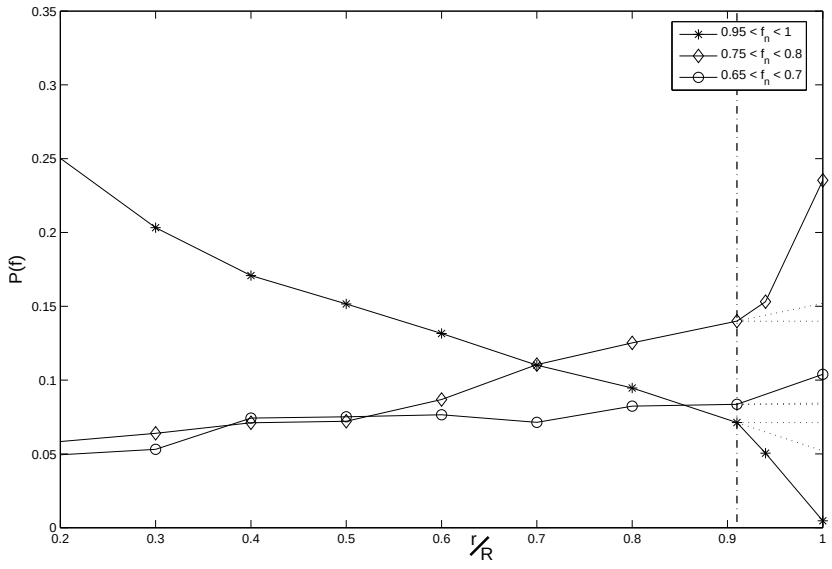

Figure 5.3: Dependency of histogram bins of the particle wetting distribution on the area fraction that is taken into account. The boundary effect is indicated with a dotted line.

wetted decreases drastically, most of which are shifted to the $0.75 < f_n < 0.8$, which is in accordance to the extent of the boundary effect (see figure 5.2). The extent of the boundary effect is increased with increasing r/R. The distributions that are reported are those for the maximum area fraction taken into account before the boundary effect is incurred ($r/R = 0.91$).

- All functions shown in figure 5 are relatively smooth up to the boundary effect. These functions are extrapolated to give an idea of the error of the reported histograms resulting from not taking all of the area into account. The extrapolated error on the fraction of completely wetted particles (about 0.025) is bigger than for all other histogram bins.

- The dependency of other particle wetting distributions on the area fraction taken into account are very similar: well-wetted particle bins are dependent on the area taken into account, but those for poorly wetted particles exhibit a weak dependency.

5.2 Statistical Significance

5.2.1 Overall bed samples

Another question is: How representative are the generated wetting distributions? Of the between 300,000 and 400,000 particles in the bed one sample image contains only about 250 particles. It should therefore be ensured that enough samples are taken from the bed to get a representative wetting distribution. Figure 5.4 shows the average wetting as determined for 15 different samples from the same bed. It is clear that even only one sample is quite representative of the average wetting efficiency throughout the bed.

For the shape of the distribution, the standard deviation is of importance. Sample standard deviations are shown in figure 5.5. From this figure it is clear that one sample is *not* representative of the whole packing in terms of the standard deviation of the wetting of the particles in a bed.

To evaluate how many samples are needed to retrieve a representative shape of the wetting distribution, the following error function was defined:

$$\begin{aligned} E_n &= \frac{\sigma_n - \sigma_{n-1}}{\sigma_n} \\ \text{where } n &= \text{total number of samples, samples} \end{aligned} \tag{5.1}$$

For the samples to be representative of the bed, E_n should show a tendency toward zero. As shown in figure 5.6, E_n stabilizes at a total sample size of three samples, and the fifteen samples that were taken from each bed are therefore sufficient to characterize the wetting distributions.

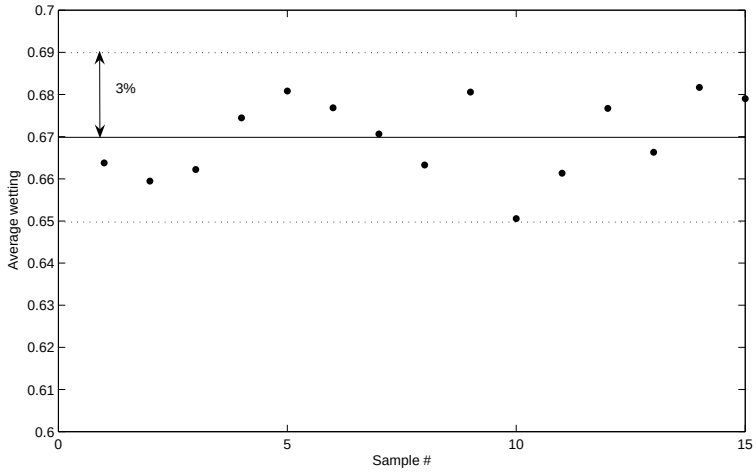

Figure 5.4: Estimated average wetting efficiency for 15 samples taken from a pulse pre-wetted bed prepared at $L = 1.6$ kg/m^2 s and $G = 0.023$ kg/m^{2}s. All values lies within 3% of the mean.

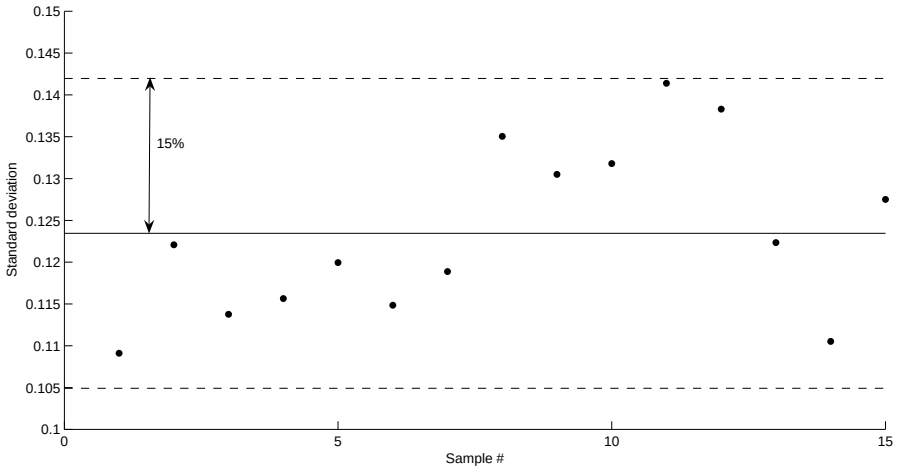

Figure 5.5: Standard deviations for the same samples as shown in figure 5.4

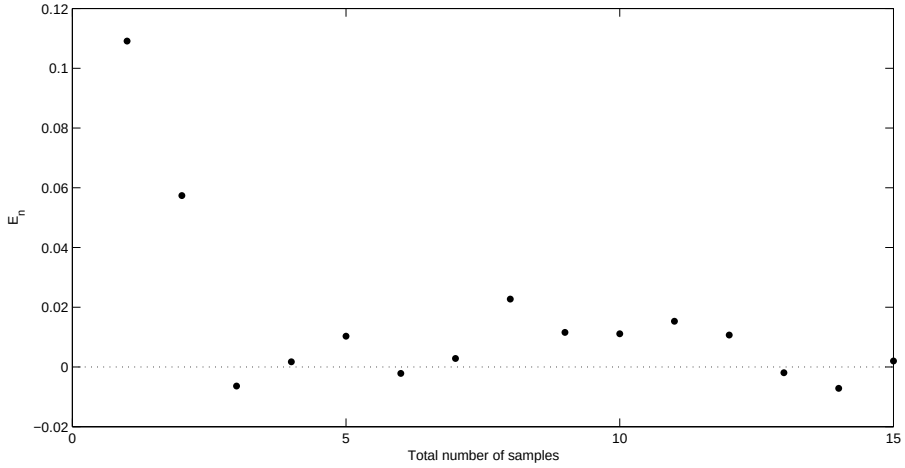

Figure 5.6: Difference in standard deviation between two successive sample sizes. The difference is expressed as a fraction of the total sample standard deviation.

5.2.2 Samples taken from different bed sections

It has been established that the data generated for the total packings are statistically representative. It is however not possible to verify the representativeness of the data generated for different bed sections in the same fashion as was done for the total packings. This is since only one sample was taken from each section. To get at least some idea as to which extend the column section data can be analysed, it was tested whether the difference between average wetting and sample standard deviation of samples taken from the different bed sections is larger than the maximum difference for the same parameters determined for the total bed packings (i.e. 3% for f_{avg} and 15% for σ_f). If so, the data can be analysed with some confidence. Figures 5.7 and 5.8 illustrate this test: According to these criteria, the only fact that can be concluded is that the average wetting efficiency at a section in the bed decreases considerably within 10 cm. No conclusions can be made in terms of the axial variation of the standard deviation. An exception to this rule is when a definite trend can be observed for several data sets. When viewing wetting and wetting distributions as a function of the bed depth, it should be kept in mind that this is most likely strongly dependent on the distributor (Stanek et al., 1981; Lutran et al., 1991; Ravindra et al., 1997; Marcandelli et al., 2000). Results are therefore only applicable for a uniform distribution.

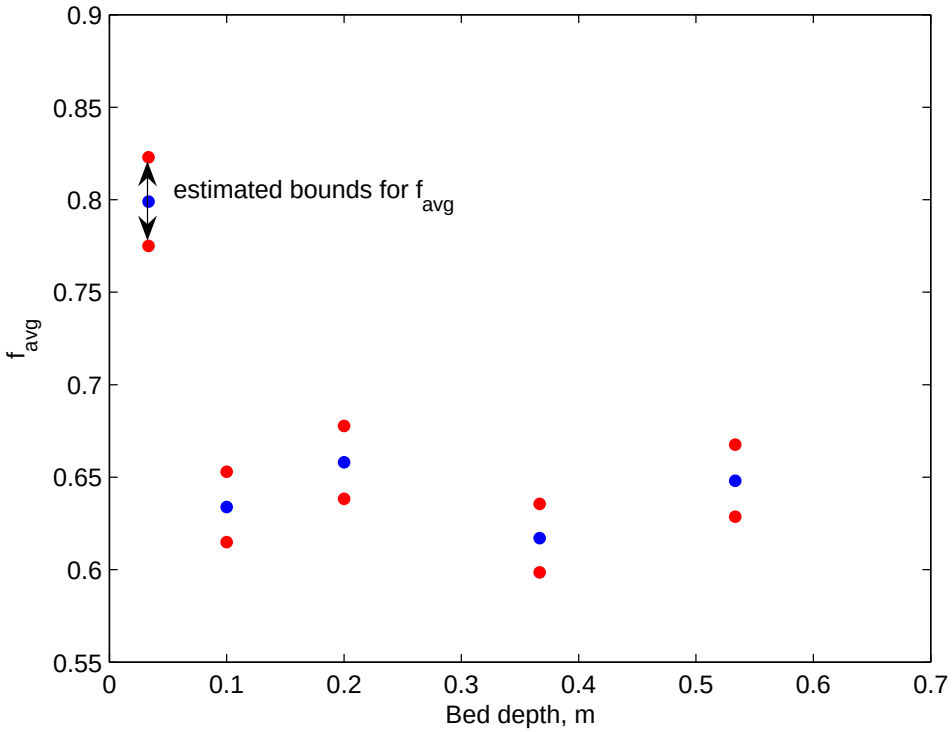

Figure 5.7: Plot of average wetting efficiency vs. bed depth, for samples taken from the same bed as in figure 5.4. The estimated range between which each datapoint may vary is also shown.

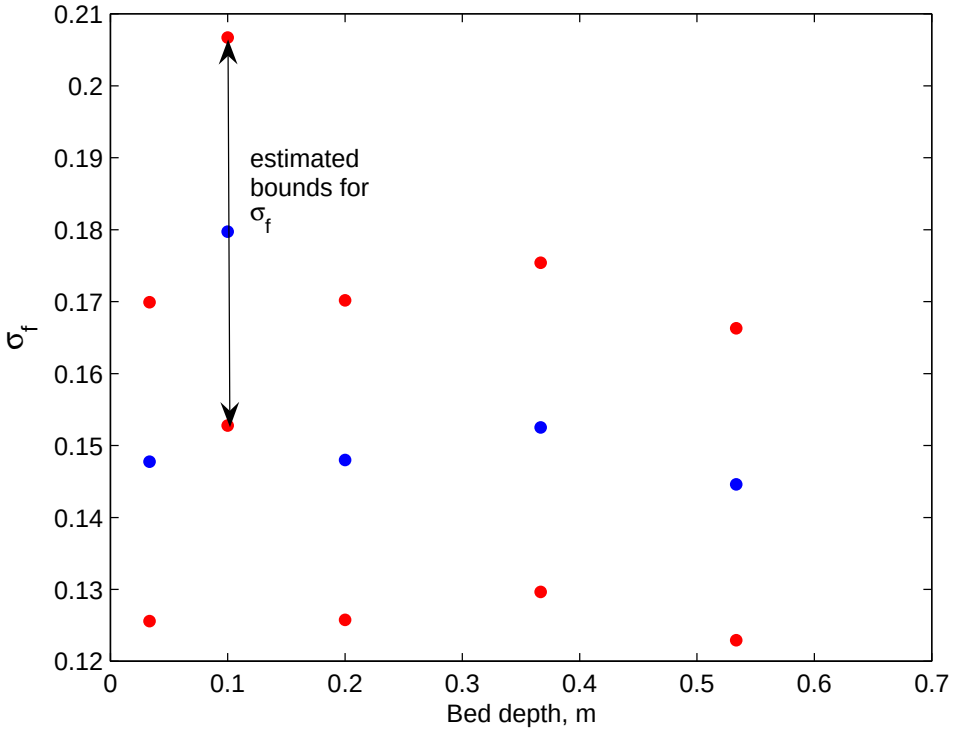

Figure 5.8: Plot of standard deviation in particle wetting vs. bed depth, for samples taken from the same bed as in figure 5.4. The estimated range between which each datapoint may vary is also shown.

5.3 Conclusions

In this chapter, the level of detail at which the data can be analysed has been estimated, and can be summed up as follows:

- Fifty-nine per cent of the total area of each particle could be estimated with accuracy. Histogram bins where $f_n > 0.75$ contain errors resulting from not taking all of the area into account, all being less than 0.025.

- Statistically, the data generated from total bed samples seem to be representative. One should however remember that the data is still a function of the method as to which it was generated (see previous bullet). Since this method was used consistently, the data is useful for detailed comparison, but not as the exact numerical truth for a certain bed on its own. Keep in mind that the figures shown in section 5.2 are all generated from data from the same bed, and other beds may differ. If the same conclusion can not be made for other beds, it will be stated in the report, before the data of such a bed is analysed.

- Definite criteria was set as to how the data generated from bed sections are to be viewed, and bed section data will be treated as was illustrated.

CHAPTER 6

Interpretation of the obtained wetting efficiency distributions in terms of flow morphology

6.1 Trickle-flow morphology according to literature

Before the respective bed data is discussed, it is good the have a second look at trickle-flow morphology as discussed in literature, specially in terms of the pre-wetting procedure.

For pulse pre-wetted beds, Lutran et al. (1991) observed film flow. The flow was predominantly over areas of low local bed porosity, and the flow pattern was not a function of liquid flow rate. All of the bed was contacted with the liquid. Kan & Greenfield (1978) did however find hysteresis with gas flow in these beds, which suggests that the pattern of flow is changed with gas flow rate. The suggested effect is that the gas flow "re-aligns" liquid connection points between particles, so that the effective tortuosity of the bed is reduced. Ravindra et al. (1997) found overall complete wetting in a pulse pre-wetted bed.

In Levec pre-wetted beds Christensen et al. (1986) found that at low liquid flow rates, filament flow prevails, rapidly changing to film flow at a certain critical flow rate. The fraction of film flow was a function of liquid and gas flow rates. Hysteresis in Levec pre-wetted beds is explained in terms of particle wettability: Recently wetted particles are more wettable than those that were not contacted by the liquid since draining the bed. All above observations were made for beds containing glass spheres.

6.2 Pulse pre-wetted beds

6.2.1 Influence of the liquid flow rate

The influence of the liquid flow rate on the particle-scale wetting distribution in pulse pre-wetted beds is depicted in figures 6.2 to 6.3. The following observations can be made from these figures:

- For all flow rates, all of the particles were in some fashion contacted by the liquid.
- All distributions follow smooth curves, which suggests that only one type of flow was present.
- The shape of all the distributions are very similar, indicating that the same type of flow was present in all beds, independent of liquid flow rate. Literature suggests that this flow type will be film flow.
- In literature, the influence of liquid flow rate in pulse pre-wetted beds is described as follows. Liquid flows in the form of films over the packing. The flow pattern in the bed is independent of liquid flow rate, and no new liquid "paths" are formed when the liquid flow is increased. Increased liquid flow rate does however increase liquid holdup, and the films on the particles therefore has to thicken and expand. In terms of wetting efficiency distributions, this means that the wetting of *each wetted particle* is increased.

  The effect on the wetting distribution that is expected when the wetting on each particle is increased equally, is shown in figure 6.1: the distribution only shifts a certain distance to the right, without a change in the overall shape. The only change in distribution shape is that one would expect a peak at $f_n = 1$, since no particles can be more than completely wetted.

  One can see from figures 6.2 and 6.3 of f_n smaller than about f_{avg}, this expected trend is closely followed (compare these figures with figure 6.1), and one can conclude that the wetting efficiency is increased more or less equally on each particle within this range of wetting efficiencies. Such an equal increase shows that with an increase in liquid flow and liquid holdup, *the "extra" liquid is divided among existing flow paths (no new channels, films or rivulets are formed).*

  At high particle wetting efficiencies, there is however a disagreement with figure 6.1: The amount of particles that are completely wetted does not increase as much as would be expected, but is distributed over a few ranges of f_n. This suggests that the maximum wetting efficiency for many of the particles in the bed is less than one, and it seems as though some mechanism prevents complete wetting of the particles. The most obvious "mechanism" is that the boundary effect was not compensated

for well enough (see chapter 5.1), but this can only account for the last two wetting intervals being misinterpreted. For both figures, there are however already peaks in the two intervals before this, and it can therefore be concluded that it is some mechanism in the flow morphology that prevents complete particle wetting. This may be either areas that are inaccessible to liquid flow, or stagnant liquid holdup. In the latter case, one would however not expect such a sharp boundary between the white and red zones on the particles as is shown in figure 4.3, since mass transfer over static and dynamic zones is possible.

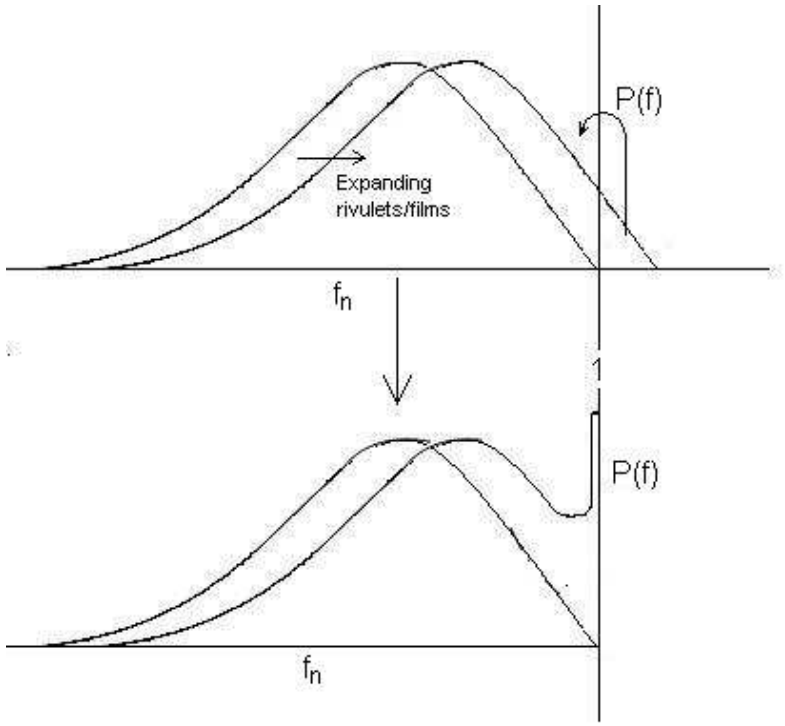

Figure 6.1: Expected change of wetting distribution when the wetting on each particle is increased equally. This expansion is likely to occur when the holdup in the bed is increased.

6.2.2 Influence of the gas flow rate

The effect of increased gas flow rate when the liquid flow rate is kept constant is shown in figures 6.4 and 6.5. On a first glance, one would conclude from these figures that the gas flow does not have any effect on the liquid flow morphology, since the distributions for a constant liquid flow rate look extremely similar, even although the gas flow rates are different.

A closer look reveals that the gas flow does have some effect: In the previous section, it has been suggested that the width of films in the bed is a function of *liquid holdup*. The obtained wetting distributions for different liquid flow rates supports this suggestion. In

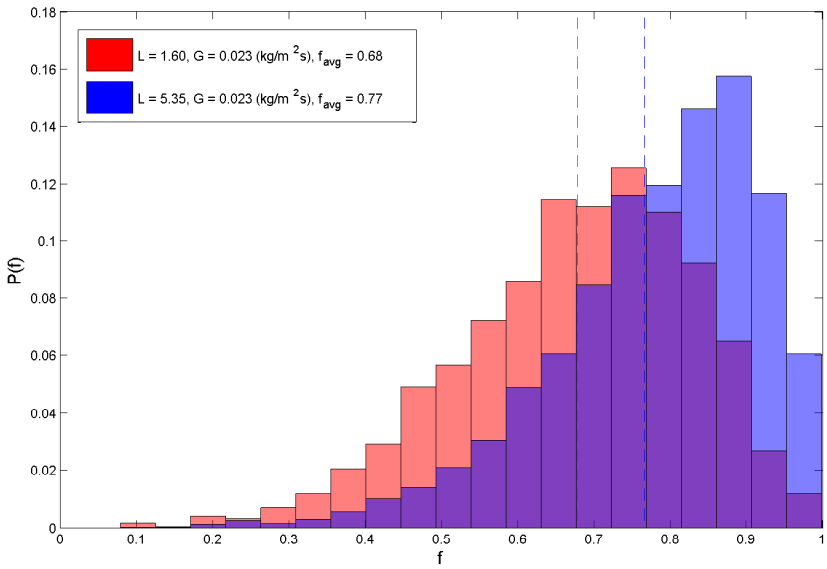

Figure 6.2: Wetting distributions for *pulse* pre-wetted beds with L = 1.60 kg/m^{2}s and L = 5.35 kg/m^{2}s. Gas flow rate was G = 0.023 kg/m^{2}s

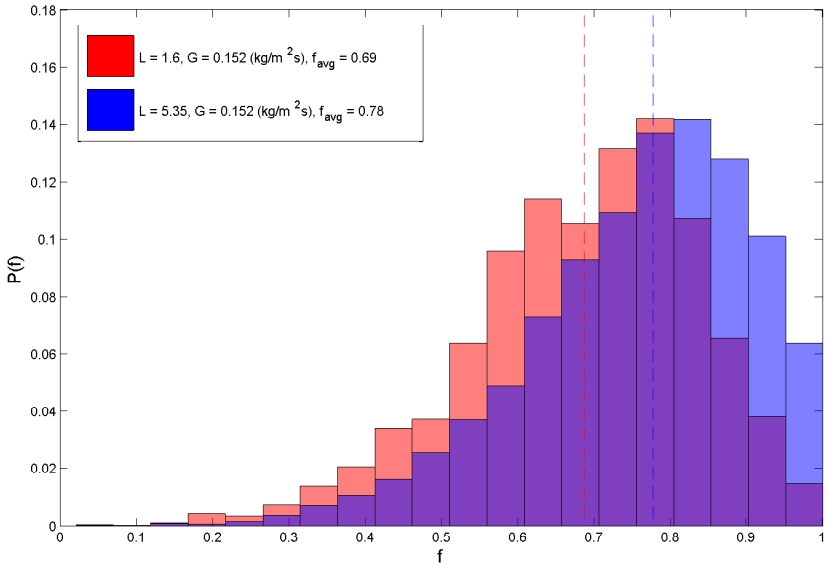

Figure 6.3: Wetting distributions for *pulse* pre-wetted beds with L = 1.60 kg/m^{2}s and L = 5.35 kg/m^{2}s. Gas flow rate was G = 0.152 kg/m^{2}s

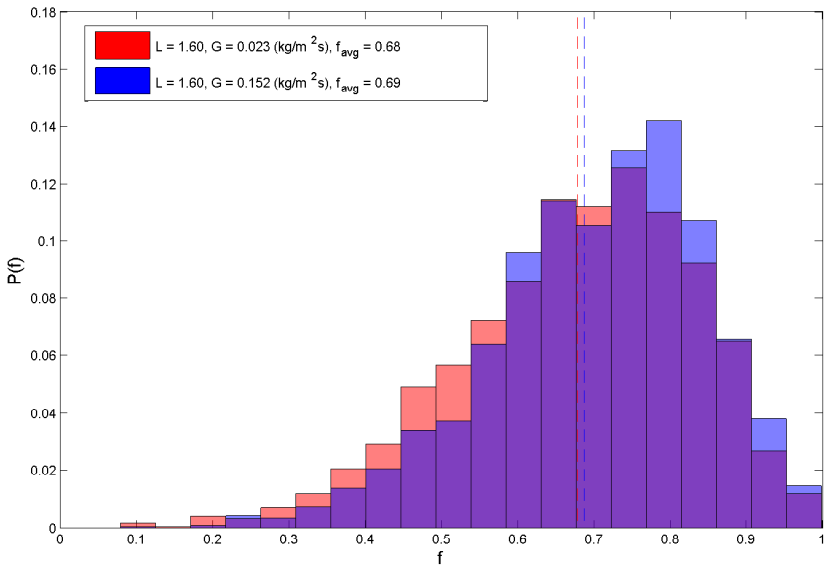

Figure 6.4: Wetting distributions for *pulse* pre-wetted beds with G = 0.023 kg/m^{2}s and G = 0.152 kg/m^{2}s. Liquid flow rate was L = 1.60 kg/m^{2}s

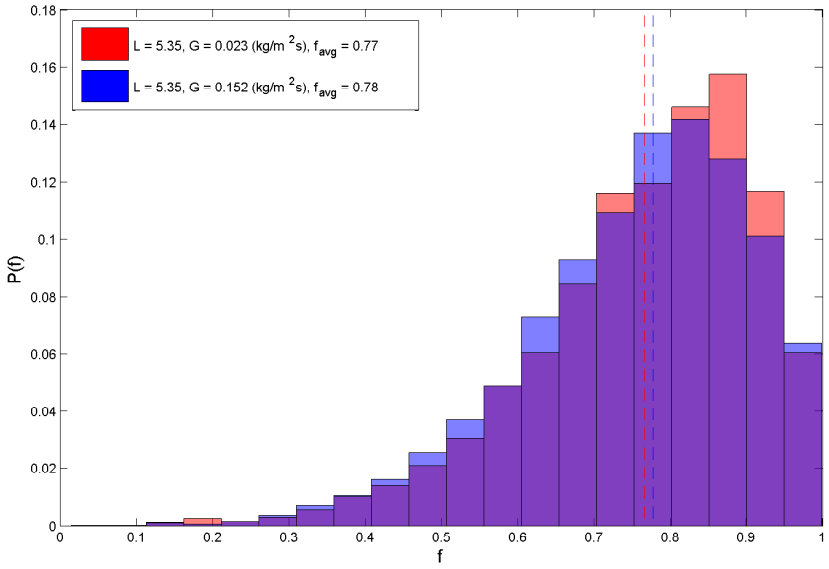

Figure 6.5: Wetting distributions for *pulse* pre-wetted beds with G = 0.023 kg/m^{2}s and G = 0.152 kg/m^{2}s. Liquid flow rate was L = 5.35 kg/m^{2}s

these figures, on the other hand, the distributions are rather constant whereas the liquid holdup is considerably lower for the beds that were exposed to higher gas flow rates. An explanation for this can be found in literature (see chapter 2.3.3): Increased gas flow rate results in increased gas-liquid shear, thereby spreading the liquid over the particles. At high pressures, many authors therefore found that the wetting efficiency increases with pressure drop for a constant liquid flow rate. According to the explanation given by Al-Dahhan & Dudukovic (1995) in terms of the trickle-flow model of Holub et al. (1992) a more general description of the influence of pressure drop on wetting efficiency is that for a constant *liquid holdup*, the pressure drop will increase the wetting efficiency.

This is what is observed here: Although the gas flow rate decreases the holdup, it spreads the liquid over the solid area thereby preventing a decrease in particle wetting efficiency. This observation is in close agreement with that of Lazzaroni et al. (1988) who found a relative constant radial distribution of wetting efficiency with increased gas flow in a super pre-wetted bed, even although the increased gas flow resulted in radial liquid holdup variations. The observation that the gas flow rate does not change the average wetting efficiency much, also agrees with literature data obtained under atmospheric conditions with gas molecular mass similar to that of N_2 (Goto et al., 1975; Lakota & Levec, 1990).

6.3 Levec pre-wetted beds

The different wetting distributions obtained from the beds that were Levec pre-wetted for two different liquid flow rates are shown in figure 6.6. The following observations can be made from the wetting distributions for Levec pre-wetted beds:

- Firstly, and importantly, it is clear that in these beds, all particles in the bed were *not* contacted with the liquid.
- At least equally important is the fact that for the same gas and liquid flow conditions, the average wetting efficiencies of the Levec pre-wetted beds are considerably lower than for the corresponding pulse pre-wetted beds. This is shown in figures 6.7 and 6.8.
- The distributions look bimodal, that is, they exhibit two local maxima, one at $0.05 < f_n < 0.2$ and one at some higher value of f_n. A bimodal distribution suggests that the data came from two different populations (Statsoft, 2005). It is therefore proposed that two different flow types might be present in Levec pre-wetted beds. In literature, these two types of flow were identified as film flow and filament flow (Christensen et al., 1986). The filament flow would then be the source of the significant amount of particles that were poorly wetted. This agrees with the nature of filament flow (see chapter 2.2.1).

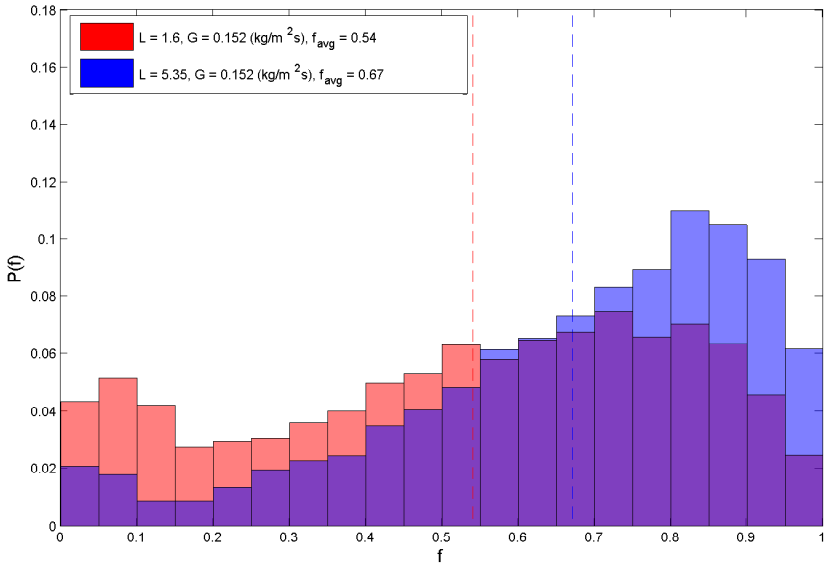

Figure 6.6: Wetting distributions for *Levec* pre-wetted beds, L = 1.60 kg/m^{2}s and L = 5.35 kg/m^{2}s. Gas flow rate was L = 0.152 kg/m^{2}s

- By increasing the liquid flow rate, the amount of particles with a very low wetting efficiency decreases significantly, and the shape of the wetting distribution at the higher liquid flow rate approaches that of a pulse pre-wetted bed (or film flow). If the explanation of two types of flow in a Levec pre-wetted bed is adopted, this suggests that the fraction of film flow is increased by the liquid flow rate. One would then expect that the wetting distribution of a Levec pre-wetted bed will become equal to that of a corresponding pulse pre-wetted bed at high liquid flow rates.

The above description of trickle-flow in Levec pre-wetted beds is in agreement with the observations of Christensen et al. (1986), who found that the fraction of film flow in a Levec pre-wetted bed is a function of the liquid flow rate. Quantitatively, the obtained distributions does not seem to agree very well with the data of these authors, who suggested a very low fraction of film flow in the beds at the liquid and gas flow rates in figure 6.6, whereas especially the shape of the distribution for L = 5.35 kg/m^{2}s suggests a high fraction of film flow. These authors did however find that ratio film to filament flow is very sensitive to the conditions in the bed and it is possible that small differences in experimental conditions may have caused this disagreement.

6.4 Flow morphology as a function of bed depth

Although it was stressed in chapter 4 that the bed depth data should be treated apprehensively, some general observations can be made.

For all the super pre-wetted beds, the value of the average wetting efficiency seem

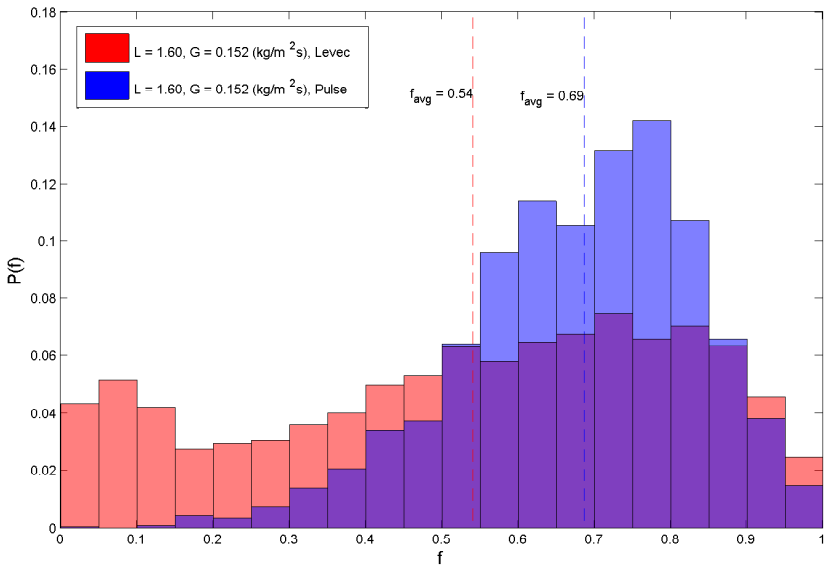

Figure 6.7: Distributions for a pulse and a Levec pre-wetted bed with L = 1.60 kg/m^{2}s and G = 0.152 kg/m^{2}s.

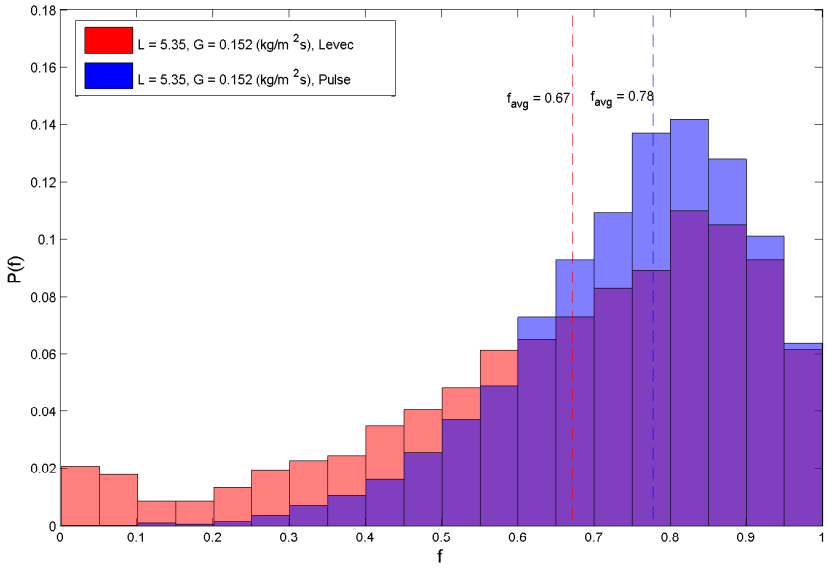

Figure 6.8: Distributions for a pulse and a Levec pre-wetted bed with L = 5.35 kg/m^{2}s and G = 0.152 kg/m^{2}s.

to stabilise before a bed depth of 10 cm is reached, and one can come to the conclusion that the flow in the bed develops within this distance. A small disagreement with this conclusion seem to come out of the sample standard deviation versus bed depth plots in figures 4.5 and 4.6: a peak in the sample standard deviations at $z \approx 0.1$ m is found for most of the pulse pre-wetted beds. This seems to be repeatable for all the pulse pre-wetted beds. An analysis of the distribution plots for the different bed depths did not show a conclusive difference in wetting distribution shape, and it is doubtful whether any significance can be attached to these observed peak.

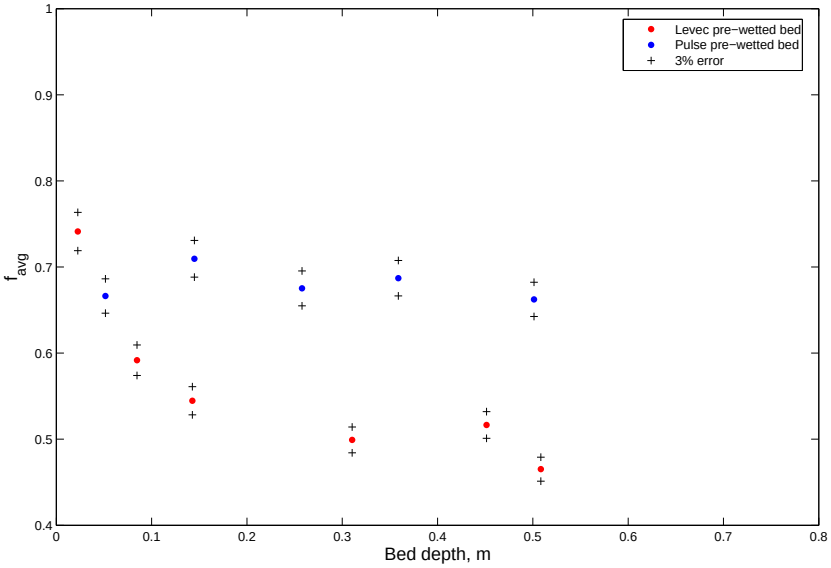

Figure 6.9: Comparison of the development of flow between a Levec- and a pulse pre-wetted bed. L = 1.60 kg/m^{2}s and G = 0.152 kg/m^{2}s.

It takes considerably longer for flow in Levec pre-wetted beds to develop. Figures 6.9 and 6.10 shows the average wetting efficiency as a function of bed depth for the Levec pre-wetted beds in comparison to the pulse pre-wetted beds at the same liquid flow rates. One could reason that the average wetting efficiency is reached later for the Levec-wetted beds only because the wetting efficiency in these beds is lower, but the shapes of the average wetting efficiency versus bed depth data for these beds suggest that the development of flow is a slower process in these beds: For the bed where L = 1.60 kg/m^{2}s and G = 0.152 kg/m^{2}s, a stable average wetting is not reached within the maximum bed depth for which wetting efficiency data was obtained. This observation is substantiated even more when one looks at the change of wetting efficiency distribution with bed depth in this bed. Figure 6.11 shows histogram plots for this bed at different bed sections. The fraction of dry particles deep in the bed is *considerably* higher than in the top of the bed. It can therefore be concluded that for this low liquid flow-rate, the liquid is more and more maldistributed while going down the bed. This effect is insignificant at the higher

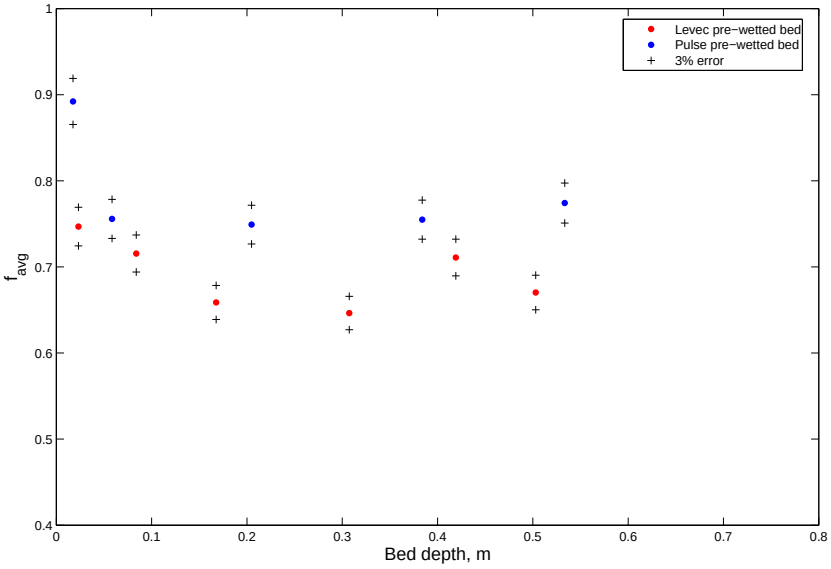

Figure 6.10: Comparison of the development of flow between a Levec- and a pulse pre-wetted bed. L = 5.35 kg/m^{2}s and G = 0.152 kg/m^{2}s.

liquid flow rate (see figure 6.12).

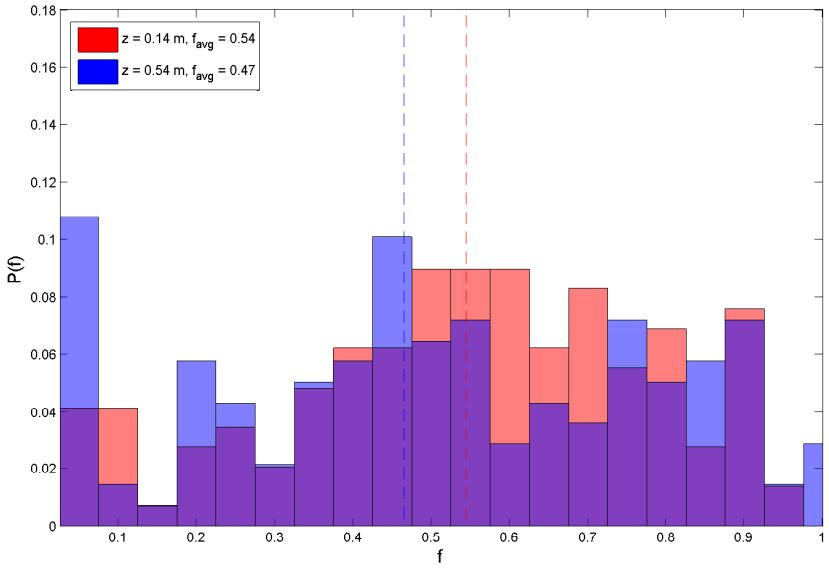

Figure 6.11: Wetting distributions obtained from different depths in a Levec pre-wetted bed. L = 1.60 kg/m^{2}s and G = 0.152 kg/m^{2}s. Note the considerable difference in the fraction of dry particles between these two distributions.

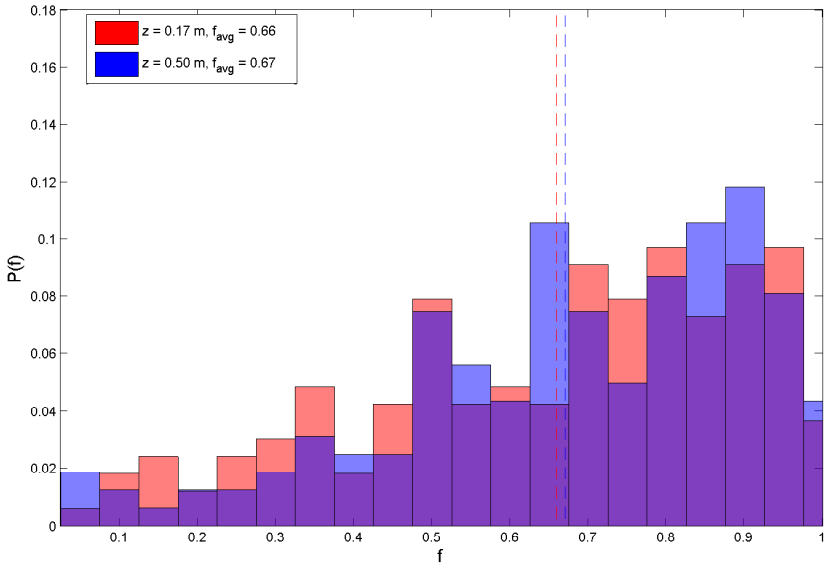

Figure 6.12: Wetting distributions obtained from different depths in a Levec pre-wetted bed. L = 5.35 kg/m^{2}s and G = 0.152 kg/m^{2}s.

6.5 Summary

The observations for pulse pre-wetted beds can be summarised as follows.

- For pulse pre-wetted beds, all particles are in some fashion contacted by the liquid. This was already observed in literature.
- The continuous shape of the wetting distributions for all pulse pre-wetted suggest that only one type of flow is present in these beds. This is in agreement with literature, which suggests exclusively film/rivulet flow.
- The flow pattern in a pulse pre-wetted bed seems to be more or less independent of liquid flow rate.
- Since the flow pattern in the bed is constant, increased liquid holdup results in thicker rivulets and films, which in turn expands the solid-liquid contacting area on each particle.
- An increase in gas flow rate results in increased liquid-gas shear, spreading the liquid over the solid area. The net effect of increased gas flow on the wetting efficiency distribution is very small since increased gas flow also results in decreased liquid holdup.
- The flow distribution in the bed does not change much as the liquid goes down the bed, and seem to stabilise within 10 cm for all pulse pre-wetted beds.

For the Levec pre-wetted beds the obtained distributions differ significantly from that of the pulse pre-wetted beds:

- The average wetting efficiencies in the Levec pre-wetted beds were significantly lower than those for the corresponding pulse pre-wetted beds.
- In all the pulse pre-wetted beds, all the particles were contacted by the liquid. In the Levec pre-wetted beds a significant fraction of the bed was completely dry. This fraction decreases with increasing liquid flow rates.
- Bimodal distributions in the Levec pre-wetted beds suggest that in these beds two different flow types are present. According to literature, this would be film and filament flow (Christensen et al., 1986). If these are the types of flow that are present, the fraction of film flow in the bed increases with increasing liquid flow rate, and it is expected that Levec pre-wetted beds will behave as pulse pre-wetted beds at high liquid flow rates.
- At the lower liquid flow rate (1.60 kg/m^{2}s), the liquid appears to be more and more maldistributed in Levec pre-wetted beds as it goes down the packing. This was not observed for the higher liquid flow rate (5.35 kg/m^{2}s).

CHAPTER 7

Effect of the distribution of particle wetting efficiency on reactor modelling

Many models that describe the effect of wetting efficiency on reactor performance are provided in literature. Most of the models are based on particle-scale phenomena, and it is possible that the distribution of the particle wetting plays an important role in the performance of a reactor. Before one can make any conclusions about the influence of pre-wetting or flow type on trickle-bed reactor performance, one has to investigate this possibility.

Most trickle-bed reactor modeling was previously performed by using only the (overall) average wetting efficiency of a bed. Results obtained from the different models that are to be investigated, will be referred to as *average wetting results*. Since particle wetting efficiency distribution data is available, one can approach reactor modeling in a different way to incorporate wetting efficiency distribution:

- The parameter of interest, for example η_{TB}, is calculated for the whole range of wetting efficiencies that were presented in the wetting efficiency distributions (i.e. between 0 and 1, in intervals of 0.05).
- The results for this range of wetting efficiencies was then weighted according to the wetting distribution and then summed, to obtain the overall value of the parameter of interest.

Thus obtained results will be referred to as *wetting distribution results*. The above approach for the estimation of the role particle wetting distribution on reactor modeling only has merit if models that describe particle-scale phenomena are used.

When reading this chapter, one has to keep in mind that all results are model-based. All modeling was performed assuming first order kinetics with respect to the limiting

reagent.

7.1 Liquid-limited reactions

The most widely utilised particle-scale model that estimate the effect of wetting efficiency on liquid limited reactions, is that of Dudukovic (1977). This model is presented in chapter 2.3.1 (equation 2.13). The average wetting trickle-bed efficiency for this model will be:

$$\eta_{TB,l} = f_{avg} \frac{\tanh\left(\frac{\phi}{f_{avg}}\right)}{\phi} \tag{7.1}$$

whereas the wetting distribution trickle-bed efficiency is given by:

$$\eta_{TB,l} = \sum^{n} P(f).f_n \frac{\tanh\left(\frac{\phi}{f_n}\right)}{\phi} \tag{7.2}$$

where P(f) is the fraction of particles in the bed with a fractional wetting of f_n. The presented model only takes into account internal mass transfer limitations. The relationship between wetting efficiency and external mass transfer limitations is linear for liquid-limited reactions so that only the average wetting has an effect on the overall external mass transfer rate.

The above calculations were performed for all the obtained wetting distributions, to compare average wetting trickle-bed efficiency with the wetting distribution trickle-bed efficiency for liquid limited reactions. The results for the Levec pre-wetted beds are shown in figures 7.1 and 7.2.

These figures show that, in Levec pre-wetted beds, the average wetting efficiency of a bed over-predicts the trickle-bed efficiency for a liquid-limited reaction with low Thiele modulus particles. This is because the relationship between wetting efficiency and particle efficiency is non-linear for these values of the Thiele modulus. The fact that the particle wetting is not equally distributed, will therefore result in a lower trickle-bed efficiency than expected (according to the average wetting efficiency). An additional effect is that some of the particles are completely dry, and will always have an adverse effect on reactor performance, even when mass transfer limitations are of no importance (very low ϕ). This can not be accounted for by an average wetting efficiency, which will always predict a 100% trickle-bed efficiency at very low values of the Thiele modulus. The dotted lines in figures 7.1 and 7.2 show the effect of dry particles on η_{TB}: average wetting trickle-bed efficiencies were calculated for the packing excluding completely dry particles, and then multiplied by one minus the fraction of completely dry particles.

It was found that for all pulse pre-wetted beds, the relationship between Thiele modulus and trickle-bed efficiency could be adequately described by means of only an average

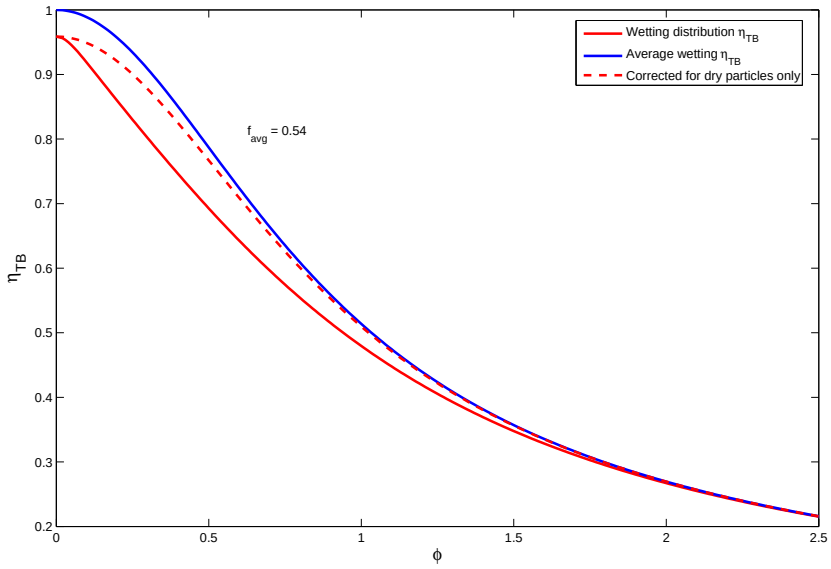

Figure 7.1: Average wetting and wetting distribution trickle-bed efficiencies as a function of Thiele modulus, for a *Levec* pre-wetted bed. L = 1.60 kg/m^{2}s; G = 0.152 kg/m^{2}s

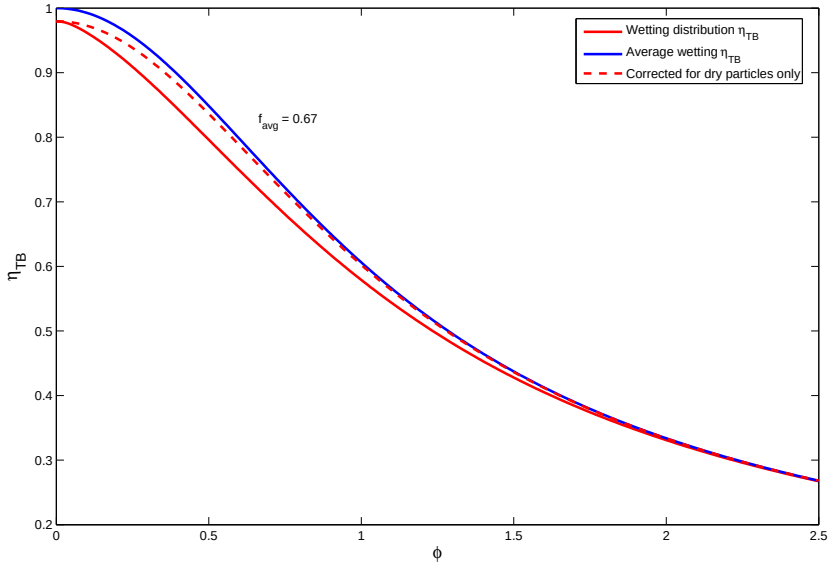

Figure 7.2: Average wetting and wetting distribution trickle-bed efficiencies as a function of Thiele modulus, for a *Levec* pre-wetted bed. L = 5.35 kg/m^{2}s; G = 0.152 kg/m^{2}s

wetting efficiency. This is shown in figure 7.3. Results for other pulse pre-wetted beds are similar to those presented in this figure.

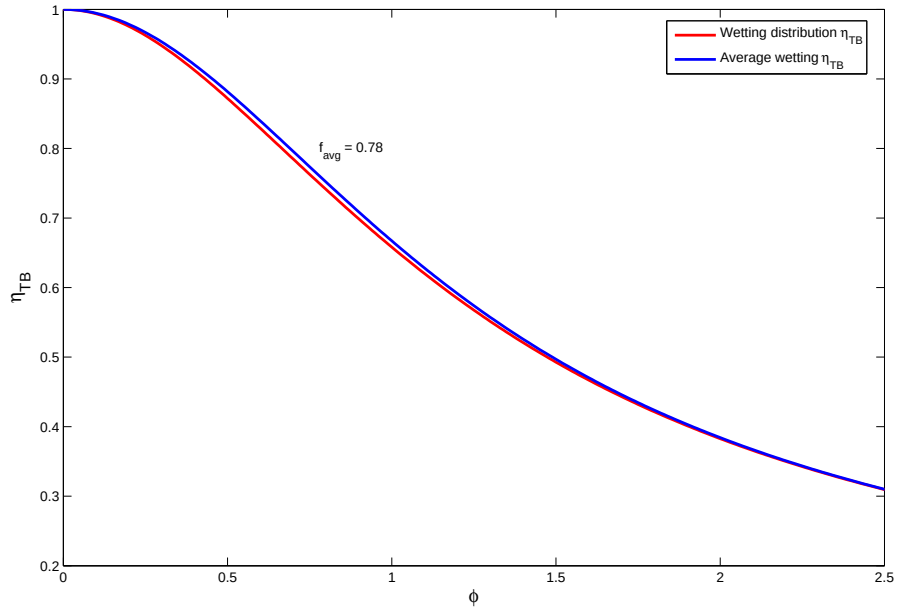

Figure 7.3: Average wetting and wetting distribution trickle-bed efficiencies as a function of Thiele modulus, for a *pulse* pre-wetted bed. L = 5.35 kg/m^{2}s; G = 0.152 kg/m^{2}s

7.2 Gas-limited reactions

To estimate the effect of wetting efficiency on gas-limited reactions, models similar to that of Ramachandran & Smith (1979) (equation 2.27) are often employed. If it is assumed that gas-solid mass transfer limitations are negligible, this model can be presented as follows:

$$\eta_{TB,g} = \frac{C_{A,int}}{C_A^*} = \frac{\eta_{CE}}{\phi}.\frac{\tanh\phi}{1+\frac{\phi}{Sh_{LS,A}}\tanh\phi} + \frac{1-\eta_{CE}}{\phi}.\tanh\phi \tag{7.3}$$

In words, this model can be described as follows. The gas-side reagent can enter a partial wetted particle from both the wetted and the dry part of the particle. The rate of mass transfer onto the dry side of the particle will however be different to the rate of mass transfer onto the wetted side of the particles. The surface concentration on the dry particle will therefore be different from that on the wetted side of the particle. An overall average surface concentration is then estimated by the weighting factors η_{CE} (wetted side of particle) and $1-\eta_{CE}$ (dry side of particle). The internal concentration is assumed to be a function of the weighted surface concentration and particle Thiele modulus. The contacting efficiency (η_{CE}) is usually replaced by the average wetting efficiency, but is actually modelled as a particle-scale wetting efficiency.

Usually, gas-solid mass transfer coefficients are *much* higher than liquid-solid mass transfer coefficients (in equation 7.3 the gas-solid mass transfer coefficient approaches infinity). The gas-side reagent can therefore be more readily transferred from the gas phase to the dry part of a particle, than through the liquid onto the wetted part of the particle. As a general rule, it is therefore suggested that a lower average wetting efficiency in a trickle-bed reactor will result in improved reactor performance if the reaction that takes place is gas-limited. There are however a few secondary effects:

- Beaudry et al. (1987) suggested that a fraction of the pores of a catalyst close to the dry catalyst surface can become liquid-limited, even although equation 2.19 would suggest that the overall reaction is completely gas-limited. This is since incomplete wetting will adversely affect the effective internal diffusivity of the liquid reagent if this reagent is non-volatile (see chapter 2.3.1).

- Particles with a very low wetting efficiency might become completely liquid-limited, that is, the external mass transfer rate of the liquid-side reagent through the wetted parts of the particles is so low, that

$$\frac{D_{eff,B}C_{B,s}}{D_{eff,A}C_{A,s}} \ll 1 \text{ although } \frac{D_{eff,B}C_{B,b}}{D_{eff,A}C_{A,b}} \gg 1 \tag{7.4}$$

  The extreme case of equation 7.4 is when the particles are completely dry so that no reaction occurs.

It is very difficult to take into account these two effects when making use of the average wetting efficiency in the bed only: If all the particles in the bed are at the average wetting efficiency, their wetting efficiency is high enough that these effects will not play a role. To model these effects, one therefore has to assume that some of the particles have a low wetting efficiency. An example of this is the model of Beaudry et al. (1987), where a very specific wetting efficiency distribution had to be assumed to model liquid limited zones in catalyst pores (see chapter 2.3.1).

It was shown that all the particles in the bed are definitely not wetted equally, and it is quite probable that for some parts of the bed, the low wetting efficiency effects discussed previously, will begin to play a role. To take these into account the following calculations were performed:

- For the complete range of particle wetting efficiencies, the trickle bed efficiency for a gas limited reaction was calculated according to equation 7.3. The internal concentration of the gaseous reaction is then given by:

$$C_{A,int} = \eta_{TB,g} C_A^* \tag{7.5}$$

- Also for the complete range of wetting efficiencies, the trickle-bed efficiency for a liquid limited reaction is calculated, according to the model of Dudukovic (1977), but with external mass transfer limitations taken into account:

$$\eta_{TB,l} = \frac{\frac{f_n}{\phi} \tanh\left(\phi / f_n\right)}{1 + \frac{\phi}{Sh_{LS,B}} \tanh\left(\phi / f_n\right)} \tag{7.6}$$

  The internal concentration of the liquid-side reagent is given by:

$$C_{B,int} = \eta_{TB,l} C_{B,b} \tag{7.7}$$

- It is assumed that the limiting reagent will be that with the lower internal concentration, and that the reaction rate is first order with respect to the limiting reagent and zeroth order with respect to the other reagent. The trickle-bed efficiency in terms of the gaseous reagent is then given by:

$$\eta_{TB,overall} = \frac{C_{int}}{C_A^*}, \text{ where } C_{int} \text{ is the internal concentration of the limiting reagent} \tag{7.8}$$

- The following values for the model parameters were chosen: $Sh_{LS,B} = Sh_{LS,A}; C_{B,b} = 20; C_A^* = 1; \phi = 10$

This procedure enables one to account for particles that are so poorly wetted that they

become liquid-limited. Possible liquid-limitations *within* a gas-limited particle (Beaudry et al., 1987) have not been accounted for.

Average wetting and wetting distribution trickle-bed efficiencies were calculated for the obtained wetting distributions, according to above procedure, as a function of Sh_{LS}. Results for the Levec pre-wetted beds are shown in figures 7.4 and 7.5. These figures show that the trickle-bed efficiency will be overestimated in Levec pre-wetted beds when only the average wetting efficiency is taken into account. This is because these beds contain dry particles (which cannot be modelled by an average wetting efficiency) and particles that are so poorly wetted that they are liquid-limited. These two groups *bring down* the trickle-bed efficiency when modelled on a particle scale (low reaction rates on liquid-limited particles, and no reaction on completely dry particles). When however modelled by the average wetting efficiency, these two groups have a *positive* effect on trickle-bed efficiency: They decrease the average wetting efficiency to such an extend that, according to the average wetting efficiency, the rate of external mass transfer onto the particles in the bed is increased.

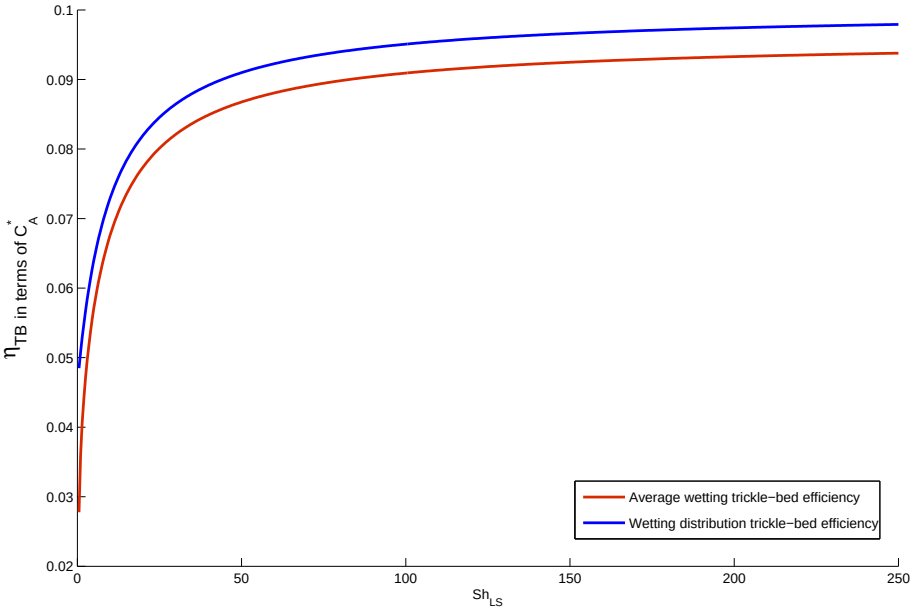

Figure 7.4: Average wetting and wetting distribution gas-limited trickle-bed efficiencies as functions of Sh_{LS} in a *Levec* pre-wetted bed. L = 1.60 kg/m^{2}s and G = 0.152 kg/m^{2}s. The following values were used for the model parameters: $\phi_A = \phi_B = 10$, $\frac{D_{eff,B}C_B}{D_{eff,A}C_A^*} = 20$, $Sh_{LS,B} = Sh_{LS,A}$ and $Sh_{gs} \to \infty$.

For gas limited systems in which external mass transfer limitations play a role, the "error" that results from modeling with only the average wetting efficiency is not only a function of Sh_{LS}, but also of ϕ and $\frac{D_{eff,B}C_{B,b}}{D_{eff,A}C_A^*}$. To characterise the dependency of gas-limited reaction rates on all of these parameters, the estimated difference between the

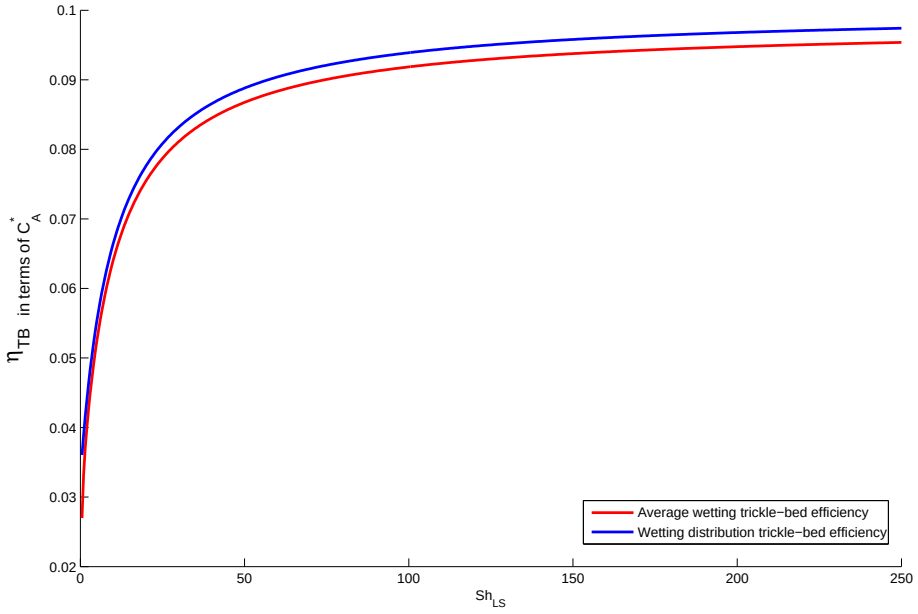

Figure 7.5: Average wetting and wetting distribution gas-limited trickle-bed efficiencies as functions of Sh_{LS} in a *Levec* pre-wetted bed. L = 5.35 kg/m^{2}s and G = 0.152 kg/m^{2}s. Model parameters are the same as for figure 7.4.

average wetting trickle-bed efficiency and the wetting distribution trickle-bed efficiency was calculated for the following cases:

- Wide range of values for $\frac{D_{eff,B}C_{B,b}}{D_{eff,A}C_A^*}$, and constant values of ϕ and Sh_{LS}.
- Wide range of values for ϕ, and constant values of $\frac{D_{eff,B}C_{B,b}}{D_{eff,A}C_A^*}$ and Sh_{LS}.
- Wide range of values for Sh_{LS}, and constant values of $\frac{D_{eff,B}C_{B,b}}{D_{eff,A}C_A^*}$ and ϕ.

Results are shown in figure 7.6

Contrary to the conclusions for liquid-limited reactions, these figures suggest that the maximum errors in the prediction of trickle-bed performance are for values of the Thiele modulus and the mass transfer coefficient for which mass transfer considerations, and therefore wetting efficiency, play the most important role, i.e. *high* Thiele moduli and *low* values for Sh$_{LS}$. On would therefore conclude that for Levec pre-wetted beds, the average wetting efficiency alone is definitely not sufficient when the effect of partial wetting is to be modelled.

As for liquid-limited systems, a pulse pre-wetted bed can be described by means of only the average wetting efficiency under gas-limited conditions. This is illustrated in figure 7.7.

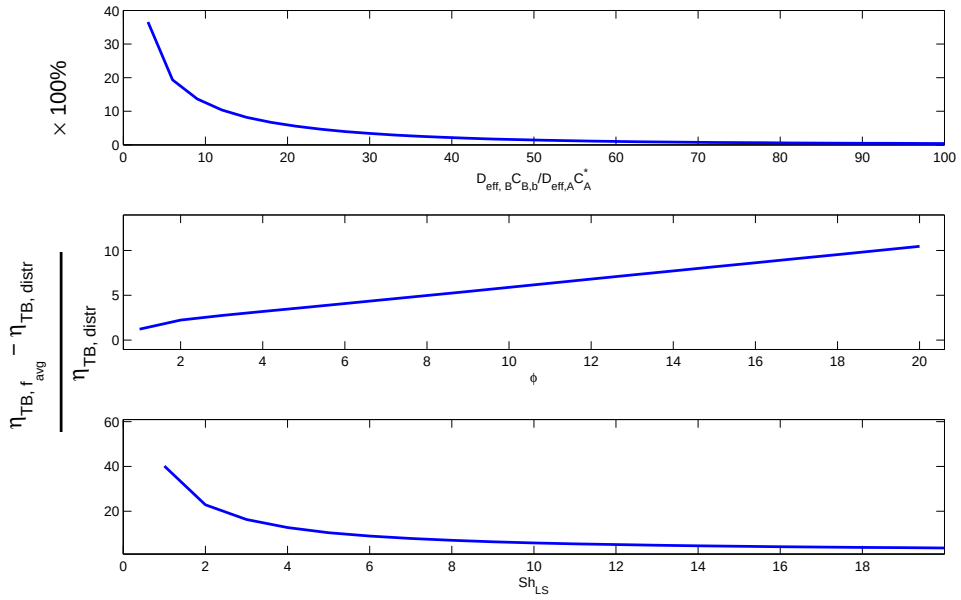

Figure 7.6: Estimated difference between the average wetting trickle-bed efficiency and the wetting distribution trickle-bed efficiency for a gas limited reaction, in the *Levec* pre-wetted bed for which L = 1.60 kg/m^{2}s. One of the three different parameters that are of importance is varied in each figure, with the other two held constant. Constant values are: $\frac{D_{eff,B}C_{B,b}}{D_{eff,A}C^*_A} = 20$; $\phi = 10$; $Sh_{LS} = 10$

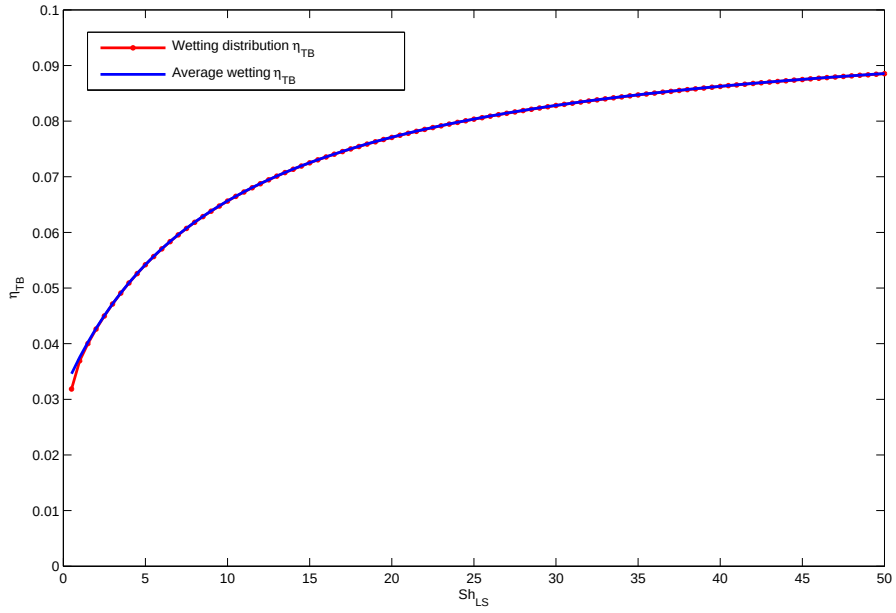

Figure 7.7: Average wetting and wetting distribution gas-limited trickle-bed efficiencies as functions of Sh_{LS} in a *pulse* pre-wetted bed. L = 1.60 kg/m^{2}s and G = 0.152 kg/m^{2}s. Model parameters are the same as for figure 7.4.

7.3 Summary

The conclusions that came from this chapter can be summarised as follows:

- For both liquid-limited and gas-limited reactions, the effect of the particle wetting distribution in pulse pre-wetted beds on reaction rates could be described adequately by the average wetting efficiency in the bed .
- For Levec pre-wetted beds, reaction rates will be overestimated by the average wetting efficiency. This applies for both liquid-limited and gas-limited reactions. For the Levec pre-wetted beds the wetting efficiency distribution therefore has to be taken into account when the reactor performance in these beds is analysed.
- In the case of liquid-limited reactions, the error caused by taking into account only the average wetting efficiency is only present at low values of the Thiele modulus, where mass transfer limitations are not very important.
- In the case of gas-limited reactions, the error of the average wetting trickle-bed efficiency is the highest where mass transfer considerations is of most importance: high values of ϕ and low values of Sh_{LS}. It is therefore very important to take the wetting efficiency distribution into account for gas-limited reactions.

Note that all above conclusions are *model-based* for first order reactions, and are only true when these models represent the physical truth.

CHAPTER 8

Influence of pre-wetting method and flow morphology on reactor performance

8.1 Liquid-limited reactions

The effect of wetting efficiency is most significant in liquid-limited reactions, since it will directly influence both *internal* and *external* mass transfer limitations. Levec pre-wetted beds will therefore be undesired for liquid-limited reactions, especially at low liquid flow rates, where a large fraction of the bed is exposed to a flow type that leads to ineffective catalyst wetting (presumably filament flow). Figures 8.1 and 8.2 compare liquid-limited trickle-bed efficiencies for Levec and pulse pre-wetted beds at the same flow conditions. All results shown are wetting distribution result, except when the contrary is stated.

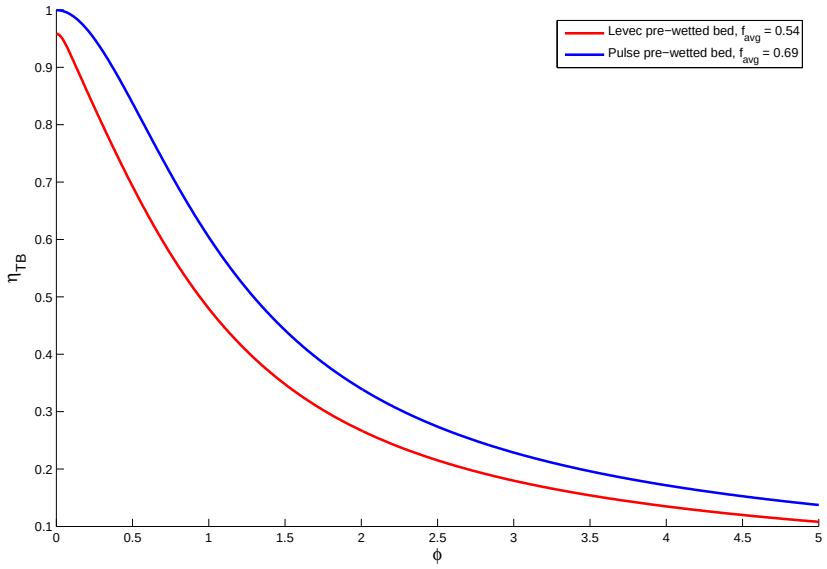

Figure 8.1: Trickle-bed efficiencies for Levec and pulse pre-wetted beds, according to the particle-scale model of Dudukovic (1977). L = 1.60 kg/m^{2}s; G = 0.152 kg/m^{2}s.

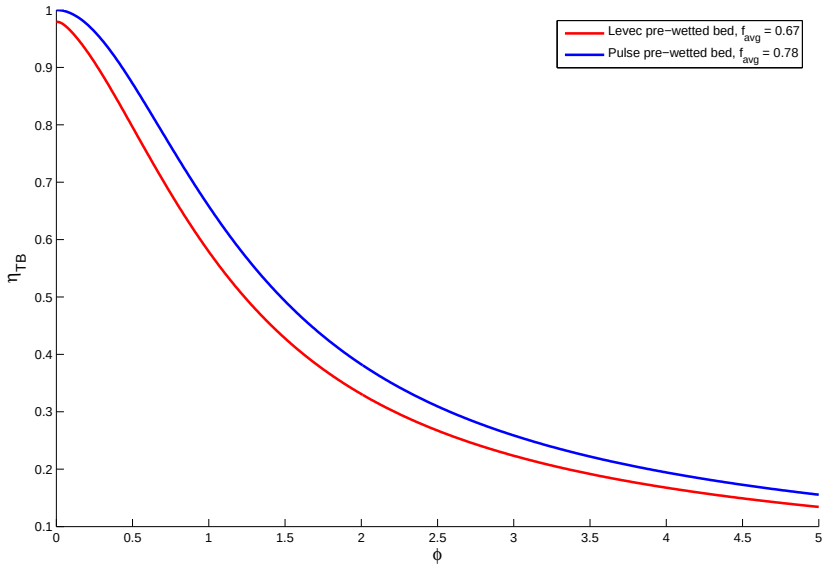

Figure 8.2: Trickle-bed efficiencies for Levec and pulse pre-wetted beds as a function of particle Thiele modulus, according to the particle-scale model of Dudukovic (1977). L = 5.35 kg/m^{2}s; G = 0.152 kg/m^{2}s.

8.2 Gas-limited reactions

If one only takes into account the average wetting efficiency in a bed, one would assume that Levec pre-wetted beds are superior to pulse pre-wetted beds, due to the lower average wetting efficiency in these beds. Figures 8.3 and 8.4 show the average wetting gas-limited trickle-bed efficiencies for the differently pre-wetted beds as calculated by the model of Ramachandran & Smith (1979) for different liquid-solid mass transfer coefficients, and a particle Thiele modulus of $\phi = 10$. According to these figures, the relative performance of these beds as a function of Sh_{LS} can be described as follows. At very high values of Sh_{LS}, external mass transfer limitations do not play a role, and the trickle bed efficiency is not a function of wetting efficiency. Therefore, the trickle-bed efficiencies of both beds will tend toward one another at high values of Sh_{LS}. The Levec pre-wetted bed will become increasingly superior to the pulse pre-wetted bed as Sh_{LS} is decreased, since external liquid-solid mass transfer limitations and therefore external wetting efficiencies play an increasingly important role.

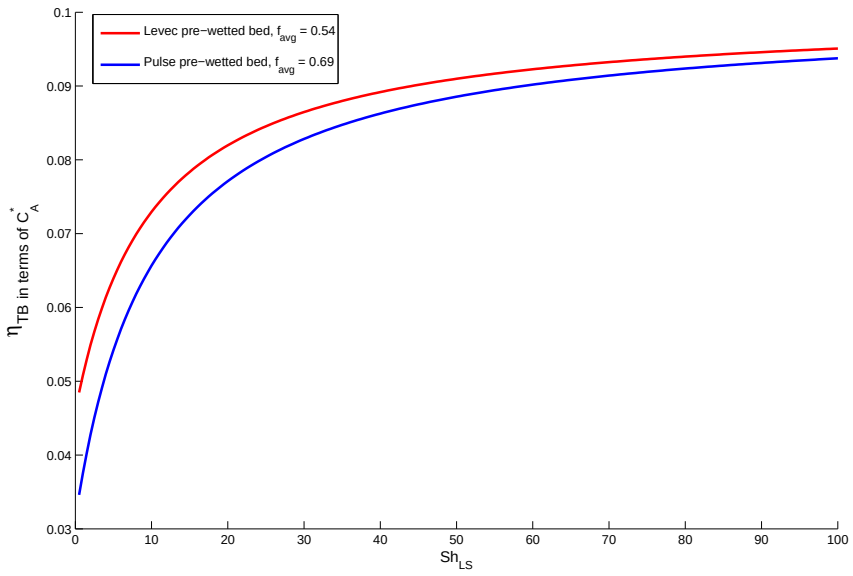

Figure 8.3: Average wetting trickle-bed efficiencies as a function of Sh_{LS} in a pulse- and a Levec pre-wetted bed, according to the model of Ramachandran & Smith (1979). L = 1.60 kg/m^{2}s and G = 0.152 kg/m^{2}s. Particle Thiele modulus was taken as $\phi = 10$.

The wetting distribution trickle-bed efficiencies as a function of Sh_{LS} were also calculated for all the different wetting distributions. The effect of pre-wetting according to these calculations as a function of Sh_{LS} is shown in figures 8.5 and 8.6. The importance of taking into account not only overall wetting efficiency, but also the distribution of wetting efficiencies is best observed in figure 8.5. In this figure, one can observe three zones, where different properties of the wetting in the bed are of importance:

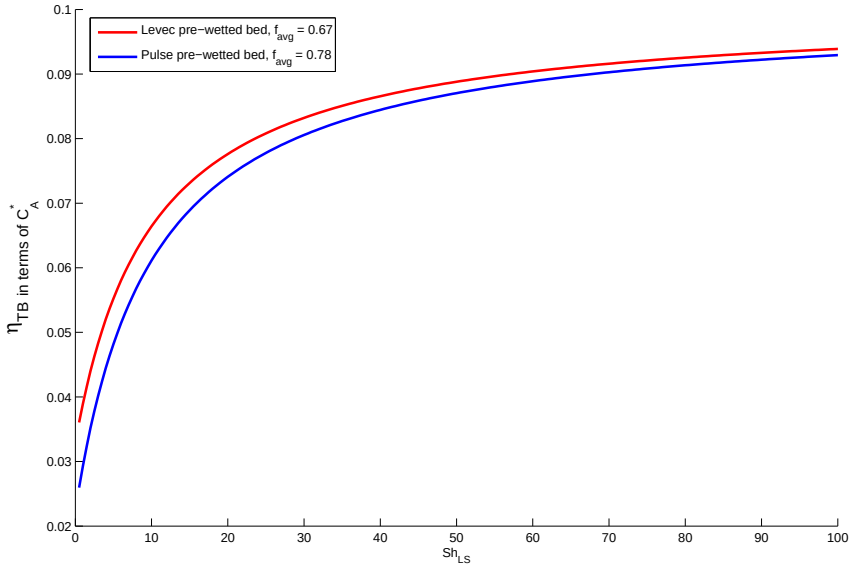

Figure 8.4: Average wetting efficiencies as a function of Sh_{LS} in a pulse- and a Levec pre-wetted bed, according to the model of Ramachandran & Smith (1979). L = 5.35 kg/m^{2}s and G = 0.152 kg/m^{2}s. Particle Thiele modulus was taken as $\phi = 10$.

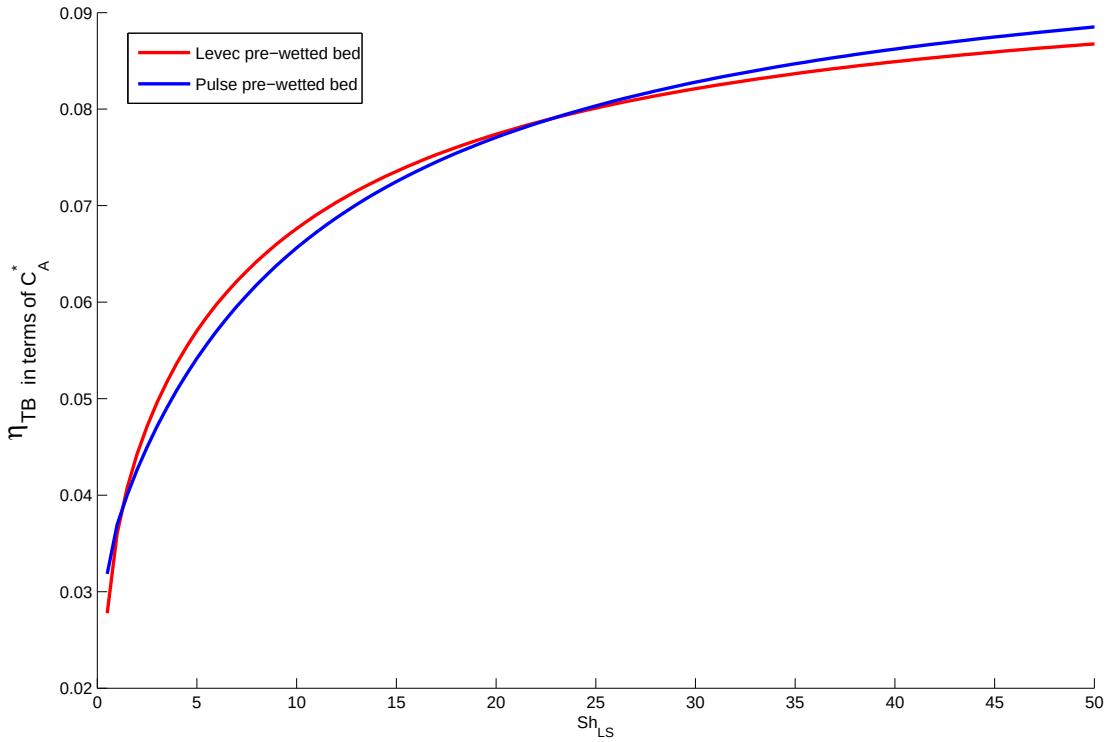

Figure 8.5: Wetting distribution trickle-bed efficiency as a function of Sh_{LS} in a pulse- and a Levec pre-wetted bed, according to the models of Ramachandran & Smith (1979) and Dudukovic (1977). L = 1.60 kg/m^{2}s and G = 0.152 kg/m^{2}s. The following values were used for the model parameters: $\phi_A = \phi_B = 10$, $\frac{D_{eff,B}C_{B,b}}{D_{eff,A}C^*_A} = 20$, $Sh_{LS,B} = Sh_{LS,A}$ and $Sh_{gs} \rightarrow \infty$.

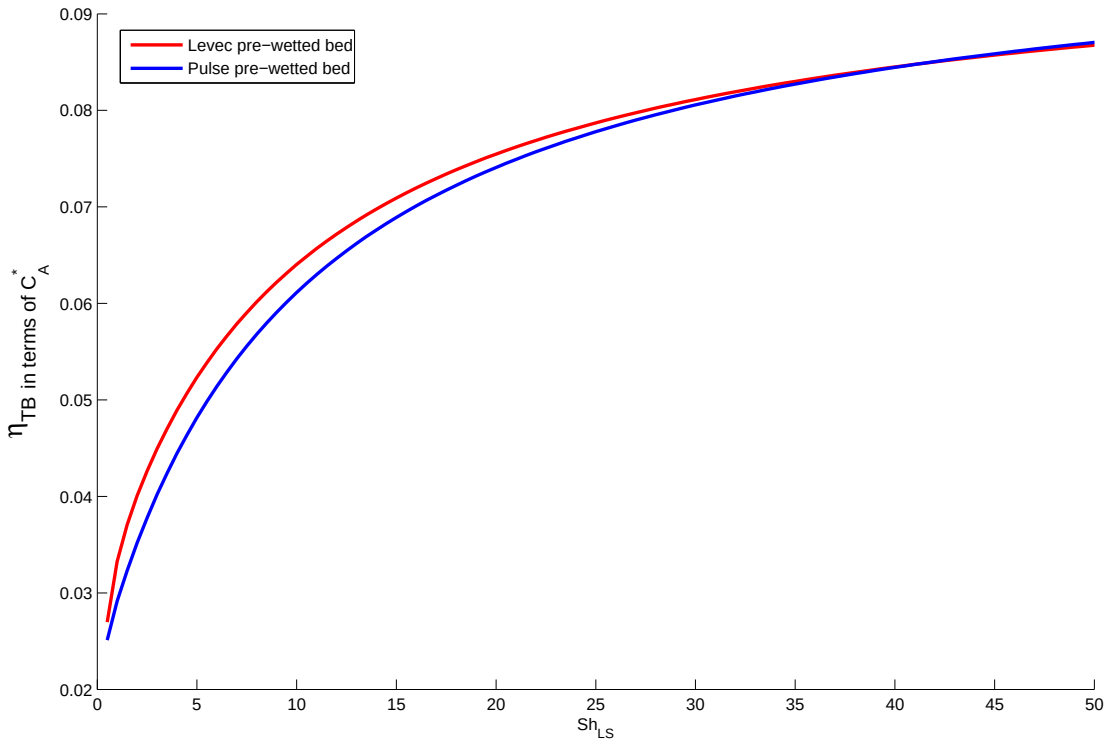

Figure 8.6: Wetting distribution trickle-bed efficiency as a function of Sh_{LS} in a pulse- and a Levec pre-wetted bed, according to the models of Ramachandran & Smith (1979) and Dudukovic (1977). L = 5.35 kg/m^{2}s and G = 0.152 kg/m^{2}s. The following values were used for the model parameters: $\phi_A = \phi_B = 10$, $\frac{D_{eff,B}C_{B,b}}{D_{eff,A}C_A^*} = 20$, $Sh_{LS,B} = Sh_{LS,A}$ and $Sh_{gs} \rightarrow \infty$.

- At intermediate values of Sh_{LS}, the Levec pre-wetted bed is superior to the pulse pre-wetted bed, since the wetting efficiencies of most of the particles are lower in this bed. The liquid-solid mass transfer coefficient is low enough to play a role in the trickle-bed performance, and the efficiencies of poorly wetted particles are higher than for the well wetted particles. There are however some dry and some liquid-limited particles (very poorly wetted particles) in the Levec pre-wetted bed, and the overall trickle-bed efficiency is lower than predicted when one only takes into account the overall average wetting efficiency (see figure 8.3).

- At high values of Sh_{LS}, external mass transfer limitations and hence wetting efficiency play a less and less important role. What is of more importance is not how much, but whether the particles are contacted by the liquid. The pulse-prewetted bed therefore becomes more and more superior to the Levec pre-wetted bed as Sh_{LS} is increasing, since only the latter contains dry particles (about 6-10%)[1].

- At very low values of Sh_{LS} the external liquid-solid mass transfer limitations are very severe. Here it is observed that the performance of the pulse pre-wetted bed is superior to that of the Levec pre-wetted bed. This is in sharp contrast to the trend predicted by taking into account only the average wetting efficiencies in the respective beds, where it was suggested that the Levec pre-wetted beds become increasingly superior to the pulse pre-wetted beds as Sh_{LS} is decreased (see figure 8.3). The reason for this is that, as the external liquid-solid mass transfer limitations become more and more severe, the maximum fractional wetting for which a particle will be liquid-limited is increased. Since the Levec pre-wetted bed contains a high amount of particles with low wetted area fractions, a high amount of particles in this bed will be liquid-limited when external liquid-solid mass transfer limitations are severe. This is shown in figure 8.7. One should keep in mind that the amount of liquid limited particles at a certain value of Sh_{LS} is of course also a strong function of $\frac{D_{eff,B}C_{B,b}}{D_{eff,A}C_A^*}$ and ϕ, so that this figure is very specific. The fact that particles can become partially liquid-limited *within* its pores will further enhance the effect that is observed at low values of Sh_{LS}.

If one studies figures 8.5 and 8.6 one can easily come to the conclusion that the above described effects are not of practical importance, seeing that they appear so small. The values of the model parameters were however chosen to illustrate all the effects *simultaneously* on one figure and the effects can be more severe, depending on reaction rates and catalyst and reagent properties. For example, if $\frac{D_{eff,B}C_{B,b}}{D_{eff,A}C_A^*}$ is low, the effect at low values of Sh_{LS} is of more importance (even at higher values of Sh_{LS}), but the superiority

[1]For the results discussed here and shown in figures 8.5 and 8.6, all particles that had an estimated wetting efficiency of $f_i < 5\%$ were considered to be completely dry. This translates to 6% in the Levec pre-wetted bed shown in figure 6.7

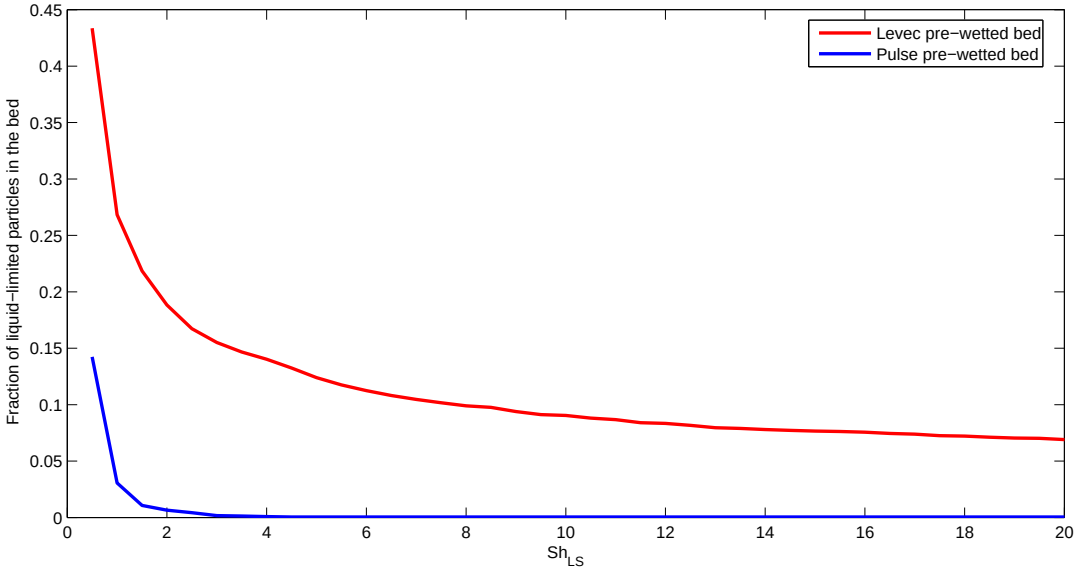

Figure 8.7: Fraction of liquid limited particles in a Levec and pulse pre-wetted beds as a function of Sh_{LS}. L = 5.35 kg/m^{2}s and G = 0.152 kg/m^{2}s. All the model parameters are the same as for figure 8.5

of the Levec pre-wetted bed at intermediate values of Sh_{LS} is much less. Likewise, for low Thiele moduli, external mass transfer limitations are of less importance, the pulse pre-wetted will faster become superior to the Levec pre-wetted than was illustrated in figure 8.5. The pre-wetting procedure that is suggested for a gas-limited trickle-bed reactor is therefore a strong function of its reaction conditions and catalyst and reagent properties. The effect of the distribution is of course also a function of liquid flow rate, and the effects will be more significant at lower liquid flow rates.

For Levec pre-wetting and low liquid flow rates, one also needs to remember that the liquid is most likely more and more maldistributed as it moves down the bed (see chapter 6.4), and reactor performance may be unexpectedly low when the bed is long. To illustrate this, the modelled reactor efficiency at $z = 0.5$ m in the Levec pre-wetted bed with L = 1.60 kg/m^{2}s is shown in figure 8.8.

8.3 Volatile reagents

Sedriks & Kenney (1972) found that for volatile reagents, reaction rates are considerably higher when the liquid in the bed is poorly distributed since dry particles exhibit extremely high reaction rates. This suggests that Levec pre-wetting is preferable for these type of reactions. However, when the reaction is strongly exothermic, liquid maldistribution lead to hot spots and possibly undesirable side reactions. Before one can say which type of flow is desirable, on should therefore take into account properties such as reaction heat and desired reaction temperature. Pulse pre-wetted beds will of course always be

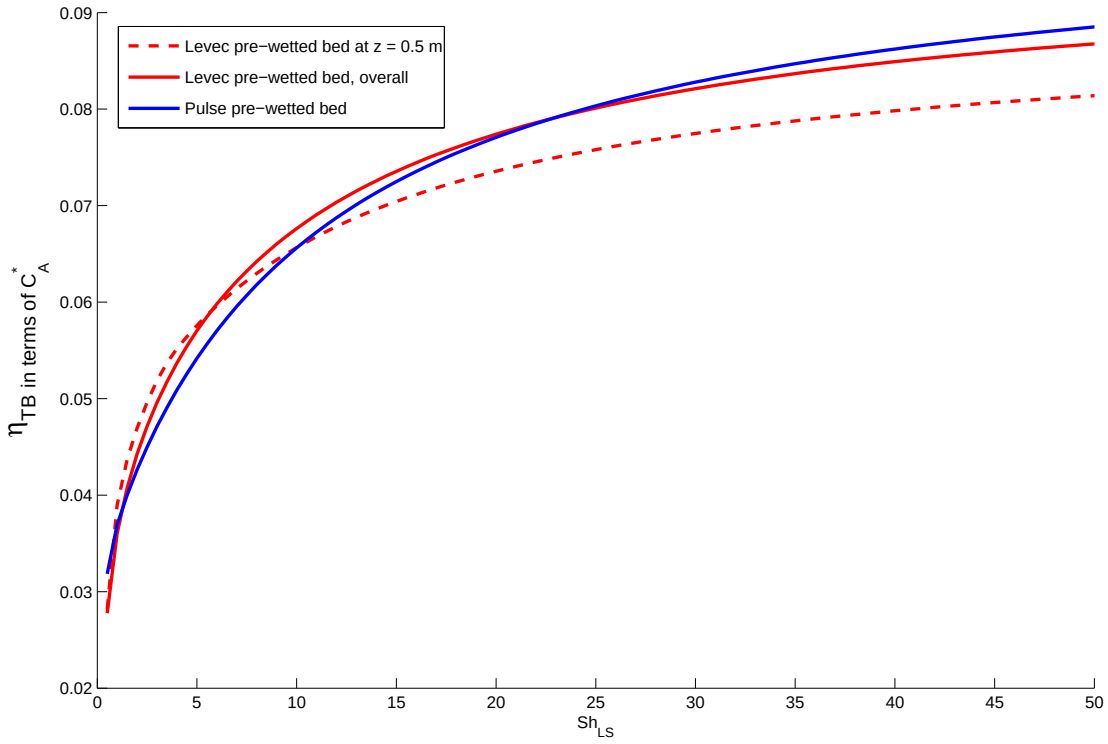

Figure 8.8: Gas-limited trickle-bed efficiencies of *Levec* pre-wetted beds as a function of Sh_{LS} for different heights. The gas limited trickle-bed efficiency as a function of Sh_{LS} is also shown. L = 5.35 kg/m^{2}s and G = 0.152 kg/m^{2}s. All the model parameters are the same as for figure 8.5

safer than Levec pre-wetted beds: Temperature control is much easier for this type of flow due to the fact that all of the packing is exposed to the flowing liquid.

8.4 Summary

Reaction efficiencies for liquid-limited and gas limited reactions in trickle-bed reactors have been estimated for the two different pre-wetting methods, according to the models of Dudukovic (1977) and Ramachandran & Smith (1979) respectively. It was shown that the pre-wetting procedure has a significant influence on reaction rates, due to its effect on flow morphology and the distribution of wetting in the bed:

- For the investigated liquid and gas flow rates, it seems as though pulse pre-wetted beds (presumably film flow) will outperform Levec pre-wetted beds (presumably film *and* filament flow) in liquid-limited reactions, irrespective of reaction kinetics and particle Thiele modulus, due to dry and poorly wetted particles that are a result of filament flow. The difference between pulse- and Levec pre-wetted beds is however likely to vanish at high liquid flow rates.

- For gas-limited reactions, the comparison between pulse- and Levec pre-wetted beds is more complex: As a rule, reactor performance under gas-limited conditions will be better when the wetting efficiency is low, due to increased gas reagent to solid mass transfer rates. At very low wetting efficiencies however, liquid-solid mass transfer rates are so low, that the reaction can become liquid-limited. This effect is present in Levec pre-wetted beds, where a significant amount of particles have a very low wetting efficiency. Despite their low wetting efficiency as compared to pulse pre-wetted beds, Levec pre-wetted beds *might* become less effective than pulse pre-wetted beds under gas-limiting conditions. A very rough rule of thumb is that the pulse pre-wetted beds will outperform Levec pre-wetted beds under *severe* mass transfer limited conditions and *severe* reaction limited conditions when the liquid reagent concentration to gas reagent concentration ratio is low (less than about 30, see figure 7.6), and low liquid flow rates. In all other cases, it seems as though a Levec pre-wetted bed will have a higher efficiency that a pulse pre-wetted bed at the same flow conditions.

- In reactors containing a volatile liquid reagent, one will expect higher reaction rates in a Levec pre-wetted bed than in a pulse pre-wetted bed. For exothermic reactions it is quite possible that hot spots and unwanted side reactions are present in Levec pre-wetted beds, due to dry parts in the bed.

CHAPTER 9

Conclusions and recommendations

9.1 Conclusions

A new colorometric method was developed for the investigation of the distribution of wetting efficiency in trickle-bed reactors. In this method, particles from the bed were photographed from two sides and the fraction on the particles that were contacted by the liquid during flow were estimated from these photographs. Fifty-six per cent of the area of each particle could be evaluated with good accuracy ($\pm$ 5%). The method was shown to give representative wetting efficiency distributions.

By means of this experimental method, particle wetting efficiency distributions for Levec and pulse pre-wetted under various flow conditions were obtained. These distributions seem to fit into literature's description of trickle-flow for the different types of pre-wetting (film flow for pulse pre-wetted beds; film and filament flow for Levec pre-wetted beds). If these types of flow are ascribed to the pulse and Levec pre-wetted beds, the influence of liquid and gas flow on trickle flow morphology can be visualised as follows.

- In pulse pre-wetted beds (presumably film flow), the liquid flow rate does not influence the pattern or the morphology in the bed. Increased liquid holdup due to increased liquid flow rate therefore have to thicken and expand the films that flow over the packing. This expansion of liquid films can be observed from the wetting efficiency distributions for pulse pre-wetted beds at different liquid flow rates.

- It was found that the gas flow rate does not have a significant effect on the wetting distribution in pulse pre-wetted beds. This is most probably due to two opposing effects of the gas flow rate: An increased gas flow rate leads to a decrease in liquid holdup and therefore smaller liquid films, whereas the increased pressure drop results in spreading of the liquid over the solid packing.

- In Levec pre-wetted beds, the obtained distributions suggest that two types of flow are present. This agrees with literature, where it was found that film and filament flow is present in Levec pre-wetted beds. Distributions obtained for different liquid flow rates in these beds show that the ratio of film to filament flow is increased with increased liquid flow rate. It is therefore likely that the flow in Levec pre-wetted beds will approach flow in a pulse pre-wetted bed at high liquid flow rates.

- Wetting distributions were obtained for several bed sections at each experimental flow condition, to get an idea of how the trickle-flow morphology changes as it goes down the bed. Stable flow was much faster encountered in pulse pre-wetted beds than in Levec pre-wetted beds. Stable flow was not reached in the Levec pre-wetted bed with liquid flow rate L = 1.60 kg/m^{2}s, and the liquid was more and more maldistributed as it goes down the packing.

Additional results that came from the obtained wetting distributions are that a fraction of the packing was never contacted by the liquid for the Levec pre-wetted beds (5-10% at L = 1.60 kg/m^{2}s and 2-4% at L = 5.35 kg/m^{2}s), and that the average wetting efficiencies in these beds are much lower than in pulse pre-wetted beds.

The effect that the wetting distributions have on reactor modeling was verified, based on popular models that describe the influence of wetting efficiency on reactor performance on a particle scale (Dudukovic, 1977; Ramachandran & Smith, 1979). If these models are correct, pulse pre-wetted beds can be adequately described by means of only the average wetting efficiency. I was shown that the distribution of wetting efficiency in Levec pre-wetted beds needs to be taken into account, for the following cases:

- Liquid-limited reactions and low values of the particle Thiele modulus (< 2).

- Gas-limited reactions for external and internal mass transfer limited systems, where the liquid to gas concentration ratio is relatively low (smaller than about 20 to 30).

It should be noted that these results are highly dependent on the models that were assumed.

Based on these models, the relative performance of pulse to Levec pre-wetted beds was described. It was shown that pulse pre-wetted beds will outperform Levec pre-wetted beds in liquid-limited reactions, and for gas-limited reactions where mass transfer limitations are high, so that the poorly wetted particles in Levec pre-wetted beds become liquid-limited. In a completely reaction limited system, pulse pre-wetted beds will also give higher conversions of gas-limited reactions than Levec pre-wetted beds, due to the dry particles that are present in Levec pre-wetted beds. For all other cases, Levec pre-wetted beds will have higher rates of gas-limited reactions than super pre-wetted beds. Although model-based, these results suggest that reactor conversions can be well manipulated by means of pre-wetting.

9.2 Recommendations

This study leaves much scope for further investigation. Possible areas of interest are:

- The data stated in this report is very limited in terms of flow conditions. More results will help in a better understanding of flow, especially for Levec pre-wetted beds.
- Levec pre-wetting and pulse pre-wetting may not be feasible pre-wetting procedures for industrial scale reactors. The feasibility of other pre-wetting procedures can be investigated.
- It was shown that flow morphology can play a very important role in the performance of trickle-bed reactors. All morphology work was previously done on small scale trickle-bed reactors for a limited time span and the effect of pre-wetting can be more pronounced than for industrial trickle-bed reactors that are operated continuously for a long period of time. Having such an important influence on small scale trickle-bed reactors, it is important to identify whether such effects are also present in industrial scale reactors, and what type of flow is "reached" after a long period of time.
- Liquids other than water should be used in the investigation of trickle-flow morphology, since the surface tension of water is extremely high as compared to petrochemical process streams.
- The effect of pre-wetting on volatile reactions has not been investigated in detail. It is probable that pre-wetting procedure has the most significant effect in these reactors (Sedriks & Kenney, 1972).
- Other particle-scale models can be evaluated and applied to compare reactor performance for different flow conditions and pre-wetting procedures.
- Wetting efficiency measurement methods can be investigated, since the wetting efficiency distributions gives an extra dimension for flow modelling.

BIBLIOGRAPHY

Al-Dahhan, M. H. and Dudukovic, M. P. (1995) "Catalyst wetting efficiency in trickle-bed reactors at high pressure", *Chemical Engineering Science, 50* (15), 2377–2389.

Al-Dahhan, M. H.; Larachi, F.; Dudukovic, M. P. and Laurent, A. (1997) "High-pressure trickle-bed reactors: A review", *Industrial Engineering Chemistry Research, 36*, 3292–3314.

Aris, R. (1957) "On shape factors for irregular particles-1. the steady state problem. diffusion and reaction", *Chemical Engineering Science, 6*, 262.

Beaudry, E. G.; Dudukovic, M. P. and Mills, P. L. (1987) "Trickle-bed reactors: Liquid diffusional effects in a gas-limited reaction", *AIChe Journal, 33*, 1435–1447.

Bondi, A. March (1971) "Handling kinetics from trickle-phase reactors", *Chemical Technology,* page 185.

Burghardt, A.; Bartelmus, G.; Jaroszynski, M. and Kolodziej, A. (1995) "Hydrodynamics and mass transfer in a three-phase fixed-bed reactor with cocurrent gas-liquid downflow", *The Chemical Engineering Journal, 58*, 83–99.

Christensen, G.; McGovern, S. G. and Sudaresan, G. (1986) "Cocurrent downflow of air and water in a two-dimensional packed column", *AIChe Journal, 32*, 1677.

Colombo, A. J.; Baldi, G. and Sicardi, S. (1976) "Solid-liquid contacting effectiveness in trickle-bed reactors", *Chemical Engineering Science, 31*, 1101–1108.

Crine, M.; Marchot, P. and L'Homme, G. A. (1980) "Liquid flow maldistributions in trickle-bed reactors", *Chemical Engineering Communications, 7*, 377.

Danckwerts, P. V. (1953) "Continuous flow systems: Distribution of residence times", *Chemical Engineering Science, 2*, 1–13.

Dudukovic, M. P. (1977) "Catalyst effectiveness factor and contacting efficiency in trickle-bed reactors", *AIChe Journal, 23*, 940.

Dudukovic, M. P.; Larachi, F. and Mills, P. L. (1999) "Multiphase reactors – revisited", *Chemical Engineering Science, 54*, 1975–1995.

Dudukovic, M. P.; Larachi, F. and Mills, P. L. (2002) "Multiphase catalystic reactors: A perspective on current knowledge and future trends", *Catalysis Reviews, 44*, 123–246.

El-Hisnawi, A. A.; Dudukovic, M. P. and Mills, P. L. (1982) "Trickle-bed reactors: dynamic tracer tests, reaction studies and modeling of reactor performance", *ACS Symposium series, 196*, 431.

Germain, A. H.; Lefebvre, A. G. and L'Homme, G. A. (1974) "Experimental study of catalytic trickle-bed reactors", *Advances in Chemistry Series, 133*, 164.

Gianetto, A. and Specchia, V. (1992) "Trickle-bed reactors: State of art and perspectives", *Chemical Engineering Science, 47*, 3197–3213.

Goto, S.; Levec, J. and Smith, J. M. (1975) "Mass transfer in packed beds with two-phase flow", *Industrial Engineering Process Design and Development, 14*, 473.

Henry, H. C. and Gilbert, J. B. (1973) "Scale up of pilot plant data for catalytic hydroprocessing", *Industrial Engineering Chemistry Process Design and Development, 12*, 328–334.

Herskowitz, M.; Carbonell, R. G. and Smith, J. M. (1979) "Effectiveness factors and mass transfer in trickle-bed reactors", *AIChe Journal, 25*, 272–283.

Herskowitz, M. and Smith, J. (1983) "Trickle-bed reactors: A review", *AIChe Journal, 29*, 1–17.

Holub, R. A.; Dudukovic, M. P. and Ramachandran, P. A. (1992) "A phenomenological model of pressure drop, liquid holdup and flow regime transition in gas-liquid trickle flow", *Chemical Engineering Science, 47*, 2343.

Hutton, B. E. T. and Leung, L. S. (1974) "Cocurrent gas-liquid flow in packed columns", *Chemical Engineering Science, 29*, 1681–1685.

Iliuta, I. and Larachi, F. (2000) "Double-slit model for partially wetted trickle flow hydrodynamics", *AIChe Journal, 46* (3), 597–609.

Iliuta, I.; Larachi, F. and Grandjean, B. P. A. (1999) "Residence time, mass transfer and back-mixing of the liquid in trickle flow reactors containing porous particles", *Chemical Engineering Science, 54*, 4099–4109.

Jiang, Y.; Khadilkar, M. R.; Al-Dahhan, M. H. and Dudukovic, M. P. (1999) "Two-phase flow distribution in 2d trickle-bed reactors", *Chemical Engineering Science, 54*, 2409–2419.

Kan, K. M. and Greenfield, P. F. (1978) "Multiple hydrodynamics tates in cocurrent two-phase downflow through packed beds", *Industrial Engineering Chenistry Process Design and Development, 17*, 482.

Kan, K. M. and Greenfield, P. F. (1979) "Pressure drop and holdup in two-phase cocurrent trickle flows through beds of small packings", *Industrial Engineering Chemistry Process Design and Development, 18*, 740–745.

Khadilkar, M. R.; Mills, P. L. and Dudukovic, M. P. (1999) "Trickle-bed reactor models for systems with a volatile liquid phase", *Chemical Engineering Science, 54*, 2421–2431.

Khadilkar, M. R.; Wu, Y. X.; Al-Dahhan, M. H. and Dudukovic, M. P. (1996) "Comparison of trickle-bed and upflow reactor performance at high pressure: Model predictions and experimental observations", *Chemical Engineering Science, 51*, 2139–2148.

Kheshgi, H. S.; Reyes, S. C.; Hu, R. and Ho, T. C. (1992) "Phase transition andsteady-state multiplicity in a trickle-bed reactor.", *Chemical Engineering Science, 47*, 1771–1777.

Krauze, R. and Scrwinski, M. (1971) "Moisted surface and fractional wetted surface area of ceramic raschig rings", *Inzineria Chemiczna, 1*, 415.

Kundu, A.; Nigam, K. D. P. and Verma, R. P. (2003) "Catalyst wetting characteristics in trickle-bed reactors", *AIChe Journal, 49*, 2253–2263.

Lakota, A. and Levec, J. (1990) "Solid-liquid mass transfer in packed beds with concurrent downward two-phase flow", *AIChe Journal, 36*, 1444.

Lapidus, L. (1957) "Flow distribution and diffusion in fixed-bed two-phase reactors", *Industrial Engineering Chemistry, 49*, 1000.

Larachi, F.; Laurent, A.; Wild, G. and Midoux, N. (1992) "Pressure effect on gas-liquid interfacial areas in cocurrent trickle-flow reactors", *Chemical Engineering Science, 47*, 2325.

Lazzaroni, C. L.; Kesselman, H. R. and Figoli, H. S. (1988) "Colorimetric evaluation of efficiency of liquid-solid contacting in trickle-bed reactors", *Industrial Engineering Chemistry, 27*, 1132.

Lazzaroni, C. L.; Kesselman, H. R. and Figoli, H. S. (1989) "Trickle bed reactors. multiplicity of hydrodynamic states. relation between the pressure drop and the liquid holdup", *Industrial Engineering Chemistry Research, 28*, 119–121.

Leung, P. C.; Recasens, F. and Smith, J. M. (1987) "Hydration of isobutene in a trickle-bed reactor: Wetting efficiency and mass transfer", *AIChe Journal, 33*, 996–1007.

Levec, J.; Grosser, K. and Carbonell, R. G. (1988) "The hysteretic behaviour of pressure drop and liquid holdup in trickle beds", *AIChe Journal, 34*, 1027–1030.

Levenspiel, O. (2002) "Modeling in chemical engineering", *Chemical Engineering Science, 57*, 4691–4696.

Llano, J. J.; Rosal, R.; Sastre, H. and Diez, F. V. (1997) "Determination of wetting efficiency in trickle-bed reactors by a reaction method", *Industrial Engineering Chemistry Research, 36*, 2616–2625.

Lutran, P. G.; Ng, K. M. and Delikat, E. P. (1991) "Liquid distribution in trickle-beds. an experimental study using computer-assisted tomography", *Industrial Engineering Chemistry Research, 30*, 1270–1280.

Marcandelli, C.; Lamine, A. S.; Bernard, J. R. and Wild, G. (2000) "Liquid distribution in trickle-bed reactor", *Oil & Gas Science and Technology, 55* (4), 407–415.

Mata, A. and Smith, J. M. (1981) "Transport processes in multiphase reaction systems", *AIChe Symposium Series,* pages 29–35.

Mears, D. E. (1974) "The role of liquid holdup and effective wetting in the performance of trickle-bed reactors", *Adv. Chem. Ser.,* page 218.

Melli, T. R. and Scriven, L. E. (1991) "Theory of two-phase cocurrent downflow in networks of pasages", *Industrial Engineering Chemistry Research, 30*, 951.

Mills, P. L. and Dudukovic, M. P. (1979) "A dual-series solution for the effectiveness factor of partially wetted catalysts in trickle-bed reactors", *Industrial Engineering Chemisrty Fundamentals, 18*, 139–149.

Mills, P. L. and Dudukovic, M. P. (1980) "Analysis of catalyst effectiveness in trickle-bed reactors processing volatile or nonvolatile reactants", *Chemical Engineering Science, 35*, 2267–2279.

Mills, P. L. and Dudukovic, M. P. (1981) "Evaluation of liquid-solid contacting in trickle-beds by tracer methods", *AIChe Journal, 27*, 893.

Mills, P. L. and Dudukovic, M. P. (1984) "A comparison of current models for isothermal trickle-bed reactors. application to a model reaction system", *ACS Symposium Series, 237*, 37.

Mills, P. L. and Dudukovic, M. P. (1989) "Convolution and deconvolution of nonideal tracer response data with application to three-phase packed beds", *Computers and Chemical Engineering, 13*, 881–898.

Moller, L. B.; Halken, C.; Hansen, J. A. and Bartholdy, J. (1996) "Liquid and gas distribution in trickle-bed reactors", *Industrial Engineering Chemistry Research, 35*, 926–930.

Morita, S. and Smith, J. M. (1978) "Mass transfer and contacting efficiency in a trickle-bed reactor", *Industrial Engineering Chemistry Fundamentals, 17*, 113.

Nigam, K. D. P.; Iliuta, I. and Larachi, F. (2001) "Liquid back-mixing and mass transfer effect in trickle-bed reactors filled with porous catalyst particles", *Chemical Engineering and Processing, 41*, 365–371.

Onda, K.; Takeuchi, H. and Kayama, Y. (1967) "Effect of packing materials on wetted surface area", *K. Kagaku Kogaku, 31*, 126.

Pathwardan, V. S. (1978) "Effective interfacial area in packed beds for absorption with chemical reaction", *Canadian Journal of Chemical Engineering, 56*, 56–64.

Pironti, F.; Mizrahi, D.; Acosta, A. and Gonzalez-Mendizabal, D. (1999) "Liquid-solid wetting factor in trickle-bed reactors: its determination by a physical method", *Chemical Engineering Science, 54*, 3793–3800.

Puranik, S. S. and Vogelpohl, V. (1974) "Effective interfacial area irrigated packed columns", *Chemical Engineering Science, 29*, 501.

Ramachandran, P. A.; Dudukovic, M. P. and Mills, P. L. (1986) "A new model for assessment of external liquid-solid contacting in trickle-bed reactors from tracer response measurements", *Chemical Engineering Science, 41*, 855–860.

Ramachandran, P. A. and Smith, J. M. (1979) "Effectiveness factors in trickle-bed reactors", *AIChe Journal, 25*, 538.

Ravindra, P. V.; Rao, D. P. and Rao, M. S. (1997) "Liquid flow texture in trickle-bed reactors: An experimental study", *Industrial Engineering Chemistry Research, 36*, 5133–5145.

Ring, Z. E. and Missen, R. W. (1991) "Trickle-bed reactors: tracers study of liquid holdup and wetting efficiency at high temperature and pressure", *Canadian Journal of Chemical Engineering, 26*, 164.

Ross, L. D. (1965) "Performance of trickle bed reactors", *Chemical Engineering Progress, 61*, 77.

Roy, S.; Kemoun, A.; Al-Dahhan, M. H.; Dudukovic, M. P.; Skourlis, T. B. and Dautzenberg, F. M. (2004) "Countercurrent flow distribution in structured packing via computed tomography", *Chemical Engineering and Processing, 45*, 59–69.

Ruiz, P.; Crine, M.; Germain, A. and L'Homme, G. (1984) "Influence of the reactional system on the irrigation rate in trickle-bed reactors", *ACS Symposium Series,* (237), 15.

Saez, A. E. and Carbonell, R. G. (1975) "Hydrodynamic parameters for gas-liquid cocurrent flow in trickle-beds", *AIChe Journal, 21*, 209–227.

Satterfield, C. N. (1975) "Trickle-bed reactors", *AIChe Journal, 21*, 209.

Schwartz, T. G.; Wegwe, E. and Dudukovic, M. P. (1976) "A new tracer method for determination of liquid-solid contacting effectiveness in trickle-bed reactors", *AIChe Journal, 22*, 894.

Sederman, A. J. and Gladden, L. F. (2001) "Magnetic resonance imaging as a quantitative probe of gas-liquid distribution and wetting efficiency in trickle-bed reactors", *Chemical Engineering Science, 56*, 2615–2628.

Sedriks, W. and Kenney, C. N. (1972) "Partial wetting in trickle-bed reactors: the reduction of crotonaldehyde over a palladium catalyst", *Chemical Engineering Science, 28*, 559–568.

Sicardi, S.; Baldi, G.; Gianetto, A. and Specchia, V. (1980) "Catalyst areas wetted by flowing and semistagnant liquid in trickle-bed reactors", *Chemical Engineering Science, 35*, 67.

Sicardi, S.; Baldi, G.; Specchia, V.; Mazzarino, I. and Gianetto, A. (1981) "Packing wetting in trickle bed reactors: influence of the gas flow rate", *Chemical Engineering Science, 36*, 226–228.

Souadnia, A. and Latifi, M. A. (2001) "Analysis of two-phase flow distribution in trickle-bed reactors", *Chamical Engineering Science, 56*, 5977–5985.

Specchia, V.; Baldi, G. and Gianetto, A. (1978) "Solid-liquid mass transfer in cocurrent two-phase flow through packed beds", *Industrial Engineering Chemistry Design and Development, 17*, 362–367.

Stanek, V.; Hanika, J.; Hlavacek, V. and Trnka, O. (1981) "The effect of liquid flow distribution on the behaviour of a trickle-bed reactor", *Chemical Engineering Science, 36*, 1045.

Statsoft "Descriptive statistics homepage", http://www.statsoft.com November (2005).

Tan, C. S. and Smith, J. M. (1980) "Catalyst particle effectiveness with unsymmetrical boundary conditions", *Chemical Engineering Science, 35*, 1601–1609.

Tsamatsoulis, D. C. and Papayannakos, N. G. (1996) "Partial wetting of cylindical catalytic carriers in trickle-bed reactors", *AIChe Journal, 42*, 1853–1863.

Tsochatzidis, N. A.; Karabelas, A. J.; Giakoumakis, D. and Huff, G. (2002) "An investigation of liquid maldistribution in trickle beds", *Chemical Engineering Science, 57*, 3543–3555.

van der Merwe, W. and Nicol, W. (2005) "Characterization of multiple flow morphologies within the trickle flow regime", *Industrial Engineering Chemistry Research, ASAP Article*.

Villermaux, J. and vanSwaaij, W. P. M. (1969) "Modele represasentatif de la distribution des temps de sejour dans un reacteur semi-infi a dispersion axiale avec zones stagnantes. application a l'ecoulement ruisselant dans des colonnes d'anneux raschig", *Chemical Engineering Science, 24*, 1097–1111.

Wammes, W. J. A.; Middelkamp, J.; Huisman, W. J.; de Baas, C. M. and Westerterp, K. R. (1991) "Hydrodynamics in a cocurrent gas-liquid trickle-bed at elevated pressures", *AIChe Journal, 37*, 1849–1862.

Wang, R.; Mao, Z. S. and Chen, J. (1995) "Experimental and theoretical studies of pressure drop hysteresis in trickle bed reactors", *Chemical Engineering Science, 50*, 2321–2328.

Wu, Y.; Al-Dahhan, M. A.; Khadilkar, M. R. and Dudukovic, M. P. (1996) "Evaluation of trickle-bed reactor models for a liquid limited reaction", *Chemical Engineering Science, 51*, 2721–2725.

Zimmerman, S. P. and Ng, K. M. (1986) "Liquid distribution in trickling flow trickle-bed reactors", *Chemical Engineering Science, 41*, 861.

Dudukovic, M. P. (1977) "Catalyst effectiveness factor and contacting efficiency in trickle-bed reactors", *AIChe Journal, 23*, 940.

Dudukovic, M. P.; Larachi, F. and Mills, P. L. (1999) "Multiphase reactors – revisited", *Chemical Engineering Science, 54*, 1975–1995.

Dudukovic, M. P.; Larachi, F. and Mills, P. L. (2002) "Multiphase catalystic reactors: A perspective on current knowledge and future trends", *Catalysis Reviews, 44*, 123–246.

El-Hisnawi, A. A.; Dudukovic, M. P. and Mills, P. L. (1982) "Trickle-bed reactors: dynamic tracer tests, reaction studies and modeling of reactor performance", *ACS Symposium series, 196*, 431.

Germain, A. H.; Lefebvre, A. G. and L'Homme, G. A. (1974) "Experimental study of catalytic trickle-bed reactors", *Advances in Chemistry Series, 133*, 164.

Gianetto, A. and Specchia, V. (1992) "Trickle-bed reactors: State of art and perspectives", *Chemical Engineering Science, 47*, 3197–3213.

Goto, S.; Levec, J. and Smith, J. M. (1975) "Mass transfer in packed beds with two-phase flow", *Industrial Engineering Process Design and Development, 14*, 473.

Henry, H. C. and Gilbert, J. B. (1973) "Scale up of pilot plant data for catalytic hydroprocessing", *Industrial Engineering Chemistry Process Design and Development, 12*, 328–334.

Herskowitz, M.; Carbonell, R. G. and Smith, J. M. (1979) "Effectiveness factors and mass transfer in trickle-bed reactors", *AIChe Journal, 25*, 272–283.

Herskowitz, M. and Smith, J. (1983) "Trickle-bed reactors: A review", *AIChe Journal, 29*, 1–17.

Holub, R. A.; Dudukovic, M. P. and Ramachandran, P. A. (1992) "A phenomenological model of pressure drop, liquid holdup and flow regime transition in gas-liquid trickle flow", *Chemical Engineering Science, 47*, 2343.

Hutton, B. E. T. and Leung, L. S. (1974) "Cocurrent gas-liquid flow in packed columns", *Chemical Engineering Science, 29*, 1681–1685.

Iliuta, I. and Larachi, F. (2000) "Double-slit model for partially wetted trickle flow hydrodynamics", *AIChe Journal, 46* (3), 597–609.

Iliuta, I.; Larachi, F. and Grandjean, B. P. A. (1999) "Residence time, mass transfer and back-mixing of the liquid in trickle flow reactors containing porous particles", *Chemical Engineering Science, 54*, 4099–4109.

Jiang, Y.; Khadilkar, M. R.; Al-Dahhan, M. H. and Dudukovic, M. P. (1999) "Two-phase flow distribution in 2d trickle-bed reactors", *Chemical Engineering Science, 54*, 2409–2419.

Kan, K. M. and Greenfield, P. F. (1978) "Multiple hydrodynamics tates in cocurrent two-phase downflow through packed beds", *Industrial Engineering Chenistry Process Design and Development, 17*, 482.

Kan, K. M. and Greenfield, P. F. (1979) "Pressure drop and holdup in two-phase cocurrent trickle flows through beds of small packings", *Industrial Engineering Chemistry Process Design and Development, 18*, 740–745.

Khadilkar, M. R.; Mills, P. L. and Dudukovic, M. P. (1999) "Trickle-bed reactor models for systems with a volatile liquid phase", *Chemical Engineering Science, 54*, 2421–2431.

Khadilkar, M. R.; Wu, Y. X.; Al-Dahhan, M. H. and Dudukovic, M. P. (1996) "Comparison of trickle-bed and upflow reactor performance at high pressure: Model predictions and experimental observations", *Chemical Engineering Science, 51*, 2139–2148.

Kheshgi, H. S.; Reyes, S. C.; Hu, R. and Ho, T. C. (1992) "Phase transition andsteady-state multiplicity in a trickle-bed reactor.", *Chemical Engineering Science, 47*, 1771–1777.

Krauze, R. and Scrwinski, M. (1971) "Moisted surface and fractional wetted surface area of ceramic raschig rings", *Inzineria Chemiczna, 1*, 415.

Kundu, A.; Nigam, K. D. P. and Verma, R. P. (2003) "Catalyst wetting characteristics in trickle-bed reactors", *AIChe Journal, 49*, 2253–2263.

Lakota, A. and Levec, J. (1990) "Solid-liquid mass transfer in packed beds with concurrent downward two-phase flow", *AIChe Journal, 36*, 1444.

Lapidus, L. (1957) "Flow distribution and diffusion in fixed-bed two-phase reactors", *Industrial Engineering Chemistry, 49*, 1000.

Larachi, F.; Laurent, A.; Wild, G. and Midoux, N. (1992) "Pressure effect on gas-liquid interfacial areas in cocurrent trickle-flow reactors", *Chemical Engineering Science, 47*, 2325.

Lazzaroni, C. L.; Kesselman, H. R. and Figoli, H. S. (1988) "Colorimetric evaluation of efficiency of liquid-solid contacting in trickle-bed reactors", *Industrial Engineering Chemistry, 27*, 1132.

Lazzaroni, C. L.; Kesselman, H. R. and Figoli, H. S. (1989) "Trickle bed reactors. multiplicity of hydrodynamic states. relation between the pressure drop and the liquid holdup", *Industrial Engineering Chemistry Research, 28*, 119–121.

Leung, P. C.; Recasens, F. and Smith, J. M. (1987) "Hydration of isobutene in a trickle-bed reactor: Wetting efficiency and mass transfer", *AIChe Journal, 33*, 996–1007.

Levec, J.; Grosser, K. and Carbonell, R. G. (1988) "The hysteretic behaviour of pressure drop and liquid holdup in trickle beds", *AIChe Journal, 34*, 1027–1030.

Levenspiel, O. (2002) "Modeling in chemical engineering", *Chemical Engineering Science, 57*, 4691–4696.

Llano, J. J.; Rosal, R.; Sastre, H. and Diez, F. V. (1997) "Determination of wetting efficiency in trickle-bed reactors by a reaction method", *Industrial Engineering Chemistry Research, 36*, 2616–2625.

Lutran, P. G.; Ng, K. M. and Delikat, E. P. (1991) "Liquid distribution in trickle-beds. an experimental study using computer-assisted tomography", *Industrial Engineering Chemistry Research, 30*, 1270–1280.

Marcandelli, C.; Lamine, A. S.; Bernard, J. R. and Wild, G. (2000) "Liquid distribution in trickle-bed reactor", *Oil & Gas Science and Technology, 55* (4), 407–415.

Mata, A. and Smith, J. M. (1981) "Transport processes in multiphase reaction systems", *AIChe Symposium Series,* pages 29–35.

Mears, D. E. (1974) "The role of liquid holdup and effective wetting in the performance of trickle-bed reactors", *Adv. Chem. Ser.,* page 218.

Melli, T. R. and Scriven, L. E. (1991) "Theory of two-phase cocurrent downflow in networks of pasages", *Industrial Engineering Chemistry Research, 30*, 951.

Mills, P. L. and Dudukovic, M. P. (1979) "A dual-series solution for the effectiveness factor of partially wetted catalysts in trickle-bed reactors", *Industrial Engineering Chemisrty Fundamentals, 18*, 139–149.

Mills, P. L. and Dudukovic, M. P. (1980) "Analysis of catalyst effectiveness in trickle-bed reactors processing volatile or nonvolatile reactants", *Chemical Engineering Science, 35*, 2267–2279.

Mills, P. L. and Dudukovic, M. P. (1981) "Evaluation of liquid-solid contacting in trickle-beds by tracer methods", *AIChe Journal, 27*, 893.

Mills, P. L. and Dudukovic, M. P. (1984) "A comparison of current models for isothermal trickle-bed reactors. application to a model reaction system", *ACS Symposium Series, 237*, 37.

Mills, P. L. and Dudukovic, M. P. (1989) "Convolution and deconvolution of nonideal tracer response data with application to three-phase packed beds", *Computers and Chemical Engineering, 13*, 881–898.

Moller, L. B.; Halken, C.; Hansen, J. A. and Bartholdy, J. (1996) "Liquid and gas distribution in trickle-bed reactors", *Industrial Engineering Chemistry Research, 35*, 926–930.

Morita, S. and Smith, J. M. (1978) "Mass transfer and contacting efficiency in a trickle-bed reactor", *Industrial Engineering Chemistry Fundamentals, 17*, 113.

Nigam, K. D. P.; Iliuta, I. and Larachi, F. (2001) "Liquid back-mixing and mass transfer effect in trickle-bed reactors filled with porous catalyst particles", *Chemical Engineering and Processing, 41*, 365–371.

Onda, K.; Takeuchi, H. and Kayama, Y. (1967) "Effect of packing materials on wetted surface area", *K. Kagaku Kogaku, 31*, 126.

Pathwardan, V. S. (1978) "Effective interfacial area in packed beds for absorption with chemical reaction", *Canadian Journal of Chemical Engineering, 56*, 56–64.

Pironti, F.; Mizrahi, D.; Acosta, A. and Gonzalez-Mendizabal, D. (1999) "Liquid-solid wetting factor in trickle-bed reactors: its determination by a physical method", *Chemical Engineering Science, 54*, 3793–3800.

Puranik, S. S. and Vogelpohl, V. (1974) "Effective interfacial area irrigated packed columns", *Chemical Engineering Science, 29*, 501.

Ramachandran, P. A.; Dudukovic, M. P. and Mills, P. L. (1986) "A new model for assessment of external liquid-solid contacting in trickle-bed reactors from tracer response measurements", *Chemical Engineering Science, 41*, 855–860.

Ramachandran, P. A. and Smith, J. M. (1979) "Effectiveness factors in trickle-bed reactors", *AIChe Journal, 25*, 538.

Ravindra, P. V.; Rao, D. P. and Rao, M. S. (1997) "Liquid flow texture in trickle-bed reactors: An experimental study", *Industrial Engineering Chemistry Research, 36*, 5133–5145.

Ring, Z. E. and Missen, R. W. (1991) "Trickle-bed reactors: tracers study of liquid holdup and wetting efficiency at high temperature and pressure", *Canadian Journal of Chemical Engineering, 26*, 164.

Ross, L. D. (1965) "Performance of trickle bed reactors", *Chemical Engineering Progress, 61*, 77.

Roy, S.; Kemoun, A.; Al-Dahhan, M. H.; Dudukovic, M. P.; Skourlis, T. B. and Dautzenberg, F. M. (2004) "Countercurrent flow distribution in structured packing via computed tomography", *Chemical Engineering and Processing, 45*, 59–69.

Ruiz, P.; Crine, M.; Germain, A. and L'Homme, G. (1984) "Influence of the reactional system on the irrigation rate in trickle-bed reactors", *ACS Symposium Series,* (237), 15.

Saez, A. E. and Carbonell, R. G. (1975) "Hydrodynamic parameters for gas-liquid cocurrent flow in trickle-beds", *AIChe Journal, 21*, 209–227.

Satterfield, C. N. (1975) "Trickle-bed reactors", *AIChe Journal, 21*, 209.

Schwartz, T. G.; Wegwe, E. and Dudukovic, M. P. (1976) "A new tracer method for determination of liquid-solid contacting effectiveness in trickle-bed reactors", *AIChe Journal, 22*, 894.

Sederman, A. J. and Gladden, L. F. (2001) "Magnetic resonance imaging as a quantitative probe of gas-liquid distribution and wetting efficiency in trickle-bed reactors", *Chemical Engineering Science, 56*, 2615–2628.

Sedriks, W. and Kenney, C. N. (1972) "Partial wetting in trickle-bed reactors: the reduction of crotonaldehyde over a palladium catalyst", *Chemical Engineering Science, 28*, 559–568.

Sicardi, S.; Baldi, G.; Gianetto, A. and Specchia, V. (1980) "Catalyst areas wetted by flowing and semistagnant liquid in trickle-bed reactors", *Chemical Engineering Science, 35*, 67.

Sicardi, S.; Baldi, G.; Specchia, V.; Mazzarino, I. and Gianetto, A. (1981) "Packing wetting in trickle bed reactors: influence of the gas flow rate", *Chemical Engineering Science, 36*, 226–228.

Souadnia, A. and Latifi, M. A. (2001) "Analysis of two-phase flow distribution in trickle-bed reactors", *Chamical Engineering Science, 56*, 5977–5985.

Specchia, V.; Baldi, G. and Gianetto, A. (1978) "Solid-liquid mass transfer in cocurrent two-phase flow through packed beds", *Industrial Engineering Chemistry Design and Development, 17*, 362–367.

Stanek, V.; Hanika, J.; Hlavacek, V. and Trnka, O. (1981) "The effect of liquid flow distribution on the behaviour of a trickle-bed reactor", *Chemical Engineering Science, 36*, 1045.

Statsoft "Descriptive statistics homepage", http://www.statsoft.com November (2005).

Tan, C. S. and Smith, J. M. (1980) "Catalyst particle effectiveness with unsymmetrical boundary conditions", *Chemical Engineering Science, 35*, 1601–1609.

Tsamatsoulis, D. C. and Papayannakos, N. G. (1996) "Partial wetting of cylindical catalytic carriers in trickle-bed reactors", *AIChe Journal, 42*, 1853–1863.

Tsochatzidis, N. A.; Karabelas, A. J.; Giakoumakis, D. and Huff, G. (2002) "An investigation of liquid maldistribution in trickle beds", *Chemical Engineering Science, 57*, 3543–3555.

van der Merwe, W. and Nicol, W. (2005) "Characterization of multiple flow morphologies within the trickle flow regime", *Industrial Engineering Chemistry Research, ASAP Article*.

Villermaux, J. and vanSwaaij, W. P. M. (1969) "Modele represasentatif de la distribution des temps de sejour dans un reacteur semi-infi a dispersion axiale avec zones stagnantes. application a l'ecoulement ruisselant dans des colonnes d'anneux raschig", *Chemical Engineering Science, 24*, 1097–1111.

Wammes, W. J. A.; Middelkamp, J.; Huisman, W. J.; de Baas, C. M. and Westerterp, K. R. (1991) "Hydrodynamics in a cocurrent gas-liquid trickle-bed at elevated pressures", *AIChe Journal, 37*, 1849–1862.

Wang, R.; Mao, Z. S. and Chen, J. (1995) "Experimental and theoretical studies of pressure drop hysteresis in trickle bed reactors", *Chemical Engineering Science, 50*, 2321–2328.

Wu, Y.; Al-Dahhan, M. A.; Khadilkar, M. R. and Dudukovic, M. P. (1996) "Evaluation of trickle-bed reactor models for a liquid limited reaction", *Chemical Engineering Science, 51*, 2721–2725.

Zimmerman, S. P. and Ng, K. M. (1986) "Liquid distribution in trickling flow trickle-bed reactors", *Chemical Engineering Science, 41*, 861.